

JRC SCIENTIFIC AND POLICY REPORTS

Systemic Seismic Vulnerability and Risk Analysis for Buildings, Lifeline Networks and Infrastructures Safety Gain

SYNER-G Synthetic Document

Authors: Kyriazis Pitilakis, Sotiris Argyroudis,
Kalliopi Kakderi, Anastasia Argyroudi

Reviewers: Helen Crowley

Publishing Editor: Fabio Taucer

2013



European Commission
Joint Research Centre
Institute for the Protection and Security of the Citizen

Contact information

Fabio Taucer

Address: Joint Research Centre, Via Enrico Fermi 2749, TP 480, 21027 Ispra (VA), Italy

E-mail: fabio.taucer@jrc.ec.europa.eu

Tel.: +39 0332 78 5886

Fax: +39 0332 78 9049

<http://elsa.jrc.ec.europa.eu/>

<http://www.jrc.ec.europa.eu/>

Legal Notice

Neither the European Commission nor any person acting on behalf of the Commission is responsible for the use which might be made of this publication.

Europe Direct is a service to help you find answers to your questions about the European Union

Freephone number (*): 00 800 6 7 8 9 10 11

(*) Certain mobile telephone operators do not allow access to 00 800 numbers or these calls may be billed.

A great deal of additional information on the European Union is available on the Internet.

It can be accessed through the Europa server <http://europa.eu/>.

JRC84703

EUR 26157 EN

ISBN 978-92-79-33135-0

ISSN 1831-9424

doi: 10.2788/23242

Luxembourg: Publications Office of the European Union, 2013

© European Union, 2013

Reproduction is authorised provided the source is acknowledged.

Printed in Ispra (Va) - Italy



D 8.20

DELIVERABLE

PROJECT INFORMATION

Project Title: **Systemic Seismic Vulnerability and Risk Analysis for Buildings, Lifeline Networks and Infrastructures Safety Gain**

Acronym: SYNER-G

Project N°: 244061

Call N°: FP7-ENV-2009-1

Project start: 01 November 2009

Duration: 41 months

DELIVERABLE INFORMATION

Deliverable Title: **D8.20 - SYNER-G synthetic document**

Date of issue: 01 March 2013

Work Package: WP8 – Guidelines, recommendations and dissemination

Aristotle University of Thessaloniki (AUTH)

Deliverable/Task Leader: & Commission of the European Communities – Directorate General Joint Research Centre (JRC)

Reviewer: University of Pavia (UPAV)

REVISION: Final



Project Coordinator: Prof. Kyriazis Pitilakis

Institution: Aristotle University of Thessaloniki

e-mail: kpitilak@civil.auth.gr

fax: + 30 2310 995619

telephone: + 30 2310 995693

Abstract

This report summarizes the main achievements and results of the work carried out within the European collaborative research project SYNER-G. SYNER-G developed an innovative methodological framework for the systemic assessment of physical as well as socio-economic seismic vulnerability at urban and regional level. The built environment is modeled according to a detailed taxonomy into its component systems, grouped in the following categories: buildings, transportation and utility networks, and critical facilities. Each category may have several types of components. The framework encompasses in an integrated fashion all aspects in the chain, from regional hazard to fragility assessment of components to the socioeconomic impacts of an earthquake, accounting for relevant uncertainties within an efficient quantitative simulation scheme, and modeling interactions between the multiple component systems in the taxonomy. The prototype software (OOFIMS) is implemented in the SYNER-G platform, which provides several pre and post-processing tools. The methodology and software tools are applied and validated in selected sites and systems in urban and regional scale: the city of Thessaloniki (Greece), the city of Vienna (Austria), the harbour of Thessaloniki, the gas system of L'Aquila (Italy), the electric power network in Sicily, a roadway network in South Italy and a hospital facility again in Italy. Adequate guidelines and appropriate dissemination schemes for all products of the project at European and international level have been proposed, including among others seven comprehensive Reference Reports, synthetic documents and deliverables, high quality brochure and leaflet, three technical workshops, a special session in the 15WCEE, peer review publications in journal and conferences, and preparation of two books in Springer Editions.

Keywords: SYNER-G methodology, utility systems, transportation networks, critical facilities, fragility curve, performance indicator, taxonomy, uncertainty, validation studies, synthetic report

Acknowledgments

The research leading to these results has received funding from the European Community's Seventh Framework Programme [FP7/2007-2013] under grant agreement n° 244061.

Deliverable Contributors

AUTH Kyriazis Pitilakis
 Sotiris Argyroudis
 Kalliopi Kakderi
 Anastasia Argyroudi

Table of Contents

Abstract	i
Acknowledgments	iii
Deliverable Contributors	v
Table of Contents.....	vii
List of Figures	xi
List of Tables.....	xv
1 Introduction.....	1
2 SYNER-G methodology for systemic analysis, performance and loss estimates	4
2.1 INTRODUCTION	4
2.2 TAXONOMY OF THE INFRASTRUCTURE	7
2.3 THE SYNER-G METHODOLOGY	10
2.3.1 Object-oriented approach	12
2.3.2 Infrastructure model.....	14
2.3.3 Seismic hazard model	18
2.3.4 Probabilistic analysis	19
3 SYNER-G fragility curves for all elements at risk.....	21
3.1 INTRODUCTION	21
3.1.1 Background.....	21
3.1.2 Derivation of fragility curves.....	22
3.1.3 Typology	22
3.1.4 Performance levels	22
3.1.5 Intensity measures.....	23
3.1.6 Performance indicators.....	24
3.1.7 Treatment of uncertainties	24
3.1.8 Relation with socio-economic losses	25
3.1.9 Main results	25
3.2 FRAGILITY CURVES FOR BUILDINGS.....	27
3.2.1 Introduction	27
3.2.2 SYNER-G Taxonomy.....	27
3.2.3 Examples of proposed fragilities	30
3.3 FRAGILITY CURVES FOR LIFELINES	33

3.3.1	Electric power network.....	33
3.3.2	Natural gas and oil networks	38
3.3.3	Water and waste-water networks	42
3.4	FRAGILITY CURVES FOR TRANSPORTATION INFRASTRUCTURES	45
3.4.1	Roadway and railway bridges.....	46
3.4.2	Roadway networks	50
3.4.3	Railway networks.....	52
3.4.4	Harbour elements	54
3.5	FRAGILITY CURVES FOR CRITICAL FACILITIES	57
3.5.1	Health care facilities.....	57
3.5.2	Fire-fighting systems.....	60
3.6	CONCLUSIONS.....	62
3.6.1	Fragility functions for reinforced concrete and masonry buildings	62
3.6.2	Fragility functions for utility networks	63
3.6.3	Fragility functions for transportation infrastructures	63
3.6.4	Fragility functions for critical facilities.....	64
4	Socio-economic vulnerability and losses	65
4.1	SHELTER NEEDS MODEL	66
4.2	HEALTH IMPACT MODEL	69
5	Systemic vulnerability specification.....	70
5.1	GENERAL SPECIFICATION	70
5.1.1	Taxonomy of components within each system	70
5.1.2	System evaluation and performance indicators	71
5.1.3	Interdependencies	71
5.2	DESCRIPTION OF THE CONSIDERED SYSTEMS	72
5.2.1	Building and aggregates	72
5.2.2	Utility Networks	73
5.2.3	Transportation network.....	74
5.2.4	Critical Facilities.....	75
6	SYNER-G toolbox and web portal.....	76
7	Pilot studies and application of SYNER-G methodology.....	78
7.1	INTRODUCTION	78
7.2	THE CASE STUDIES	78
7.3	FRAGILITY CURVES	86

7.4	SEISMIC AND GEOTECHNICAL HAZARD.....	90
7.5	SYSTEMIC VULNERABILITY ANALYSIS AND SOFTWARE IMPLEMENTATION ..	92
7.5.1	City of Thessaloniki, Greece.....	92
7.5.2	City of Vienna, Austria	94
7.5.3	Road network (application in Calabria region, Southern Italy).....	95
7.5.4	Electric power network (application in Sicily).....	95
7.5.5	Hospital facility and regional health-care system (application in Italy).....	95
7.5.6	Harbour (application in Thessaloniki)	96
7.5.7	Summary of systemic vulnerability analysis.....	97
7.6	RESULTS	99
7.6.1	City of Thessaloniki.....	99
7.6.2	City of Vienna	109
7.6.3	Gas system in L'Aquila, Italy.....	113
7.6.4	Road network in Calabria region, Southern Italy	119
7.6.5	Electric power network of Sicily	122
7.6.6	Hospital facility and regional health-care system IN Italy.....	125
7.6.7	Harbour of Thessaloniki.....	127
7.7	CONCLUSIONS.....	131
8	Guidelines, recommendations and dissemination	135
8.1	MAIN DISSEMINATION ACTIVITIES	135
9	Conclusions and recommendations for further improvement and actions	137
	References.....	139

List of Figures

Fig. 1.1 The SYNER-G consortium.....	2
Fig. 1.2 Graphical layout of SYNER-G methodology and software tools.....	2
Fig. 1.3 Main steps of the SYNER-G methodology.....	3
Fig. 2.1 The three dimensions in an Infrastructure vulnerability study.....	5
Fig. 2.2 Illustration of the different categories of components/sub-systems of the Infrastructure.....	6
Fig. 2.3 Integrated evaluation of physical and socio-economic performance indicators.....	10
Fig. 2.4 Class diagram for the hazard class (the grey hatch, as indicated, denotes classes that have been included at the conceptual level but have not yet been implemented in the software)	13
Fig. 2.5 Class diagram for the WSS and EPN classes (the grey hatch denotes classes included at the conceptual level but not yet implemented in the software)	13
Fig. 2.6 Sample WSS (top) and corresponding object-diagram (bottom)	14
Fig. 2.7 State diagram to model the inter-dependencies: sequence in the evaluation of states of the objects and messages (quantities) transmitted between objects.	17
Fig. 2.8 The sequence of models with associated input and output quantities.....	20
Fig. 3.1 Examples of (a) vulnerability function and (b) fragility function	21
Fig. 3.2 Screenshot of the main window of the Fragility Function Manager tool.....	26
Fig. 3.3 Mean curve for yielding limit state in left column (a, c, e, g) and collapse limit state in right column (b, d, f, h) for reinforced concrete buildings	32
Fig. 3.4 Mean curve for yielding limit state (a) and collapse limit state (b) for masonry buildings	33
Fig. 3.5 European high voltage transmission grid ($V \geq 220\text{kV}$). Higher voltage lines in blue, lower voltage lines in red. Line thickness is proportional to voltage (Poljansek et al. 2010).....	34
Fig. 3.6 Overview of the gas networks in Europe (Nies, 2008)	38
Fig. 3.7 Mean and individual fragility curves for (left column) minor damage limit state and (right column) collapse limit state, for reinforced concrete bridges. (a, b, c, d) isolated pier-to-deck connection and (e, f, g, h) for non-isolated pier-to-deck connection. (a, b, e, f) regular or semi-regular bridges type and (c, d, g, h) irregular bridge type.....	49
Fig. 3.8 System taxonomy of a hospital	58
Fig. 4.1 Integrated evaluation of physical and socio-economic performance indicators.....	66

Fig. 4.2 Relationship between severely damaged and destroyed buildings and displaced persons after earthquakes (n = 457 earthquakes from 1900-2012 from the CATDAT database in Khazai 2013.....	67
Fig. 4.3 Multi-criteria decision model for computing Shelter Needs Index (SNI).....	68
Fig. 4.4 Ratio of actual population in shelters (Observed data) shown against the ranking of displaced persons and shelter needs in the 8 COMs after the 2009 L'Aquila earthquake.....	68
Fig. 4.5 Ranking of Shelter Needs Index (SNI) for sub-city districts of Thessaloniki	69
Fig. 5.1 Example of a specified UML diagram for the Road Network System	71
Fig. 6.1 The plug-in based structure of the software.....	76
Fig. 6.2 Layout of the SYNER-G platform.....	77
Fig. 7.1 Sub-city districts (SCD) of Thessaloniki study area as defined by Urban Audit.....	79
Fig. 7.2 The city of Vienna with the part of the 20th district	79
Fig. 7.3 Case study of L'Aquila gas system	80
Fig. 7.4 Calabria region road network topology (left) and location of hospitals and landslides areas (right)	81
Fig. 7.5 Position of municipalities and EPN nodes in Sicily case study	81
Fig. 7.6 The hypothetical study area.....	82
Fig. 7.7 General plan of the examined hospital system	82
Fig. 7.8 Thessaloniki's port	83
Fig. 7.9 Flowchart of the building class computation	92
Fig. 7.10 Update procedure of the adjacency matrix	94
Fig. 7.11 Functionality simulation of port facilities.....	97
Fig. 7.12 Moving average μ , $\mu+\sigma$, $\mu-\sigma$ curves for ECL.....	99
Fig. 7.13 MAF curve for electric power network connectivity loss (ECL)	99
Fig. 7.14 Correlation of non-functional transmission substations to electric power network connectivity loss.	100
Fig. 7.15 Moving average μ , $\mu+\sigma$, $\mu-\sigma$ curves for WCL.....	100
Fig. 7.16 MAF curve for water connectivity loss (WCL) with and without interaction with electric power network (EPN)	101
Fig. 7.17 Correlation of damaged pipes and non-functional EPN transmission stations to water network connectivity	102
Fig. 7.18 Water supply system damages for an event (#2379, M=7.4, R=72km) that corresponds to WCL with $T_m=500$ years	102
Fig. 7.19 Moving average μ , $\mu+\sigma$, $\mu-\sigma$ curves (up) and MAF curve (down) for deaths	103
Fig. 7.20 Distribution of estimated damages (collapsed and yielding buildings) into cells of the study area for an event (#1488, M=5.5, R=24 km) that corresponds to death rate with $T_m=500$ years.....	104

Fig. 7.21 Correlation of damaged EPN and WSS components to displaced people	105
Fig. 7.22 Moving average μ , $\mu+\sigma$, $\mu-\sigma$ curves for SCL (left) and WCL (right).	106
Fig. 7.23 MAF curves for simple (SCL) and weighted (WCL) connectivity loss with and without interaction with building collapses.....	106
Fig. 7.24 Correlation of broken edges (bridges) to road network connectivity (PI=WCL) ...	107
Fig. 7.25 Correlation of blocked by buildings edges to road network connectivity (PI=WCL)	107
Fig. 7.26 Accessibility to hospitals for Thessaloniki SCDs (zone based technique)	108
Fig. 7.27 Average building collapse (left) and building yielding distribution (right).....	109
Fig. 7.28 Average death (left) and injured (right) distribution.....	110
Fig. 7.29 Mean annual frequency of exceedance and moving average (death persons) ..	110
Fig. 7.30 Average blocked roads (left) and unusable ones (right)	111
Fig. 7.31 Pipes broken (left) and non-functional nodes (right)	111
Fig. 7.32 Number of buildings collapsed (left) and yield (right) for the selected event of M = 5.4.....	112
Fig. 7.33 Number of deaths (left) and injured (right) persons for the selected event of M = 5.4.....	113
Fig. 7.34 Ccdf and confidence bounds for CL (top) and SR (bottom)	114
Fig. 7.35 Histograms of broken pipes in the simulations (top) and scatter plots of PIs with respect to percentage of broken pipes (bottom).....	115
Fig. 7.36 Histograms of damaged M/R stations in the simulations (top) and scatter plots of PIs with respect to percentage of damaged M/R stations (bottom)	116
Fig. 7.37 Relative frequency of the number of broken pipes conditional to CL (left) and SR (right)	117
Fig. 7.38 Relative frequency of the number of damaged M/R stations conditional to CL (left) and SR (right)	117
Fig. 7.39 Relative frequency of percentage of pipes vulnerable to PGD conditional to CL (left) and SR (right)	118
Fig. 7.40 Exceedance curve of CL (top) and SR (bottom) for the three grid sizes.....	118
Fig. 7.41 Moving average μ , $\mu+\sigma$ and $\mu-\sigma$ curves for SCL (left) and WCL (right)	119
Fig. 7.42 MAF curves for SCL and WCL (left) and TR matrix (right).....	120
Fig. 7.43 Contour maps of minimum travel time to hospitals, in non-seismic conditions (left) and of expected increment of minimum travel time to hospitals (right)	120
Fig. 7.44 Comparison of moving average μ obtained from MCS, ISS and ISS-KM, for SCL (left) and WCL (right)	121
Fig. 7.45 Comparison of MAF curves obtained from MCS, ISS and ISS-KM, for SCL (left) and WCL (right)	121
Fig. 7.46 Moving average μ , $\mu+\sigma$ and $\mu-\sigma$ curves for CL (left) and SSI (right).....	122

Fig. 7.47 MAF curves for CL (left) and SSI (right)	123
Fig. 7.48 Contour map of expected values of VR	123
Fig. 7.49 Comparison of moving average μ obtained from MCS, ISS and ISS-KM, for CL (left) and SSI (right)	124
Fig. 7.50 Comparison of MAF curves obtained from MCS, ISS and ISS-KM, for CL (left) and SSI (right)	124
Fig. 7.51 MAF curves of normalised casualties (divided in two categories) that are not allocated in hospitals	125
Fig. 7.52 Evolution of maximum travel time for hospitalisation	126
Fig. 7.53 $P(HTD \geq HTC)$, for the three region hospitals	126
Fig. 7.54 Moving average μ , $\mu+\sigma$, $\mu-\sigma$ curves for TCoH (left) and TCaH (right)	128
Fig. 7.55 MAF curve for TCoH and TCaH performance loss	128
Fig. 7.56 MAF curves for TCoH (left) and TCaH (right) for Thessaloniki's port, with and without interaction with building collapses	129
Fig. 7.57 MAF curves for TCoH (left) and TCaH (right) for Thessaloniki's port, with and without interaction with EPN and building collapses	130
Fig. 7.58 Correlation of damaged cranes to port performance (PI=TCaH)	131
Fig. 7.59 Correlation of non-functional electric power distribution substations to port performance (PI=TCaH)	131
Fig. 8.1 Graphical representation of SYNER-G Dissemination scheme	136

List of Tables

Table 2.1 Infrastructure taxonomy	7
Table 2.2 Interdependencies for sample system from the Taxonomy.	16
Table 3.1 SYNER-G Taxonomy for buildings	27
Table 3.2. Description of building types, taxonomy and available number of fragility curves	30
Table 3.3 Mean and c_v of lognormal fragility parameters for reinforced concrete buildings..	31
Table 3.4 Mean and c_v of lognormal fragility parameters for low-rise masonry buildings	32
Table 3.5 Main typologies of EPN components in Europe.....	35
Table 3.6 Fragility functions of macro-components 1, 2, 3 and 4	36
Table 3.7 Fragility functions of 11 micro-components	37
Table 3.8 SYNER-G Taxonomy for oil network	39
Table 3.9 SYNER-G Taxonomy for natural gas network	40
Table 3.10 Summary of the proposed fragility functions for elements of gas and oil systems	41
Table 3.11 SYNER-G Taxonomy for water supply network.....	42
Table 3.12 SYNER-G taxonomy for waste-water network.....	44
Table 3.13 Summary of the proposed fragility functions for water and waste water elements	45
Table 3.14 SYNER-G Taxonomy for bridges.....	46
Table 3.15 Mean and c_v of lognormal fragility parameters for reinforced concrete, isolated pier-to-deck connection, regular or semi-regular bridges type	50
Table 3.16 SYNER-G Taxonomy for roadway Network.....	51
Table 3.17 Summary of the proposed fragility functions for road elements	52
Table 3.18 SYNER-G Taxonomy for railway network.....	53
Table 3.19 Summary of the proposed fragility functions for railway elements	54
Table 3.20 SYNER-G Taxonomy for harbour elements.....	55
Table 3.21 Summary of the proposed fragility functions for harbour elements.....	57
Table 3.22 SYNER-G Taxonomy for health-care facilities.....	59
Table 3.23 SYNER-G Taxonomy for fire-fighting system	61
Table 5.1 Interactions between systems considered in SYNER-G.....	72
Table 7.1. Summary of elements at risk in each case study.....	83
Table 7.2 Fragility curves used in the case studies	86
Table 7.3 Parameters of fragility curves for RC buildings in Thessaloniki	88

Table 7.4 Parameters of fragility curves for masonry buildings in Thessaloniki.....	88
Table 7.5 Bridge types in the Thessaloniki study area	89
Table 7.6 Fragility curves used in Vienna test case for RC and masonry buildings	90
Table 7.7 Summary of seismic and geotechnical hazard for the case studies	91
Table 7.8 Systemic analysis for the case studies	97
Table 7.9 Data from the selected event for Vienna case study	112
Table 8.1 Consolidated List for the production of the SYNER-G Reference Reports	136

1 Introduction

SYNER-G is a European collaborative research project focusing on systemic seismic vulnerability and risk analysis of buildings, transportation and utility networks and critical facilities. The methodology is implemented in an open source software tool and it is applied and validated in selected case studies. SYNER-G is integrated across different disciplines with an internationally recognized partnership from Europe, USA and Japan. The 14 participants in the consortium (Fig. 1.1) represent a variety of organizations, from universities and academic institutions to research foundations and SMEs. The objectives and the deliverables are focused to the needs of the administration, local authorities, responsible for the management of seismic risk, private and public services managing utility systems and infrastructures, insurance industry, as well as the needs of the construction, consulting and insurance.

SYNER-G developed an innovative methodological framework for the assessment of physical as well as socio-economic seismic vulnerability at urban and regional level. The built environment is modeled according to a detailed **taxonomy** into its component systems, grouped into the following categories: buildings, transportation and utility networks, and critical facilities. Each category may have several types of components. The framework encompasses in an integrated fashion all aspects in the chain, from regional **hazard** to **fragility** assessment of components to the **socioeconomic impacts** of an earthquake, accounting for relevant **uncertainties** within an efficient quantitative simulation scheme, and **modeling interactions** between the multiple component systems in the taxonomy. The **prototype software** (OOFIMS) which provides several pre and post-processing tools, is implemented in the **SYNER-G platform**. The methodology and software tools are applied and **validated** in selected sites and systems in urban and regional scale: the city of Thessaloniki (Greece), the city of Vienna (Austria), the harbour of Thessaloniki (Greece), the gas system of L'Aquila (Italy), the electric power network in Sicily, a roadway network in South Italy and a hospital facility again in Italy. Adequate **guidelines** and appropriate **dissemination** schemes for all products of the project at European and international level have been proposed, including among others seven European Reference Reports, synthetic documents and deliverables, high quality brochure and leaflet, three technical workshops, a special session in the 15WCEE, peer review publications in journal and conferences, and preparation of two books in Springer Editions. The layout of SYNER-G methodology and software tools is illustrated in Fig. 1.2. The main steps of the SYNER-G methodology are outlined in Fig. 1.3.

This report presents, in a synthetic way, the general methodology developed within the SYNER-G project for the assessment of the seismic vulnerability of infrastructures (Chapter 2); an overview of proposed typology and taxonomy for buildings, lifelines, transportation infrastructures and critical facilities, and examples of the fragility functions proposed within the project for all elements at risk (Chapter 3). Chapter 4 summarizes the key outputs and scientific achievements related to the shelter needs and health impact models. The main features of the systemic vulnerability specification are outlined for each system in Chapter 5. Chapter 6 briefly presents the main features of the SYNER-G software. The application of SYNER-G methodology and tools to selected case studies of regional and urban extension are summarized in Chapter 7: the city of Thessaloniki in Greece; the city of Vienna in Austria; the gas system of L'Aquila in Italy; the road network of Calabria region in Southern Italy; the electric power network of Sicily (Italy); a hospital facility and a regional health-care system in Italy; the harbour of Thessaloniki in Greece. Finally, the main dissemination actions together with the final recommendations are presented (Chapter 8).

Aristotle University of Thessaloniki (coordinator), Greece		Middle East Technical University, Turkey	
Vienna Consulting Engineers, Austria		AMRA, University of Naples Federico II, Italy	
Bureau de Recherches Geologiques et Minieres, France		University of Karlsruhe, Germany	
Commission of the EC - Joint Research Centre, Belgium		University of Patras, Greece	
Norwegian Geotechnical Institute, Norway		Willis Group Holdings, United Kingdom	
University of Pavia, Italy		Mid-America Earthquake Center, University of Illinois, USA	
University of Roma "La Sapienza", Italy		Kobe University, Japan	

Fig. 1.1 The SYNER-G consortium

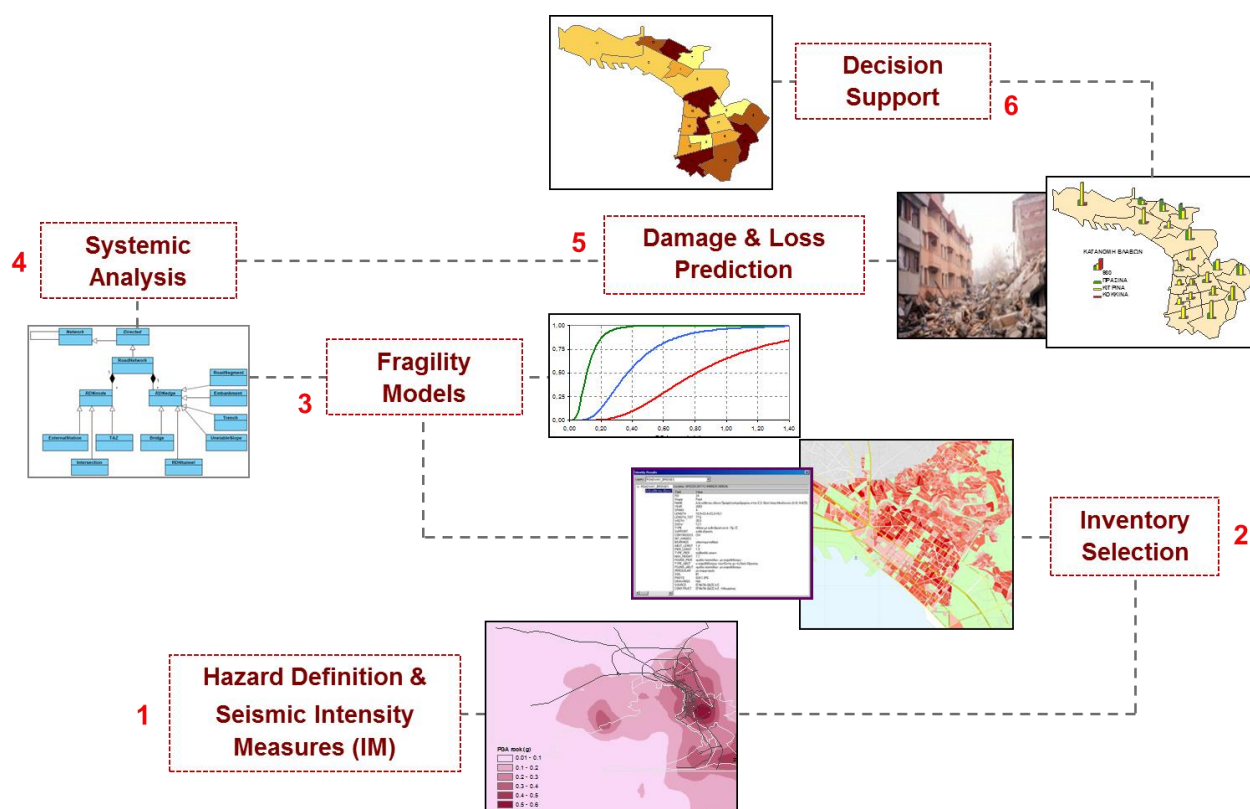
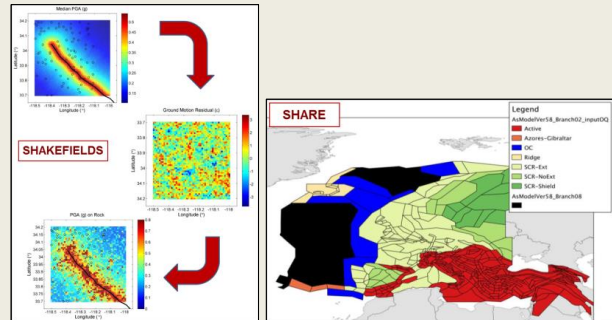


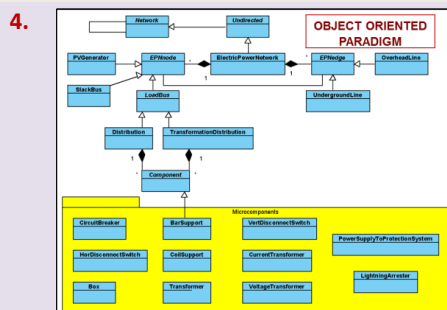
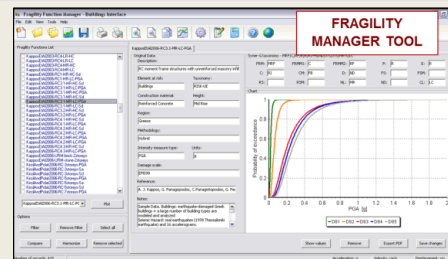
Fig. 1.2 Graphical layout of SYNER-G methodology and software tools

1. The **seismic hazard** is defined based on the SHARE EC/FP7 project results. A stochastic simulation is performed for the generation of spatially correlated and cross-correlated fields for ground motion intensity measures (Shake-fields). Site effects and various geotechnical hazards (liquefaction, fault crossing, landslide displacements) are also considered.



The physical elements are the built environment (buildings, lifeline networks, transportation infrastructures, critical facilities) while the social elements are represented by the demographic and socio-economic data. It is essential to compile **inventory** databases of elements at risk and to make a classification on the basis of pre-defined typology definitions. Inventories are obtained from Census Data, Owner/Operators Data, and ground surveys or through remote sensing techniques. Unified and harmonized **typology and taxonomy** definitions are proposed for the European physical assets at risk.

3. **Fragility curves** based on SYNER-G taxonomy are selected, developed and proposed for all elements at risk. A **Fragility Function Manager Tool** is available for the storage, harmonization and comparison of all available fragility functions.



A **systemic analysis** methodology and tool is developed for buildings (BDG), utilities and lifelines (electrical power, water, waste water, gas, transportation and harbor networks and health care facilities). The **Object-Oriented Modeling paradigm** is used, where the problem is decomposed in a number of interacting objects. Each system is specified with its components, solving algorithms – interactions between components, performance indicators (PIs) and interactions with other systems.

5. An advanced innovative systemic vulnerability assessment is carried out considering uncertainties based on Monte Carlo or importance sampling simulation. **Damages and losses** for all assets are assessed. Representative results are building damages, casualties (deaths, injuries, displaced people), connectivity or flow analysis-based performance indicators for networks and infrastructures and mean annual frequency of exceedance of the PIs. Distribution of estimated damages and losses for specific events is given through thematic maps.

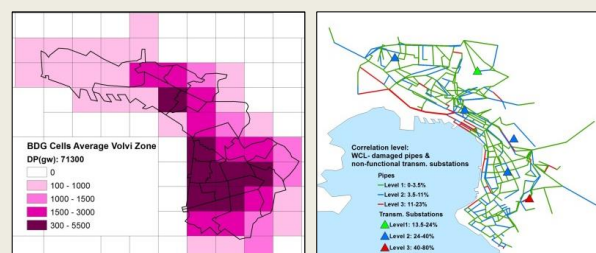


Fig. 1.3 Main steps of the SYNER-G methodology

2 SYNER-G methodology for systemic analysis, performance and loss estimates

2.1 INTRODUCTION

This chapter presents, in a synthetic way, the general methodology developed within the SYNER-G project for the assessment of the seismic vulnerability of infrastructures. First a brief introduction is given to the dimensions that have to be considered in a systemic study and on the spatial characterization of the components of the infrastructure. This is followed by a presentation of a schematic and identified taxonomy of infrastructural systems. Then the synthesis of the general methodology is given, presenting first the object-oriented approach that has been adopted and then the infrastructure and the hazard model that have been implemented. Finally the uncertainties and the probabilistic evaluation of the performance of an infrastructure are presented. For more details the reader is referred to SYNER-G Deliverable 2.1 (Franchin et al. 2011) and Reference Report 1 (Franchin 2013). This developed methodology is based on smart simulation of an object-oriented model of the system to account for the uncertainties involved (in the hazard, as well as in the system) and to tackle the complexity of the interactions existing within each system between its components, and across the systems. The methodology integrates within the same framework the hazard, the physical vulnerability and the social consequences/impact. The strength of the object-oriented foundation of the model is that it can be easily expanded and developed step-wise, allowing for multiple choices for each intermediate model. This allows also the integration of previous research results and models within a larger simulation framework for distributed infrastructural systems.

When the focus is on a systemic study, there are three main dimensions that have to be considered: time, space and stakeholders. The impact of the disaster caused by a natural hazard (which is an earthquake within SYNER-G) on a system evolves with *time* elapsed from the event and in *space*. Furthermore, different *stakeholders* may have different stakes and play different roles in dealing with the various phases of the disaster, and are correspondingly interested in the assessment of the impact in different ways. These dimensions of the systemic study are represented in Fig. 2.1. As far as the time dimension is concerned, two aspects are of interest: the *time-frame* and the *observation point-in-time*. Typically, three frames are considered:

- **short-term:** in the aftermath of the event the damaged Infrastructure operates in a state of emergency;
- **mid-term:** the Infrastructure progressively returns to a new state of normal functionality;
- **long-term:** the Infrastructure is upgraded/retrofitted with available resources to mitigate the risk from the next event.

Correspondingly, the spatial extent of interest to the study of the Infrastructure response increases with time, initially (short-term) involving only the local impacted area, then, an increasingly wide area covering adjacent regions, up to the national scale in the economic recovery phase and long-term risk mitigation actions.

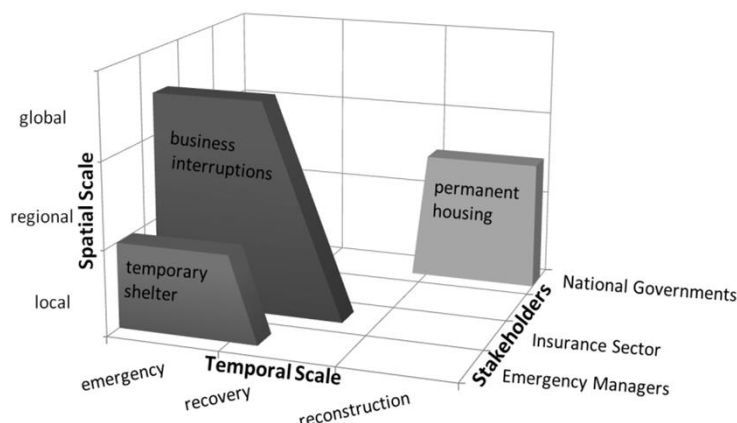


Fig. 2.1 The three dimensions in an Infrastructure vulnerability study.

The position on the time axis of the observer with respect to the time-frame changes the goal of the systemic study:

- **before the time-frame:** the goal of the system analyst is forecasting the impact in order to set-up mitigation measures. It is important to underline how the information basis in this case can be considered as constant.
- **within the time-frame:** the goal of the system analyst is that of providing the managers with a real-time decision support system, which updates the Infrastructure state based on the continuously incoming flow of information.
- **after the time-frame:** the goal of the system analyst is to validate the models against occurred events.

Systemic studies of different nature most commonly address the following two phases:

- Emergency phase: short-term (a few days/weeks) at the urban/regional scale
- Economic recovery phase: medium to long-term, at the regional/national scale

The contribution of Engineering disciplines is obviously capital to the first phase. During the second phase their role becomes to some extent ancillary, due to the intervention of political and economic factors in the decision-making process.

The developed SYNER-G methodology focuses on the first phase only, to Emergency managers as reference Stakeholders, and with the goal of forecasting before the event the expected impact for the purpose of planning and implementing risk mitigation measures.

The spatial characterization of the components (sub-systems) of the infrastructure has a direct relation with the approaches to be used for the definition of both the corresponding hazard and vulnerability. From a *geometric* point of view three categories can be identified:

- **Point-like components (Critical facilities):** single-site facilities whose importance for the functionality of the Infrastructure makes them critical, justifying a detailed description and analysis. Examples include hospitals, power-plants.
- **Line-like components (networks, lifelines):** distributed systems comprising a number of vulnerable point-like sub-systems in their vertices, and strongly characterized by their *flow-transmission function*. Examples include Electric networks with vulnerable power plants, sub-stations, etc, or road networks with vulnerable bridges.
- **Area-like components:** this is a special category specifically intended to model large populations of residential, office and commercial buildings, that cannot be treated individually. These buildings make up the largest proportion of the built environment and

generally give the predominant contribution to the total direct loss due to physical damage.

The approach for a vulnerability study of the area-like components is not homogeneous with that of the point-like and line-like sub-systems. The area-like components, for the purpose of a systemic study within SYNER-G, have been modelled with geo-cells characterized in terms of physical (distribution of buildings amongst standardized typologies with associated fragilities) and socio-economic (population, income, etc) parameters. In Fig. 2.2 the different categories of components/sub-systems of the Infrastructure are shown and the area-like component is represented by a *census tract*.

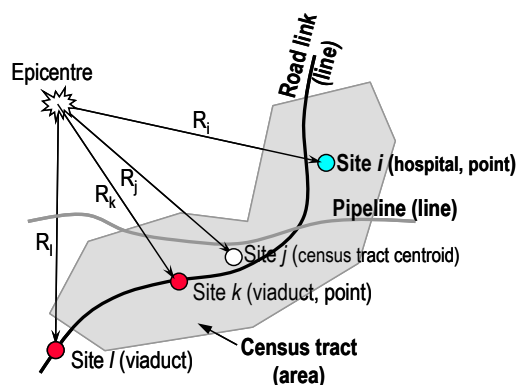


Fig. 2.2 Illustration of the different categories of components/sub-systems of the Infrastructure.

2.2 TAXONOMY OF THE INFRASTRUCTURE

In order to tackle the complexity of devising a model of the entire infrastructure the first task undertaken within the project was the identification and description of a set of systems, sub-systems and components to focus on. This has resulted in what is called the SYNER-G taxonomy and a more detailed version of this taxonomy can be found in the deliverable D2.1 (Franchin et al. 2011), Appendix B, with description of each component type. All considered systems and their components have been assigned unique tags used consistently throughout the project. This taxonomy has been the guidance for the fragility models that have been revised and/or developed for each component (see chapter 3), with a focus on European distinctive features, and for the modelling of the systems (see chapter 5).

For the purpose of summarising the taxonomy, in the following table all the systems, components and their sub-components considered in the infrastructure are reported with their tags.

Table 2.1 Infrastructure taxonomy

System	Component (and sub-components)
1. BDG: buildings	Force Resisting Mechanism (FRM1), FRM Material (FRMM1), Plan (P), Elevation (E), Cladding (C), Detailing (D), Floor System (FS), Roof System (RS), Height Level (HL), Code Level (CL)
2. HCS: health-care system	HCS01: organisational HCS02: human HCS03: physical <ul style="list-style-type: none"> - HCS03-1: structural elements (of the buildings within the complex/facility) - HCS03-2: non-structural elements - HCS03-3: architectural (walls, ceilings, windows etc) - HCS03-4: basic installations (generation/distribution) - HCS03-5: basic installations/medical gases - HCS03-6: basic installations/power system - HCS03-7: basic installations/water system - HCS03-8: basic installations/conveying system - HCS03-9: building contents
3.HBR: harbour	HBR01: waterfront components (gravity retaining structures; sheet pile wharves; piers; breakwaters mooring and breasting dolphins) HBR02: earthen embankments (hydraulic fills and native soil material)

	HBR03: cargo handling and storage components (cranes, tanks, etc)
	HBR04: buildings (sheds, warehouse, offices, etc)
	HBR05: liquid fuel system (as per the OIL system)
4. RDN: road network	<p>RDN01: bridge (material, type of deck, deck structural system, pier to deck connection, type of pier to deck connection; type of section of the pier, spans, type of connection to the abutments, skew, bridge configuration, foundation type, seismic design level)</p> <p>RDN02: tunnel</p> <p>RDN03: embankment (road on)</p> <p>RDN04: trench (road in)</p> <p>RDN05: unstable slope (road on, or running along)</p> <p>RDN06: road pavement (ground failure)</p> <p>RDN07: bridge abutment</p>
5. RWN: railway network	<p>RWN01: bridge</p> <p>RWN02: tunnel</p> <p>RWN03: embankment (track on)</p> <p>RWN04: trench (track in a)</p> <p>RWN05: unstable slope (track on, or running along)</p> <p>RWN06: track</p> <p>RDN07: bridge abutment</p> <p>RWN07: station</p>
6. WSS: water-supply network	<p>WSS01: source (springs, rivers, natural lakes, impounding reservoirs, shallow or deep wells)</p> <p>WSS02: treatment plant</p> <p>WSS03: pumping station</p> <p>WSS04: storage tank</p> <p>WSS05: pipe</p> <p>WSS06: tunnel</p> <p>WSS07: canal</p> <p>WSS08: SCADA system</p>
7. WWN: waste-water network	<p>WWN01: waste-water treatment plant</p> <p>WWN02: pumping (lift) station</p> <p>WWN03: pipe</p> <p>WWN04: tunnel</p>

	WWN05: SCADA system
8. FFS: fire-fighting system	FFS01: fire-fighters station FFS02: pumping station FFS03: storage tank FFS04: fire-hydrant FFS05: pipe
9. EPN: electric power network	EPN01: electric power grid EPN02: generation plant EPN03: substation EPN04: distribution circuits EPN05-09: substation macro-components (autotransformer line; line without transformer; bars-connecting line; bars; cluster) EPN10-23: substation micro-components (circuit breaker; lightning arrester or discharger; horizontal disconnect switch or horizontal sectionalizing switch; vertical disconnect switch or vertical sectionalizing switch; transformer or autotransformer; current transformer; voltage transformer; box or control house; power supply to protection system; coil support; bar support or pothead; regulator; bus; capacitor tank) EPN24: transmission or distribution line
10. GAS: natural gas system	GAS01: production and gathering facility (onshore, offshore) GAS02: treatment plant GAS03: storage tank GAS04: station (compression; metering/pressure reduction; regulator; metering) GAS05: pipeline GAS06: SCADA
11. OIL: oil system	OIL01: production and gathering facility (onshore, offshore) OIL02: refinery OIL03: storage tank farm OIL04: pumping plant OIL05: pipeline OIL06: SCADA

2.3 THE SYNER-G METHODOLOGY

The goal of the general methodology developed within the SYNER-G project is to assess the seismic vulnerability of an infrastructure of urban/regional extension, accounting for inter- and intra-dependencies among infrastructural components, as well as for the uncertainties characterizing the problem. The goal has been achieved setting up a model of the infrastructure and of the hazard acting upon it, and then enhancing it with the introduction of the uncertainty and of the analysis methods that can evaluate the system performance accounting for such uncertainty.

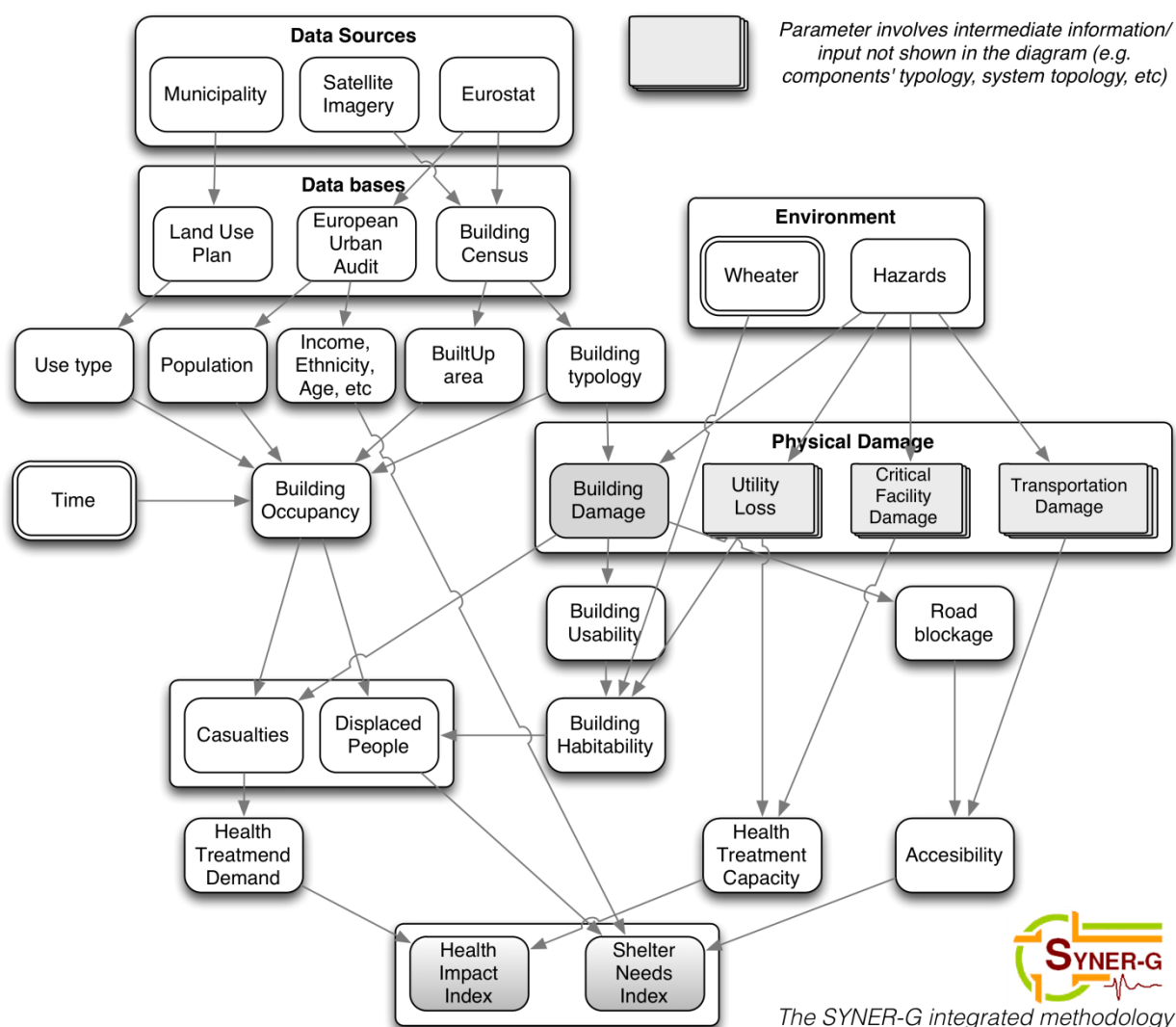


Fig. 2.3 Integrated evaluation of physical and socio-economic performance indicators.

The infrastructure model actually consists of two sets of models: the first set consists of the physical models of the systems making up the infrastructure. These models take as an input the hazards and provide as an output the state of physical/functional damage of the infrastructure. The second set of models consists of the socio-economic models that take among their input the output of the physical models and provide the socio-economic

consequences of the event¹. The SYNER-G methodology integrates these models in a unified analysis procedure. In its final form the entire procedure is based on a sequence of three models: a) seismic hazard model, b) components' physical vulnerability model, and c) system (functional and socio-economic) model.

For illustration purposes, with reference to the two socio-economic models identified and studied within the project (the SHELTER and HEALTH-CARE models), Fig. 2.3 shows in qualitative terms the integrated procedure that leads from the evaluation of the hazard to that of the demands on the shelter and health-care system in terms of Displaced Population and Casualties, down to the assessment of social indexes like the Health Impact and the Shelter Needs. For more details the reader is referred to SYNER-G Reference Report 1 (Franchin 2013).

The conceptual sketch in Fig. 2.3 can be practically implemented by developing:

- A model for the spatially distributed seismic hazard
- A physical model of the Infrastructure
- Socio-economic models

Development of the hazard model has the goal of providing a tool for: a) sampling events in terms of location (epicentre) and possibly extension, magnitude and faulting style according to the seismicity of the study region b) predicting maps of seismic intensities at the sites of the vulnerable components in the infrastructure. These maps, conditional on M, epicentre, etc. should correctly describe the variability and spatial correlation of intensities at different sites. Further, when more vulnerable components exist at the same location and are sensitive to different intensities (e.g. acceleration and displacement), the model should predict intensities that are consistent at the same site.

Development of the physical model starts from the SYNER-G Taxonomy presented in the previous paragraph and requires: a) for each system within the Taxonomy, a description of the functioning of the system under both undisturbed and disturbed conditions (i.e. in the damaged state following an earthquake); b) a model for the physical and functional (seismic) damageability of each component within each system; c) identification of all dependencies between the systems; d) definition of adequate performance indicators for components and systems, and the infrastructure as a whole.

Development of the socio-economic model starts with an interface to outputs from the physical model in each of the four domains of SYNER-G (i.e., buildings, transportation systems, utility systems and critical facilities). Thus, four main performance indicators - Building Usability, Transportation Accessibility, Utility Functionality and Healthcare Treatment Capacity – are used to determine both direct and indirect impacts on society. Direct social losses are computed in terms of casualties and displaced populations. Indirect social losses are considered in two models – Shelter Needs and Health Impact – which employ the multi-criteria decision analysis (MCDA) theory for combining performance indicators from the physical and social vulnerability models.

¹ Within the SYNER-G project physical models have been developed in WP3 and WP5, while socio-economic models were developed in WP4.

In order to tackle the complexity of the described problem the object-oriented paradigm (OOP) has been adopted. In abstract terms, within such a paradigm, the problem is described as a set of objects, characterized in terms of attributes and methods, interacting with each other (see Section 2.3.1). Objects are instances (concrete realizations) of classes (abstract models, or templates for all objects with the same set of properties and methods).

2.3.1 Object-oriented approach

As anticipated, an important choice in the development of the SYNER-G methodology has been to adopt the paradigm of object-oriented modelling. Object-oriented technology is built on a sound engineering foundation, whose elements are collectively called the object model of development or, simply, the object model, which is the conceptual framework for all things object-oriented. The object model encompasses the seven principles or elements of abstraction, encapsulation, modularity, hierarchy, typing, concurrency, and persistence. By themselves, none of these principles are new. What is important about the object model is that these elements are brought together in a synergistic way.

Having a well-defined and expressive notation is important to the process of software development, and more generally to the design of any model. For this reason, the Unified Modelling Language (UML) which is the primary modelling language used to analyze, specify, and design software systems, has been chosen. The UML has numerous types of diagrams, each providing a certain view of your system. One must understand both the structure and the function of the objects involved. One must understand the taxonomic structure of the class objects, the inheritance mechanisms used, the individual behaviours of objects, and the dynamic behaviour of the system as a whole. Amongst various available types of diagrams only two are used within this methodology: the class and the object diagrams.

A class diagram is used to show the existence of classes and their relationships in the logical view of a system. A single class diagram represents a view of the class structure of a system. The two essential elements of a class diagram are classes and their basic relationships. The class icon (used to represent a class in a class diagram) consists of three compartments, with the first occupied by the class name, the second by the properties (or attributes), and the third by the methods (or functions/operations). A name is required for each class and must be unique to its enclosing namespace. Then it is worth noting that there are also abstract classes for which no instances may be created. Classes rarely stand alone. They collaborate with other classes in a variety of ways. The essential connections among classes include association, generalization, aggregation, and composition. Fig. 2.4 shows, for instance, the class diagram for the Hazard class. This class is the *composition* of two *abstract* classes: *man-made* and *natural* hazards. The class Natural contains environmental hazards such as seismic, volcano eruption, floods, etc. The seismic hazard, in turn, is modelled as the composition of three classes: one class for seismo-genetic sources, one for events and the third one for the local intensity at each site. Objects from the SeismicSource class are, as the name suggests, sources that can generate earthquakes. The class SeismicEvent is the class from which earthquakes in terms of localization and magnitude are instantiated. The passage from macro-seismic parameters to intensity values at each site of interest is performed by objects instantiated from the third class LocalIntensity.

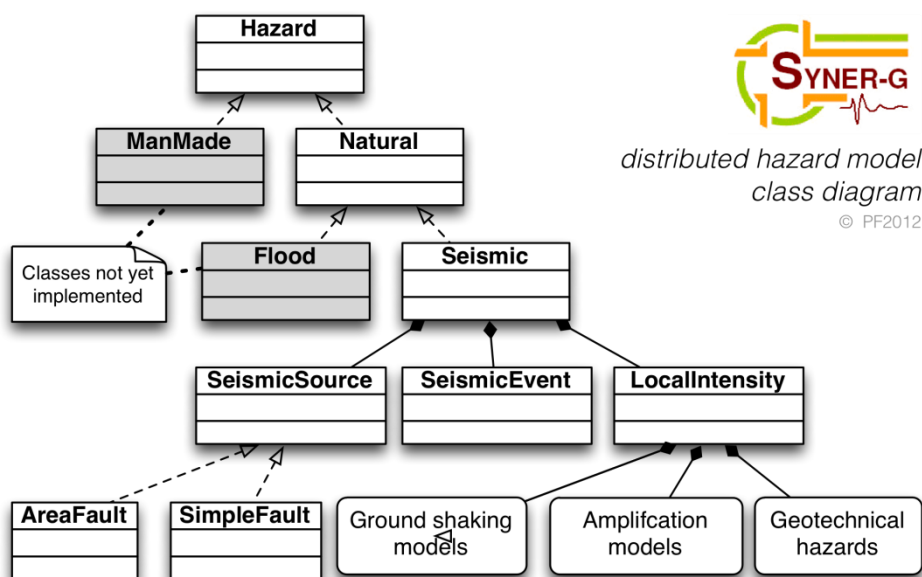


Fig. 2.4 Class diagram for the hazard class (the grey hatch, as indicated, denotes classes that have been included at the conceptual level but have not yet been implemented in the software)

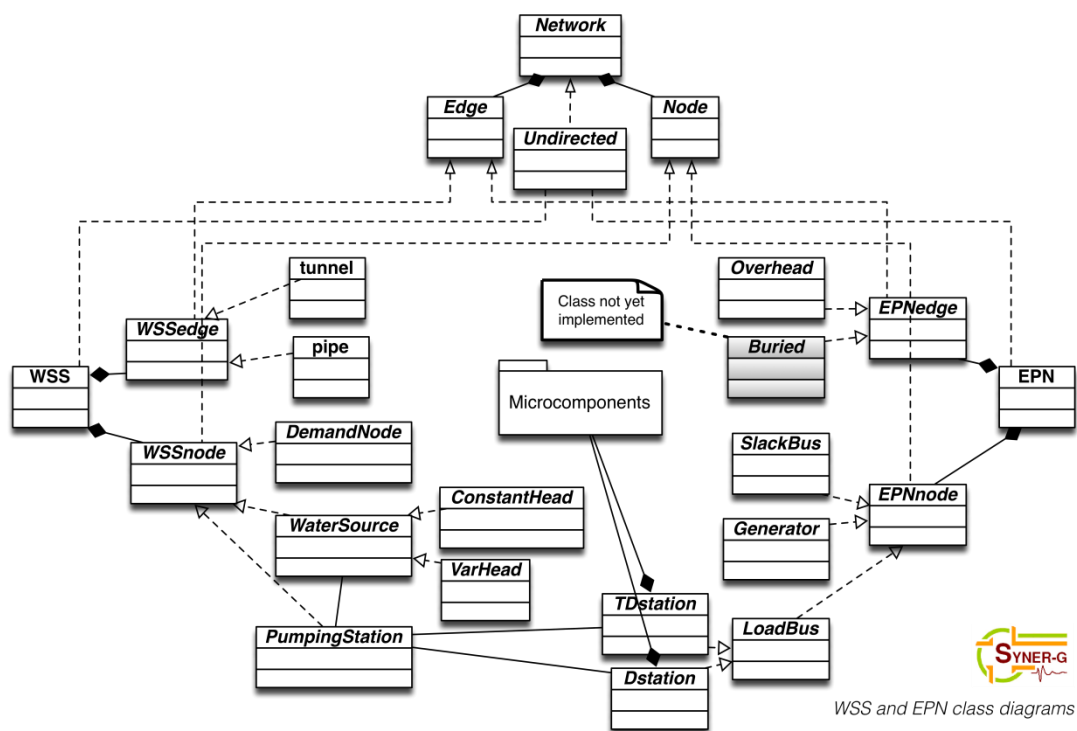


Fig. 2.5 Class diagram for the WSS and EPN classes (the grey hatch denotes classes included at the conceptual level but not yet implemented in the software)

Fig. 2.5 shows another example of class diagram for WSS and EPN classes. Both the WSS and EPN classes are composition of node and link classes. For instance, for the water-

supply system, links can either be pipes or tunnels, while nodes can be end-user demand nodes, water sources or pumping stations. As far as the electric-power network is concerned, links can be either overhead or buried lines, and there three node types: end-user demand nodes (load bus), electric power sources (generator) and a balance node, called the SlackBus, which is usually chosen as one of the power sources and is used as a mathematical expedient to solve the nonlinear alternate current (AC) equations (it provides the balance of flows during iterations in the solution). Load buses can be either distribution (D) or transformation/distribution sub-stations (TD). The two networks are shown in the same figure to highlight the association between the pumping station class in the WSS and the distribution and transformation/distribution classes in the EPN.

While classes are useful to represent all the systems with their high-level relationships, the actual models on which the vulnerability analysis is carried out are not made of them, but, rather, they are collection of objects. To better understand the difference between class and object Fig. 2.6 shows a sample WSS with the corresponding set of objects. For example, the elementary WSS has two sources, a tank and a well (with the associated pump), four demand nodes (two end-users with non-zero demands, and two junctions, which are modelled as demand nodes with zero assigned demand) and a number of connecting elements (five pipe segments and a tunnel). Correspondingly, there are five objects (pipe1 to pipe5) of the class Pipe, one object tunnel of class Tunnel, etc.

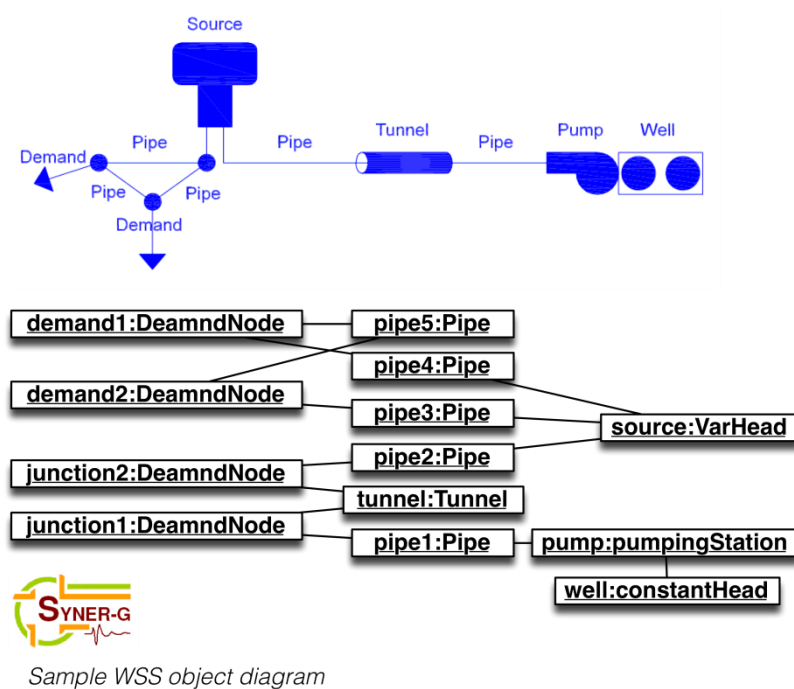


Fig. 2.6 Sample WSS (top) and corresponding object-diagram (bottom)

2.3.2 Infrastructure model

The infrastructure model provides details on the modelling of the physical behaviour of a sub-set of the system from Syner-G taxonomy such as buildings and utilities. It has to be said that a central role is played by the area-like system made up of all residential/commercial/industrial buildings and in general of buildings that are not included among critical facilities. These buildings are where people live, work and consume goods

and services. For this reason this system is the source of demands on all other systems (e.g. electric power and water supply demands, but also casualties to be transported through the road network to health-care facilities, displaced households seeking public shelter, etc.). Further, in terms of economic loss estimation, the largest proportion of direct loss due to physical damage and a considerable one of the indirect (e.g. business interruption) come from damage to these buildings.


Interaction within and between systems can be classified as Physical, Cyber, Geographic, Logical, Societal, Policy-related. Not all of them have been modelled within the methodology. Geographic interactions (physical proximity) are modelled in the seismic case by correctly incorporating within the seismic hazard model the statistical dependence structure between intensities at the same or close sites. Societal interactions are accounted for, e.g. in passing from a potential number of shelter-seeking population to the actual figure, incorporating factors such as anxiety, neighbourhood effects, income, etc.

Table 2.2 reports the interdependencies between some of the systems in the Taxonomy: the i-th row presents the influences of the i-th system on the other systems, while the j-th column collects the influences from other systems on the j-th system. The letter codes stand for: Physical (P), Demand (D) and Geographical (G) interactions. Numbers refer to the following descriptions of the interdependency type:

1. Fires in buildings can be triggered by earthquake induced damage thus raising the water-supply demand on the WSS (when this is not independent of the FFS);
2. In a urban setting, structural damage to buildings produces debris that can cause road blockages;
3. Structural and non-structural damage to buildings may result in casualties that need to be treated in a health-care facility and hence determine the demand on this system;
4. Damage to the EPN can lower the service level in the struck area, possibly below tolerance thresholds thus leading to population displacement and demand on the Shelter model;
5. Damage to the EPN can prevent functioning of pumping stations in the WSS;
6. Damage to the EPN can prevent functioning of re-gasification and regulation/metering stations in the GAS system;
7. Damage to the EPN can prevent functioning of stations in the OIL system;
8. Damage to the EPN can prevent functioning of critical components in the HBR system;
9. Damage to the EPN can prevent power to be fed to the health-care facilities hindering emergency response in case a joint failure of backup power sources occur.
10. Damage to the WSS can lower the service level in the struck area, possibly below tolerance thresholds thus leading to population displacement and demand on the Shelter model;
11. Damage to the WSS can prevent water to be delivered to the health-care facilities hindering emergency response over time in case backup reservoirs are depleted;

12. Damage to the GAS system can lower the service level in the struck area, possibly below tolerance thresholds, especially in adverse weather conditions, thus leading to population displacement and demand on the Shelter model;
13. Damage to the GAS system can stop production in generators within the EPN inducing power shortages;
14. Damage to the GAS system can prevent natural gas to be fed to the health-care facilities hindering emergency response in case backup power sources depend on gas fuel;
15. Damage to the OIL system can stop production in generators within the EPN inducing power shortages;
16. Damage to the transportation network can block access to damaged buildings hindering emergency response;
17. Damage to the transportation network can block access to the HBR preventing goods to be dispatched and causing large economic loss;
18. Damage to the transportation network can block access to health-care facilities hindering emergency response;
19. Demand for transportation (which concur to the determination of the origin-destination matrix that drives traffic flows) of goods is generated in HBR (HBR is an origin);
20. Demand for transportation is generated in HCS (as a destination).

Table 2.2 Interdependencies for sample system from the Taxonomy.



	BDG	EPN	WSS	GAS	OIL	RDN	HBR	HCS
BDG		D	D ₁	D		D G ₂		D ₃
EPN	P ₄		P ₅	P ₆	P ₇		P ₈	P ₉
WSS	P ₁₀							P ₁₁
GAS	P ₁₂	P ₁₃						P ₁₄
OIL		P ₁₅						
RDN	P ₁₆						P ₁₇	P ₁₈
HBR						D ₁₉		
HCS						D ₂₀		

The evaluation of the above interactions requires establishing a sequence of actions and messages between the objects making up the model. This sequence establishes an order in the evaluation of states of the objects, something that is described within UML with a so-called state diagram. Fig. 2.7 presents such a diagram. In any given overall system-of-systems evaluation, an initialization phase is performed first, with the BDG object setting up the region discretization into cells and passing their centroids to the other systems, which in

turn compile a list of tributary cells for each of their demand node and assign this demand node as a reference node to the cells. Demand for goods and services is then evaluated and an analysis of all systems in the pre-earthquake undisturbed conditions is carried out. Then, for all considered events, generation of shake field (local intensities at all relevant locations, i.e. the systems' components sites and cell centroids) is followed by evaluation of: 1) the EPN; 2) all other utilities, with direct damage and possible power losses from the EPN; 3) the BDG, with direct damage and utility loss; 4) the RDN, with demand from the BDG and closures due to direct damage to its elements as well as from road blockages; 5) the HCS with demand from the BDG system, service level from all utilities and accessibility from the RDN.



Sequence of actions to evaluate interactions
(state diagram)

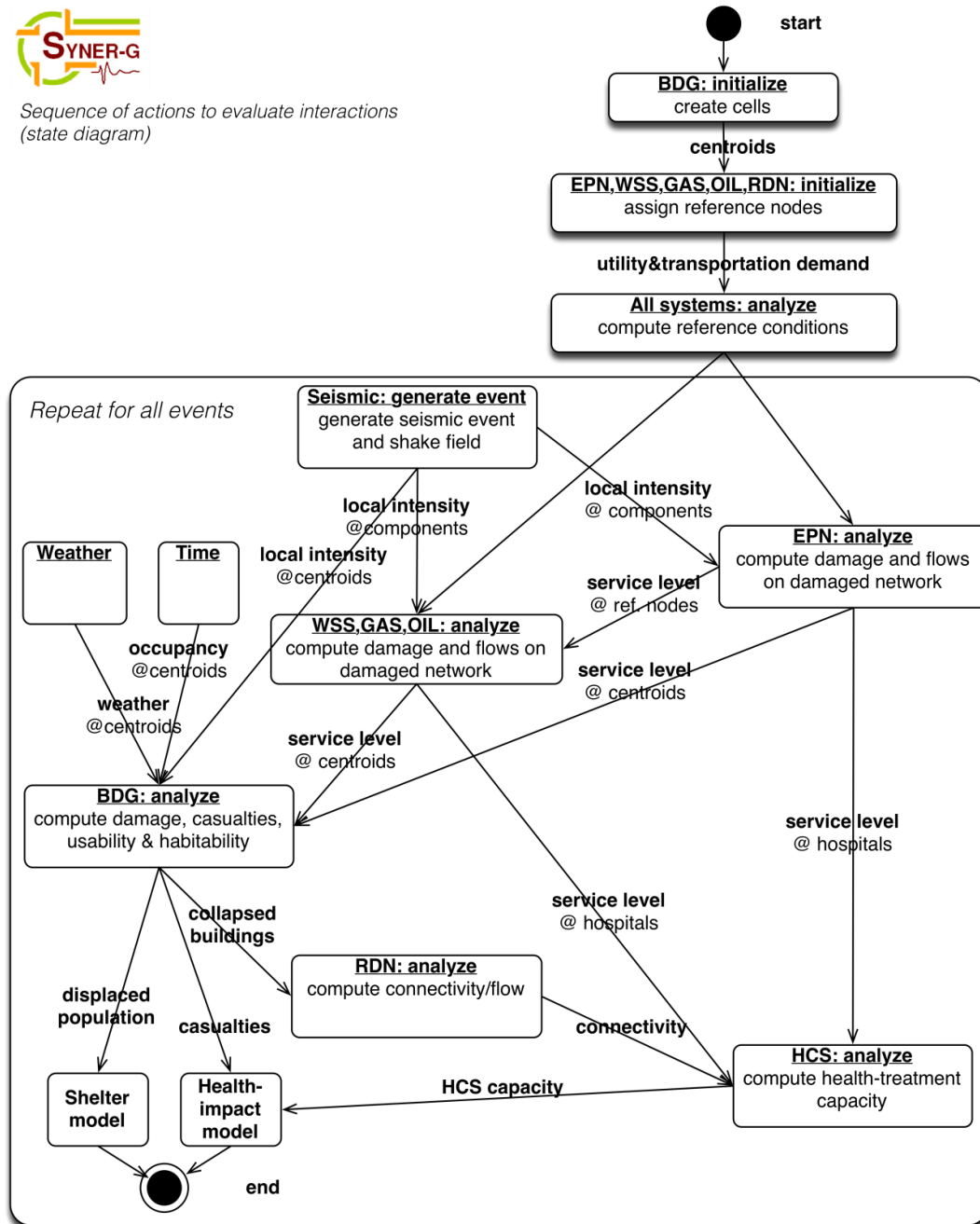


Fig. 2.7 State diagram to model the inter-dependencies: sequence in the evaluation of states of the objects and messages (quantities) transmitted between objects.

To preserve generality of the developed methodology it is paramount to devise a scheme which can accommodate information from the very detailed to the less accurate. In many practical applications there will not be enough data to adopt a modelling approach whereby all physical components are characterized and their functional links are described deterministically.

A distinction is thus made between:

- **Deterministic (hard) links:** direct physical/functional link between components that allow for deterministic evaluation of a system state from a known components' states vector. This is the case, e.g. when one knows the exact topology of an electric power network with enough details on the lines and loads that the system behaviour can be modelled through the governing power flow equations.
- **Non-deterministic (soft) links:** links of "statistical" nature, which describe the probability of a given system state, given the state of its components, or of another system. This links are an additional source of uncertainty that needs to be accounted for in the vulnerability estimation and one that ideally should be removed by improving on the data gathering phase. A typical example of a situation in which such a link is unavoidable, since the required resolution is not compatible with a realistic study, is that of road blockage due to debris.

The goal of the SYNER-G methodology is to assess the performance of the Infrastructure and of all its systems and components, when subjected to a seismic hazard. The quantitative measure of this performance is given by Performance Indicators (PIs), that express numerically either the comparison of a demand with a capacity quantity, or the consequence of a mitigation action, or the assembled consequences of all damages (the "impact"). Performance Indicators can be categorized, according to the level within the hierarchy of the infrastructure to which they refer, into component-level PIs, system-level PIs and system of systems or Infrastructure-level PIs.

2.3.3 Seismic hazard model

The seismic vulnerability assessment of an infrastructure of regional extension requires fragility models for a large number of different components. These fragility models take an intensity measure, scalar or vector, and provide the probability of each damage state. In general multiple different components may share the same site. Thus, in order to assess the damage state of the infrastructure for any given event, it is necessary to predict a vector of IMs at all sites where one or more vulnerable components are present. This is the purpose of the seismic hazard model. The vector $\mathbf{s} = \left\{ \mathbf{s}_1 \rightleftharpoons \mathbf{s}_n \right\}$ of length $m = \sum m_i$, where \mathbf{s}_i is the vector of length m_i of seismic IMs at the i -th site, exhibits a variable degree of statistical dependence between its components, decaying with the distance between the sites, and usually larger between the components within each \mathbf{s}_i (zero distance). The hazard model provides tools to sampling events in terms of location (epicentre) and possibly extension, magnitude and faulting style according to the seismicity of the study region and tools to predicting maps of seismic intensities at the sites of the vulnerable components in the infrastructure. These maps, conditional on M , epicentre, etc. should correctly describe the variability and spatial correlation of intensities at different sites.

Moreover, in modelling the seismic risk to lifeline systems, the consideration of hazard from permanent deformation of the ground (PGD_f) is paramount. For pipelines and similar systems with linear elements, fragility models are generally given in terms of PGD_f , as they are most vulnerable to the permanent displacements of the ground rather than transient shaking. For application within SYNER-G, four primary causes of permanent ground displacement are considered: liquefaction-induced lateral spread, liquefaction-induced settlement, slope displacement and coseismic fault rupture.

2.3.4 Probabilistic analysis

The uncertainties entering the regional seismic vulnerability analysis are summarized below:

- Seismic activity of the seismo-genetic sources/faults (modelled through magnitude-recurrence laws and explained in report D2.13, Weatherhill et al. 2011b);
- Local seismic intensities at the sites (modelled through ground-motion prediction equations, spatial correlation models, cross-IM correlation models and site amplification models, and explained in report D2.13, Weatherhill et al. 2011b);
- Physical damageability of the components of the infrastructure (modelled by fragility models, e.g. as reported in chapter 3 and Reference Report 4, Kaynia 2013);
- Uncertainty in the functional consequences at component and/or system level of the physical damage at the component level;
- Uncertainty in the socio-economic consequences of physical damage (non-structural components fragility models, probabilistic cost models, etc, Reference Report 5, Khazai 2013);
- Epistemic uncertainty in all the above models.

The goal of the analysis is to evaluate probabilities or mean annual rates of events E defined in terms of performance-indicators of the types of infrastructure. This requires the joint probability model (distribution) of all the above uncertainties, denoted by $f(\mathbf{x})$, where \mathbf{x} is the vector that collects all random variables in the problem. The latter variables form a sequence of cause and effect and this sequence can be represented graphically in the form of a directed acyclic graph, which illustrates the flow from the rupturing fault/source, to event location and magnitude, the local intensities, the components' state of physical damage, the functional consequences at system-level and finally the value of the performance indicators at the highest, Infrastructure, level. In Reference Report 1 (Franchin 2013) the directed acyclic graph is explained in detail. Additional uncertainty in the results of the analysis comes from the epistemic uncertainty on the models and it can be considered by setting up a logic tree of model alternatives. Finally also the soft links can be included as additional random terms that enter in the relation between the physical damage state D and the performance PI . Notwithstanding this the SYNER-G software toolbox written to illustrate the methodology in its current stage of development does not account for the epistemic uncertainties in the models, or for the soft links. Moreover it has to be noted that the uncertainty related to the socio-economic portion of the integrated model is not represented, nor included yet.

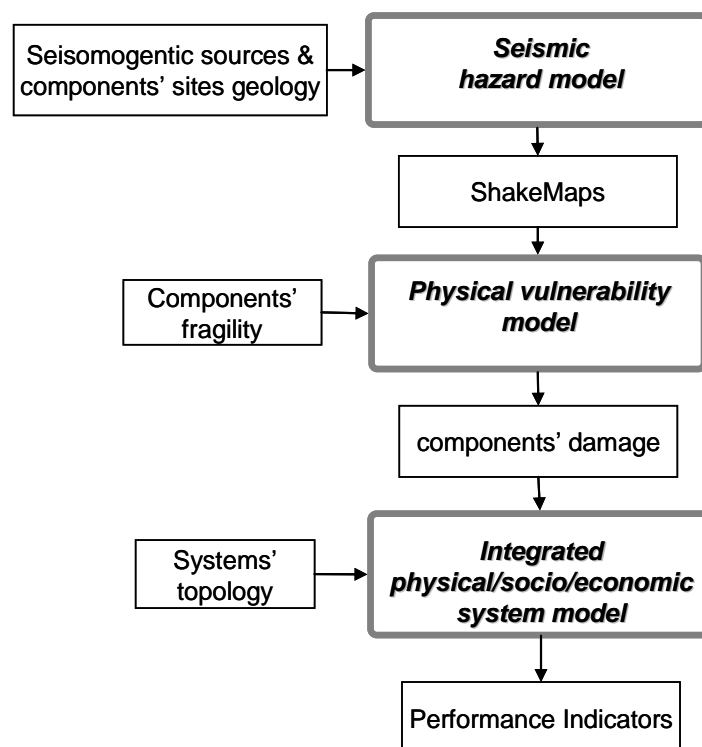


Fig. 2.8 The sequence of models with associated input and output quantities.

Fig. 2.8 summarizes in very general terms what are the inputs and outputs exchanged by the three models for hazard, physical vulnerability and systemic consequences. Probabilistic evaluation of the performance of the infrastructure can be carried out with different methods (for instance, simulation methods or non-simulation methods). Simulation methods have been adopted and implemented within the SYNER-G software toolbox due to the fact that simulation is a robust way to explore the behaviour of systems of any complexity. Pragmatically, with the current state of knowledge in mind, the option adopted within the SYNER-G project to deal with the uncertainty is to resort to simulation methods and to reduce the required number of system evaluations by using advanced variance reduction techniques in order to arrive at probability estimates of the performances of interest.

The developed methodology is implemented in the SYNER-G software toolbox. It is coded in Matlab and the user interface (EQVis platform) is based on the software MAEviz which is a seismic risk assessment software developed by the Mid-America Earthquake (MAE) Center and the National Center for Supercomputing Applications (NCSA).

3 SYNER-G fragility curves for all elements at risk

3.1 INTRODUCTION

3.1.1 Background

The vulnerable conditions of a structure can be described using vulnerability functions and/or fragility functions. According to one of possible conventions, vulnerability functions describe the probability of losses (such as social losses or economic losses) given a level of ground shaking, whereas fragility functions describe the probability of exceeding different limit states (such as damage or injury levels) given a level of ground shaking. Fig. 3.1 shows examples of vulnerability and fragility functions. The former relates the level of ground shaking with the mean damage ratio (e.g. ratio of cost of repair to cost of replacement) and the latter relates the level of ground motion with the probability of exceeding the limit states. Vulnerability functions can be derived from fragility functions using consequence functions, which describe the probability of loss, conditional on the damage state.

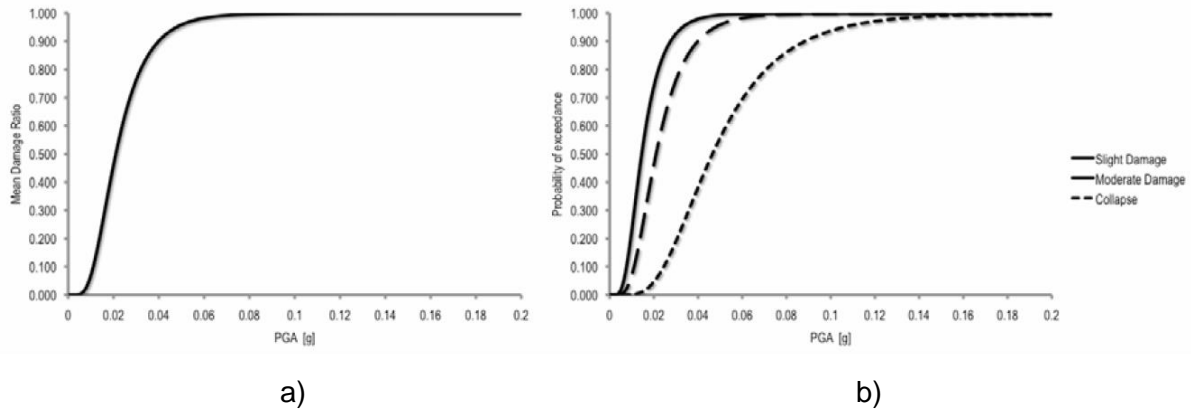


Fig. 3.1 Examples of (a) vulnerability function and (b) fragility function

Fragility curves constitute one of the key elements of seismic risk assessment. They relate the seismic intensity to the probability of reaching or exceeding a level of damage (e.g. minor, moderate, extensive, collapse) for each element at risk. The level of shaking can be quantified using different earthquake intensity parameters, including peak ground acceleration/velocity/displacement, spectral acceleration, spectral velocity or spectral displacement. They are often described by a lognormal probability distribution function as in Eq. 3.1, although it is noted that this distribution may not always be the best fit.

$$P_f(ds \geq ds_i | IM) = \Phi \left[\frac{1}{\beta_{tot}} \cdot \ln \left(\frac{IM}{IM_{mi}} \right) \right] \quad (3.1)$$

where $P_i(\cdot)$ is the probability of being at or exceeding a particular damage state, DS , for a given seismic intensity level defined by the earthquake intensity measure, IM (e.g. peak ground acceleration - PGA), Φ is the standard cumulative probability function, IM_{mi} is the median threshold value of the earthquake intensity measure IM required to cause the i_{th} damage state and β_{tot} is the total standard deviation. Therefore, the development of fragility curves according to Eq. 3.1 requires the definition of two parameters, IM_{mi} and β_{tot} .

3.1.2 Derivation of fragility curves

Several approaches can be used to establish the fragility curves. They can be grouped under empirical, judgmental, analytical and hybrid. Empirical methods are based on past earthquake surveys. The empirical curves are specific to a particular site because they are derived from specific seismo-tectonic and geotechnical conditions and properties of the damaged structures. Judgment fragility curves are based on expert opinion and experience. Therefore, they are versatile and relatively fast to derive, but their reliability is questionable because of their dependence on the experiences of the experts consulted.

Analytical fragility curves adopt damage distributions simulated from the analyses of structural models under increasing earthquake loads as their statistical basis. Analyses can result in a reduced bias and increased reliability of the vulnerability estimates for different structures compared to expert opinion (Rossetto and Elnashai, 2003). Analytical approaches are becoming ever more attractive in terms of the ease and efficiency by which data can be generated. The above methods are further described in Reference Report 4 (Kaynia 2013).

3.1.3 Typology

The key assumption in the vulnerability assessment of buildings and lifeline components is that structures having similar structural characteristics, and being in similar geotechnical conditions, are expected to perform in the same way for a given seismic loading. Within this context, damage is directly related to the structural properties of the elements at risk. Typology is thus a fundamental descriptor of a system, derived from the inventory of each element. Geometry, material properties, morphological features, age, seismic design level, anchorage of the equipment, soil conditions, foundation details, etc. are among usual typology descriptors/parameters.

The knowledge of the inventory of a specific structure in a region and the capability to create classes of structural types (for example with respect to material, geometry, design code level) are among the main challenges when carrying out a seismic risk assessment. The first step should be the creation of a reasonable taxonomy that is able to classify the different kinds of structures in the system. In case of buildings and bridges, different typology schemes have been proposed in the past studies. The typological classifications for other lifeline elements are more limited due to the lack of detailed inventory data and less variability of structural characteristics.

3.1.4 Performance levels

In seismic risk assessment, the performance levels of a structure can be defined through damage thresholds called limit states. A limit state defines the boundary between different damage conditions, whereas the damage state defines the damage condition itself. Different damage criteria have been proposed depending on the typology of element at risk and the

approach used for the derivation of fragility curves. The most common way to define earthquake consequences is a classification in terms of the following damage states: No damage; slight/minor; moderate; extensive; complete. This qualitative approach requires an agreement on the meaning and the content of each damage state. Methods for deriving fragility curves generally model the damage on a discrete damage scale. In empirical procedures, the scale is used in reconnaissance efforts to produce post-earthquake damage statistics and is rather subjective. In analytical procedures the scale is related to limit state mechanical properties that are described by appropriate indices as for example displacement capacity in case of buildings.

3.1.5 Intensity measures

A main issue related to the fragility curves is the selection of appropriate earthquake intensity measure (IM) that characterizes the strong ground motion and best correlates with the response of each element. Several measures of the strength of ground motion (IMs) have been developed. Each intensity measure may describe different characteristics of the motion, some of which may be more adverse for the structure or system under consideration. The use of a particular IM in seismic risk analysis should be guided by the extent to which the measure corresponds to damage to local elements of a system or the global system itself. Optimum intensity measures are defined in terms of practicality, effectiveness, efficiency, sufficiency, robustness and computability (Cornell, 2002; Mackie and Stojadinovich, 2003; 2005).

Practicality refers to the recognition that the IM has some direct correlation to known engineering quantities and that it “makes engineering sense” (Mackie and Stojadinovich, 2005; Mehanny, 2009). The practicality of an IM may be verified analytically via quantification of the dependence of the structural response on the physical properties of the IM (e.g. energy, response of fundamental and higher modes, etc). It may also be verified numerically by interpretation of the response of the structure under non-linear analysis using existing time histories.

Sufficiency describes the extent to which the IM is statistically independent of ground motion characteristics such as magnitude and distance (Padgett et al., 2008). A sufficient IM is one that renders the structural demand measure conditionally independent of the earthquake scenario. This term is more complex and is often at odds with the need for computability of the IM. Sufficiency may be quantified via statistical analysis of the response of a structure for a given set of records.

The *effectiveness* of an IM is determined by its ability to evaluate its relation with an engineering demand parameter (EDP) in closed form (Mackie and Stojadinovich, 2003), so that the mean annual frequency of a given decision variable exceeding a given limiting value (Mehanny, 2009) can be determined analytically.

The most widely used quantitative measure from which an optimal IM can be obtained is *efficiency*. This refers to the total variability of an engineering demand parameter for a given IM (Mackie and Stojadinovich, 2003; 2005).

Robustness describes the efficiency trends of an IM-EDP pair across different structures, and therefore different fundamental period ranges (Mackie and Stojadinovich, 2005; Mehanny, 2009). Readers are referred to Deliverable 2.12 (Weatherhill et al. 2011a) for a description of these parameters and further references.

In general two main classes exist: empirical intensity measures and instrumental intensity measures. With regards to the empirical IMs, different macroseismic intensity scales could be used to identify the observed effects of ground shaking over a limited area. As regards the instrumental IMs, the severity of ground shaking can be expressed as an analytical value measured by an instrument or computed by analysis of recorded accelerograms.

The selection of the intensity parameter is also related to the approach that is followed for the derivation of fragility curves and the typology of element at risk. For example, as the empirical curves relate the observed damages with the seismic intensity, the latter may be described based on intensity of records of seismic motions, and thus PGA, peak ground velocity (PGV) or spectral acceleration (S_a) may be suitable IMs. On the other hand, the spatial distribution of PGA values is easier to be estimated through simple or advanced methods within a seismic hazard study of a specific area (e.g. Esposito and Iervolino, 2011a). When the vulnerability of elements due to ground failure is examined (i.e. liquefaction, fault rupture, landslides) permanent ground deformation (PGD) is the most appropriate IM.

3.1.6 Performance indicators

The ultimate goal of aseismic risk assessment methodology is to assess the performance (or the expected loss) of the infrastructure and all its systems and components when subjected to a seismic hazard. The quantitative measure of this performance is given by Performance Indicators (PIs). PIs express numerically either the comparison of a demand with a capacity quantity, or the consequence of a mitigation action, or the accumulated consequences of all damages (the “impact”). The functionality of each component and therefore its performance is directly related with the expected damage levels.

3.1.7 Treatment of uncertainties

Several uncertainties are introduced in the parameters of fragility curves, as well as in the relationship between physical damage state and the performance (PI) of the element at risk. The uncertainties are usually categorized in aleatory and epistemic. Aleatory uncertainty is presumed to be due to the intrinsic randomness of a phenomenon. An epistemic uncertainty is presumed to be caused by lack of knowledge (or data). The reason for having this distinction within an engineering analysis model is that the lack-of-knowledge-part of the uncertainty can be represented in the model by introducing auxiliary non-physical variables. These variables capture information obtained through the gathering of more data or use of more advanced scientific principles (Der Kiureghian and Ditlevsen, 2009).

In general, the uncertainty of the fragility parameters is estimated through the standard deviation, β_{tot} , that describes the total variability associated with each fragility curve. Three primary sources of uncertainty are usually considered (NIBS, 2004), namely the definition of damage states, β_{DS} , the response and resistance (capacity) of the element, β_C , and the earthquake input motion (demand), β_D . The total variability is modelled by the combination of the three contributors, assuming that they are stochastically independent and lognormally distributed random variables using Eq. (3.2):

$$\beta_{tot} = \sqrt{\beta_{DS}^2 + \beta_C^2 + \beta_D^2} \quad (3.2)$$

3.1.8 Relation with socio-economic losses

One of the aims in SYNER-G has been to develop a unified approach for modelling socio-economic impacts caused by earthquake damage which integrates social vulnerability into the physical systems modelling approaches. In many earthquake loss estimation models socio-economic losses are computed as linear damage-consequence functions without consideration of social vulnerability. Contributing to the challenge of integrating social vulnerability with physical damage/performance models is the fact that social vulnerability is a fundamentally relative phenomenon and not something that can be directly observed and measured.

In SYNER-G, social losses (e.g., number of displaced people and casualties) are computed as an integrated function of hazard intensity, vulnerability of physical systems (through fragility curves) and the social vulnerability of the population at risk. The integrated approach proposed in SYNER-G provides a framework to link the degree of damage and performance of physical systems to vulnerabilities and coping capacities in society to assess: (1) Impacts on displaced populations and their shelter needs, and (2) Health impacts on exposed populations and their health-care needs. This way of conceptualizing the integrated framework emphasizes the importance of understanding the interrelations between physical and social systems. In other words, how direct physical losses can potentially aggravate existing vulnerabilities in society and how vulnerabilities in society can ultimately lead to greater impacts from physical damage and loss.

Thus, one of the main objectives has been the adoption of an indicator system and common nomenclature which posits social vulnerability in relation to the vulnerability of the physical system. For example, the number of displaced persons is not computed as a function of damaged buildings alone, but derived as a function of the habitability of buildings (defined by the tolerance to utility loss for different levels of building damage and weather conditions); and a set of key socio-economic indicators influencing a population to leave their homes and seek or not seek public shelter.

3.1.9 Main results

One of the main contribution of SYNER-G is the compilation of the existing fragility curves/functions and development of new functions for all the system elements based on the taxonomy/typology that has been derived in the framework of the SYNER-G project. A literature review on the typology, the fragility functions (analytical/empirical/expert judgment/hybrid), damage scales, intensity measures and performance indicators has been performed for all the elements. The fragility functions are based on new analyses and collection/review of the results that are available in the literature. In some cases, the selection of the fragility functions has been based on validation studies using damage data from past and recent earthquakes mainly in Europe. Moreover, the damage and serviceability states have been defined accordingly. Appropriate adaptations and modifications have been made to the selected fragility functions in order to satisfy the distinctive features of the presented taxonomy. In other cases new fragility functions have been developed based on numerical solutions or by using fault tree analysis together with the respective damage scales and serviceability rates in the framework of European typology and hazard.

A fragility function manager tool² has been developed for buildings and bridges and is connected with the SYNER-G software platform. This tool is able to store, visualize, harmonise and compare a large number of fragility functions sets. For each fragility function set, the metadata of the functions, representative plots and the parameters of the functions can be visualized in an appropriate panel or window. Once the fragility functions are uploaded, the tool can be used to harmonise and compare the curves. The harmonisation module allows one to harmonise the curves using a target intensity measure type and a number of limit states of reference. After the harmonisation, the comparison module can be used to plot together and to compare different functions, which can then be extracted and the mean and dispersion of the parameters of the curves can be calculated. In Fig. 3.2 the screenshot of the main window of the tool is presented together with a brief description of its principal panels.

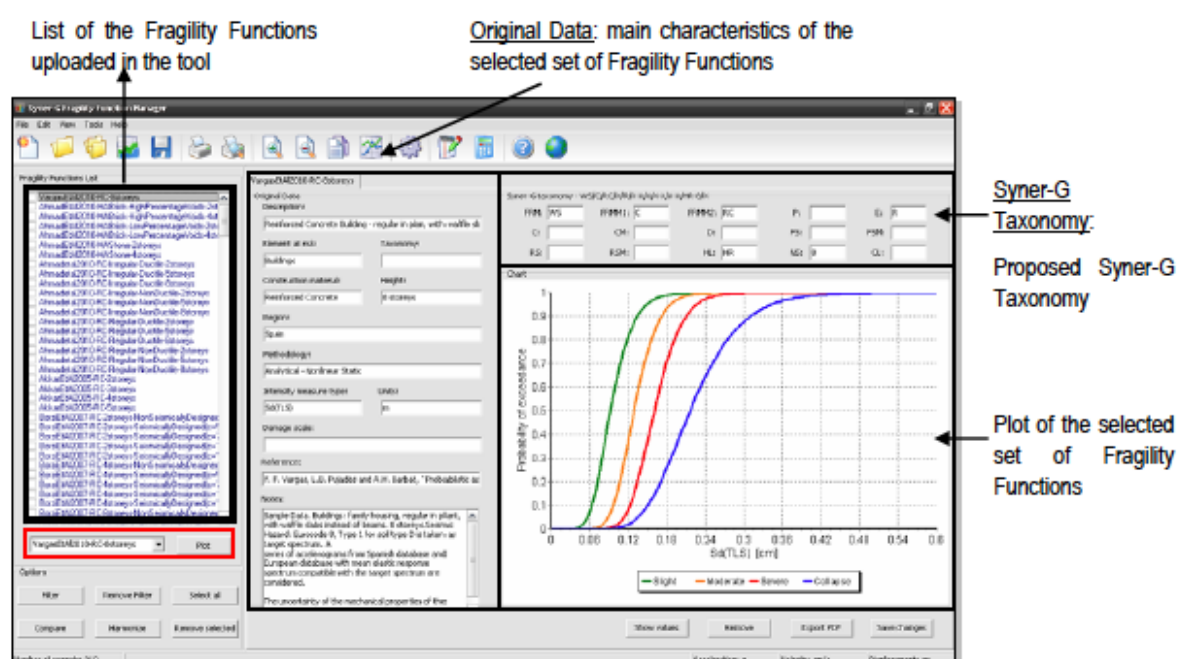


Fig. 3.2 Screenshot of the main window of the Fragility Function Manager tool

In the next sections, the proposed fragility functions for buildings, utility networks, transportation infrastructures and critical facilities along with the typology classification of each component are summarized. For more details the reader is referred to SYNER-G Reference Report 4 (Kaynia 2013).

3.2 FRAGILITY CURVES FOR BUILDINGS

3.2.1 Introduction

The identification of the seismic fragility functions for common building types is a fundamental component of a seismic risk loss assessment model and many research studies have addressed this topic in the recent past.

In the context of the SYNER-G Project, the main typologies of buildings in Europe have been identified and, focusing on reinforced concrete and masonry buildings, the existing fragility functions have been reviewed with the objective of homogenizing the existing model building types (through a new taxonomy, called the SYNER-G taxonomy) and comparing these functions amongst themselves. The main output is a set of fragility functions (with associated uncertainty) for the main reinforced concrete and masonry typologies present in Europe.

To allow for this comparison the fragility curves have been harmonized to the same intensity measure, the same number of limit states and the same building typology using the Fragility Function Manager tool. Examples of the resulting set of fragility functions (with associated uncertainties) for the main reinforced concrete and masonry typologies common in Europe are presented below. For further details, the reader is referred to Reference Report 4, (Kaynia 2013).

3.2.2 SYNER-G Taxonomy

A new taxonomy was developed in the SYNER-G project for RC and masonry buildings, as described below. It has the aim of allowing European building typologies to be classified by the users based on the same underlying classification scheme.

Different main categories have been identified to describe a building. These are presented in Table 3.1 and include such features as the lateral force resisting mechanism, material, elevation, cladding, etc. It has to be noted that a hierarchy is used for some categories where additional information might or might not be available. For example, the material is masonry but a user may or may not know whether it is reinforced or unreinforced, fired brick or stone. In the case of RC, for instance, the user may or may not know the type of concrete (e.g. high, average or low strength) or the kind of reinforcements (e.g. smooth or non-smooth rebars). In both cases the definition of the second (unknown) parameter is optional.

Table 3.1 SYNER-G Taxonomy for buildings

CATEGORY	SUB-CATEGORY
Force Resisting Mechanism (FRM1) <ul style="list-style-type: none"> • Moment Resisting Frame (MRF) • Structural Wall (W) • Flat Slab (FS) • Bearing Walls (BW) • Precast (P) • Confined Masonry (CM) 	Force Resisting Mechanism (FRM2) <ul style="list-style-type: none"> • Embedded beams (EB) • Emergent beams (EGB)
FRM Material (FRMM1) <ul style="list-style-type: none"> • Concrete (C) 	FRM Material (FRMM2) <ul style="list-style-type: none"> • Reinforced Concrete (RC)

CATEGORY	SUB-CATEGORY
<ul style="list-style-type: none"> Masonry (M) 	<ul style="list-style-type: none"> Unreinforced Masonry (URM) Reinforced Masonry (RM) High strength concrete (>50MPa) (HSC) Average strength concrete (20-50 MPa) (ASC) Low strength concrete (<20 MPa) (LSC) Adobe (A) Fired brick (FB) Hollow clay tile (HC) Stone (S) High yield strength reinforcing bars (>300MPa) (HY) Low yield strength reinforcing bars (<300MPa) (LY) Classification of reinforcing bars based on EC2 (A,B,C) Lime mortar (LM) Cement mortar (CM) Mud mortar (MM) Smooth rebars (SB) Non-smooth rebars Concrete Masonry Unit (CMU) Autoclaved Aerated Concrete (AAC) High % of voids (H%) Low % of voids (L%) Regular Cut (Rc) Rubble (Ru)
Plan (P) <ul style="list-style-type: none"> Regular (R) Irregular (IR) 	
Elevation (E) <ul style="list-style-type: none"> Regular geometry (R) Irregular geometry (IR) 	
Cladding (C) <ul style="list-style-type: none"> Regular infill vertically (RI) Irregular infill vertically (IRI) Bare (B) 	Cladding Characteristics (CM) <ul style="list-style-type: none"> Fired brick masonry (FB) High % voids (H%) Low % voids (L%) Autoclaved Aerated Concrete (AAC) Precast concrete (PC) Glazing (G) Single layer of cladding (SL) Double layer of cladding (DL) Open first floor (Pilotis) (P) Open upper floor (U)
Detailing (D) <ul style="list-style-type: none"> Ductile (D) 	

CATEGORY	SUB-CATEGORY
<ul style="list-style-type: none"> Non-ductile (ND) With tie rods/beams (WTB) Without tie rods/beams (WoTB) 	
Floor System (FS) <ul style="list-style-type: none"> Rigid (R) Flexible (F) 	Floor System Material (FSM) <ul style="list-style-type: none"> Reinforced concrete (RC) Steel (S) Timber (T)
Roof System (RS) <ul style="list-style-type: none"> Peaked (P) Flat (F) Gable End Walls (G) 	Roof System Material (RSM) <ul style="list-style-type: none"> Timber (Ti) Thatch (Th) Corrugated Metal Sheet (CMS)
Height Level (HL) <ul style="list-style-type: none"> Low-rise (1-3) (L) Mid-rise (4-7) (M) High-rise (8-19) (H) Tall (20+)(Ta) 	Number of stories (NS) [Here the number of stories is explicitly given, if known]
Code Level (CL) <ul style="list-style-type: none"> None (NC) Low (<0.1g) (LC) Moderate (0.1-0.3g) (MC) High (>0.3g) (HC) 	

The building typology is defined using the label put in the brackets for each parameter within a given category.

Example: FRM1-FRM2/FRMM1-FRMM2/P/E/C-CM/D/FS-FSM/RS-RSM/HL-NS/CL

More than one label can be used for the category separated by a dash. For example, a building with moment resisting frames and walls (i.e. dual system) would be MRF-W, a building with mixed construction of reinforced concrete and masonry would be RC-M. Not all categories need to be defined due to the fact that there might be lack of information about the structure. In this case, where information is unknown, an X symbol is used. Three examples are shown below:

- MRF/C-RC/X/X/RI-FB-H%/ND/R-RC/X/L-2/NC: moment resisting frame, in reinforced concrete with regular external infill panels in brick with a high percentages of voids, with non-ductile design details, with rigid reinforced concrete floor, low-rise, 2 storeys, not designed to a seismic code;
- CM/M-RM/R/R/RI-FB/ND/F-T/X/L-2/MC: structure in confined reinforced masonry characterized by regular layout in both plan and elevation with regular brick cladding, with non-ductile design, flexible timber floor, low-rise, 2 storeys, designed for moderate seismic code;
- BW/M/X/X/X/X/X/L/X: low-rise masonry bearing wall structure.

The proposed taxonomy is constructed with a modular structure. In this way, other categories and sub-categories can easily be added and all the different kinds of European

buildings can be taken into account. Subsequently, additional categories for describing the non-structural elements might be added in the future.

3.2.3 Examples of proposed fragilities

3.2.3.1 RC Buildings (FRMM1)

In the fragility function manager tool there are up to 400 fragility functions. In the following, four examples show in detail the capability of the tool and how it can be used for comparison between different literature studies. The selected examples going from a lower level of detail (reinforced concrete building with mid-rise) to a higher level of detail (reinforced concrete building with mid-rise, seismically designed, bare and non-ductile). The examples are from deliverable D3.1 (Crowley et al. 2011).

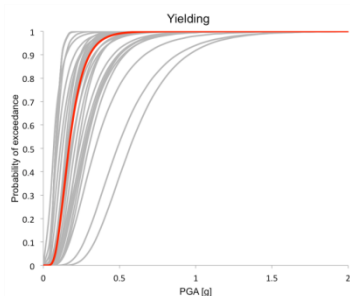
For each reinforced concrete buildings class, in Fig. 3.3 below are shown the mean curve (in red) and the individual fragility functions (in grey), whilst in the following tables are reported the mean and coefficient of variation (c_v) of the lognormal parameters of the fragility functions (i.e. logarithmic mean and logarithmic standard deviation).

Table 3.2. Description of building types, taxonomy and available number of fragility curves

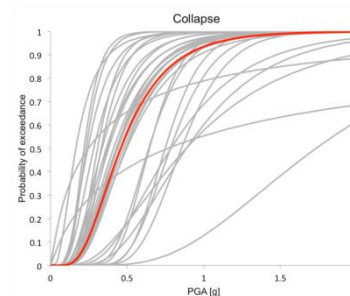
RC buildings	SYNER-G taxonomy	Number of fragility curves
mid-rise building with moment resisting frame	MRF/C/RC/X/X/X/X/X/X/MR/X	32 sets
mid-rise building with moment resisting frame with lateral load design	MRF/C/RC/X/X/X/X/X/X/MR/C	20 sets
mid-rise building with bare moment resisting frame with lateral load design	MRF/C/RC/X/X/B/X/X/X/MR/C	15 sets
mid-rise building with bare non-ductile moment resisting frame with lateral load design	MRF/C/RC/X/X/B/ND/X/X/MR/C	9 sets

Table 3.3 Mean and c_v of lognormal fragility parameters for reinforced concrete buildings.

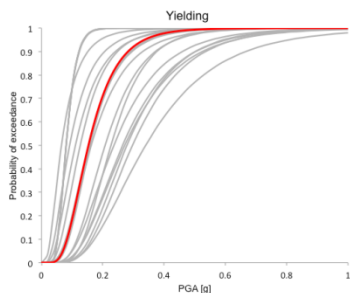
RC buildings		Yielding		Collapse	
		Logarithmic Mean	Logarithmic Standard Deviation	Logarithmic Mean	Logarithmic Standard Deviation
mid-rise building with moment resisting frame	Mean	-1.853	0.481	-0.879	0.452
	c_v (%)	26	19	48	23
mid-rise building with moment resisting frame with lateral load design	Mean	-1.876	0.476	-0.738	0.430
	c_v (%)	28	21	67	28
mid-rise building with bare moment resisting frame with lateral load design	Mean	-1.939	0.458	-0.821	0.452
	c_v (%)	28	23	64	25
mid-rise building with bare non-ductile moment resisting frame with lateral load design	Mean	-1.832	0.474	-1.091	0.485
	c_v (%)	33	21	48	24



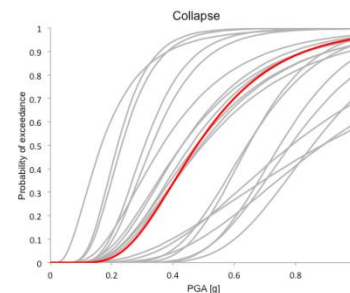
(a) with moment resisting frame



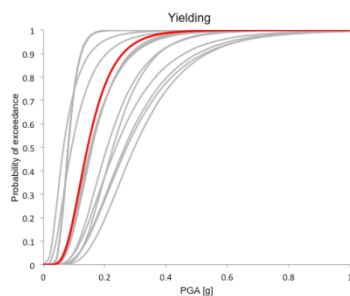
(b) with moment resisting frame



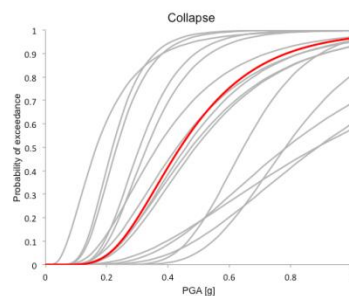
(c) with moment resisting frame with lateral load design



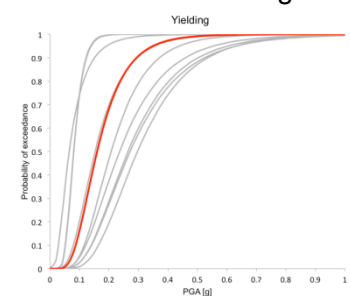
(d) with moment resisting frame with lateral load design



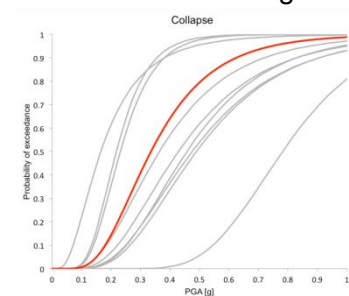
(e) with bare moment resisting frame with lateral load design



(f) with bare moment resisting frame with lateral load design



(g) with bare non-ductile moment resisting frame with lateral load design



(h) with bare non-ductile moment resisting frame with lateral load design

Fig. 3.3 Mean curve for yielding limit state in left column (a, c, e, g) and collapse limit state in right column (b, d, f, h) for reinforced concrete buildings

3.2.3.2 Masonry Buildings (FRMM1)

Below follow two examples for masonry building classes (low-rise and midrise). For each masonry building class, in Fig. 3.4 below are shown the mean curve and the individual fragility functions, whilst in the following tables are reported the mean and coefficient of variation (c_v) of the lognormal parameters of the fragility functions (i.e. logarithmic mean and logarithmic standard deviation).

Table 3.4 Mean and c_v of lognormal fragility parameters for low-rise masonry buildings

Masonry buildings		Yielding		Collapse	
		Logarithmic Mean	Logarithmic Standard Deviation	Logarithmic Mean	Logarithmic Standard Deviation
Low-rise building	Mean	-2.029	0.572	-1.320	0.552
	c_v (%)	19	16	28	24
mid-rise building	Mean	-2.417	0.587	-1.5984	0.5732
	c_v (%)	17	16	24	21

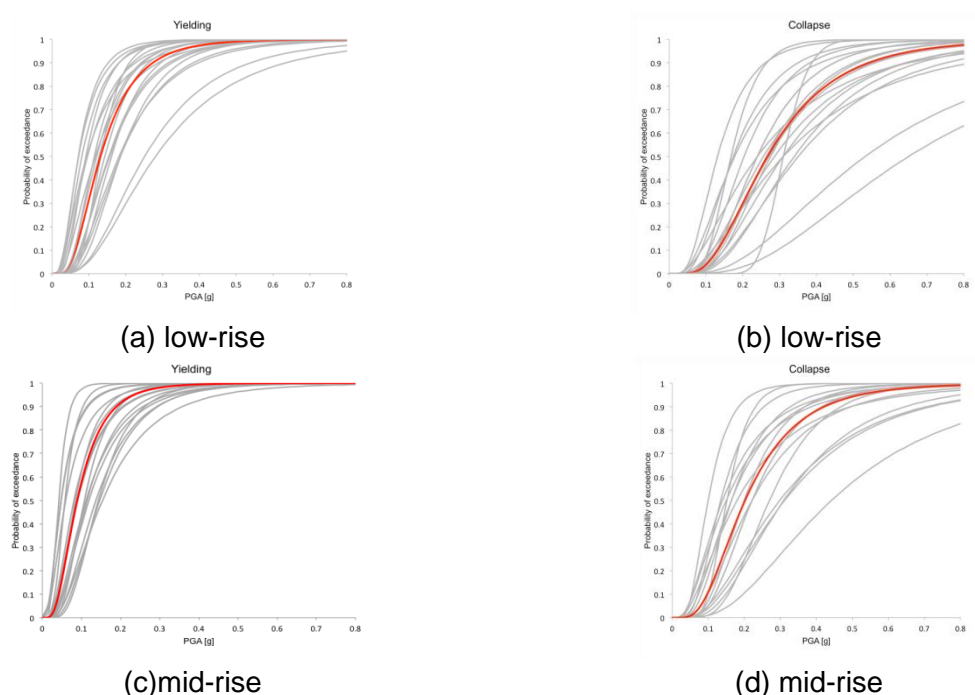


Fig. 3.4 Mean curve for yielding limit state (a) and collapse limit state (b) for masonry buildings

3.3 FRAGILITY CURVES FOR LIFELINES

Lifelines consist of utilities that supply energy (electric or fossil fuels), water, waste water, telecommunication, and infrastructure (ports, roads, and railroads) that allow for transportation between and within cities. All human activities depend on the complex networks of lifelines. Naturally it is of high importance to assess and reduce the seismic risk of lifelines.

From earthquake risk assessment viewpoint, lifelines consist of combination point wise and distributed objects that have different seismic vulnerabilities. Below follows a description of the different types of lifelines, proposed taxonomies and examples of fragility functions.

3.3.1 Electric power network

Electric power networks are very complex systems, whose spatial distribution can reach the continental scale (e.g. the European interconnected power grid as depicted in Fig. 3.5).

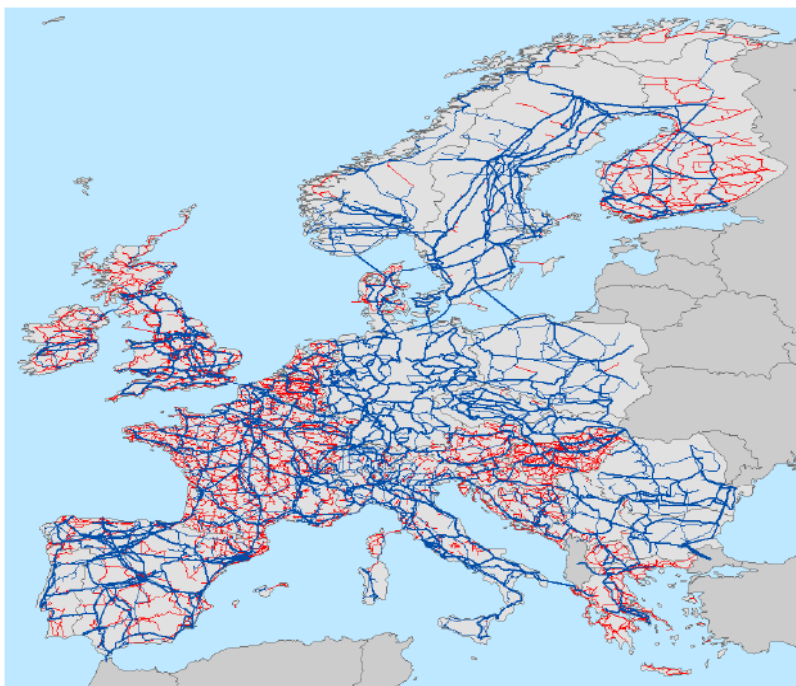


Fig. 3.5 European high voltage transmission grid ($V \geq 220\text{kV}$). Higher voltage lines in blue, lower voltage lines in red. Line thickness is proportional to voltage (Poljansek et al. 2010)

This type of system is usually broken down into three main functions:

- Generation of electric power;
- Transmission of high-voltage electric power from generation plants to consumption areas;
- Distribution of low-voltage electric power to the consumers and the electric appliances;

These functions are carried out by a wide range of components that can be regrouped into different generic categories:

- Power generation plants;
- Transformation stations;
- Transmission and distribution grid;
- Electric devices of the ends-users, referred as loads;
- Control and regulation systems;

For a more detailed description of Electric power networks the reader is referred to the review in D2.3 Pinto et al. (2011a) and in Saadi (2002).

The main typologies and proposed taxonomy, with particular reference to the European context, are listed in Table 3.5.

The distinction between micro- and macro-components is useful in terms of reliability analysis when the approach to network modelling is capacitive (i.e. power flows are

computed) and/or the internal logic of substations is modelled, i.e., partial functioning (continued service with reduced power flow) is accounted for.

Assembling sub-sets of micro-components to a macro-component, characterised by a single fragility, can reduce the computational effort. The substation is then composed of macro-components which can lead to partial functioning states, depending on the distribution of damage.

Tables 3.6 and 3.7 present two examples of the proposed in SYNER-G fragility functions of macro and micro-components. For further details, the reader is referred to Reference Report 4 (Kaynia 2013) and Deliverable 3.3 (Pinto et al. 2010).

Table 3.5 Main typologies of EPN components in Europe

Typology		Analysis level	Element code
Electric power grid		Network	EPN01
Generation plant		Station	EPN02
Substation		Station	EPN03
Distribution circuits		Distribution-system	EPN04
Macro-components		Substation's component	
1 ^[1]	Autotransformer line	Substation's component	EPN05
2	Line without transformer	Substation's component	EPN06
3	Bars-connecting line	Substation's component	EPN07
4	Bars	Substation's component	EPN08
5	Cluster	Substation's component	EPN09
Micro-components		Substation's component	
1 ^[1]	Circuit breaker	Substation's component	EPN10
2	Lightning arrester or Discharger	Substation's component	EPN11
3	Horizontal disconnect switch or Horizontal sectionalizing switch	Substation's component	EPN12
4	Vertical disconnect switch or Vertical sectionalizing switch	Substation's component	EPN13
5	Transformer or Autotransformer	Substation's component	EPN14
6	Current transformer	Substation's component	EPN15
7	Voltage transformer	Substation's component	EPN16
8	Box or Control house	Substation's component	EPN17
9	Power supply to protection system	Substation's component	EPN18
10	Coil support	Substation's component	EPN19
11	Bar support or Pothead	Substation's component	EPN20
12	Regulator	Substation's component	EPN21
13	Bus	Substation's component	EPN22
14	Capacitor bank	Substation's component	EPN23

[1] Numbers based on lists in section 4.1.3.5 and 4.1.3.6 in Ref. Report 4 (Kaynia 2013).

Table 3.6 Fragility functions of macro-components 1, 2, 3 and 4

Element at risk	4 electric macro-components	Element Code	EPN05 to 08			
Reference	Vanzi, I. 1996					
Method	Numerical, FORM/SORM methods					
Function	Lognormal, $LN(\lambda, \beta)$					
Damage states	Failure (Collapse)					
Seismic intensity parameter	PGA (m/s^2)					
Background	Fragilities of micro-components considered by the same author					
Figures						
Parameters (graphically retrieved from the curves)	Macro-component	25 th perc. (m/s^2)	Median (m/s^2)	75 th perc. (m/s^2)	λ (m/s^2)	β
	Line without transformer	1.8	2.2	2.4	0.79	0.21
	Bars-co necting line	2	.4	2.6	0.88	0.19
	Bars	1.2	1.5	2	0.41	0.38
	Autotransformer line	1.5	1.8	2.3	0.9	0.32
Comments	The considered macro-components are: (1) Line without transformer, (2) Bars-connecting line, (3) Bars, (4) Autotransformer line; The failures of interconnected vulnerable microelements are assumed as independent events					

Table 3.7 Fragility functions of 11 micro-components

Element at risk	11 electric micro-components		Element Code	EPN10 to EPN20		
Reference	Vanzi, I. 1996					
Method	Numerical		Function	Lognormal, $LN(\lambda, \beta)$		
Damage states	Failure (Collapse)					
Seismic intensity parameter		PGA (m/s^2)	Background	Cornell method		
Figures						
<div><div></div><div></div><div></div><div><div>The considered micro-components are: (1) Coil support, (2) Circuit breaker, (3) Current transformer, (4) Voltage transformer, (5) Horizontal sectionalizing switch, (6) Vertical sectionalizing switch, (7) Discharger, (8) Bar support, (9) Autotransformer, (10) Box, (11) Power supply to protection system.</div></div></div>						
Parameters (extracted from a different reference)	Component	λ (m/s^2)	β	Component	λ (m/s^2)	β
	Coil support	1.36	0.34	Discharger	2.7	0.32
	Circuit breaker	1.66	0.33	Bar support	1.48	0.44
	Current transformer	1.43	0.27	Autotransformer	3.16	0.29
	Voltage transformer	1.79	0.27	Box	2.93	0.52
	Horiz. sectionalizing switch	1.7	0.22	Power supply to protection system	1.4	0.16
	Vert. sectionalizing switch	1.69	0.34			
Comments	The retrieved fragility curves take into account the uncertainties about both the mechanical properties and the dynamic input					

Table 3.8 SYNER-G Taxonomy for oil network

CATEGORY	SUB-CATEGORY
Production and Gathering Facility (OIL01) <ul style="list-style-type: none"> Onshore Production Facilities (Production Field) Offshore Production Facilities (Marine-water Platforms) Gathering Facilities 	<ul style="list-style-type: none"> Oil and gas pools and wells (oil, gas and condensate wells) Radial line Trunk line
Refineries (OIL02)	<ul style="list-style-type: none"> Equipment: Centrifuges, compressors, cooling towers, crushers, crystallizers, distillation towers and pressure vessels, electric power generators, transformers and electric motors, electrolysis cell, evaporators, filters, furnaces, gas flares, mixers and blenders, monitoring and control systems, piping and valves, pumps, steam generators, steam turbines and gas turbines, storage tankers, wastewater treatment.
Storage Tank Farms (OIL03) <ul style="list-style-type: none"> Floating roof tank Fixed roof tank Bullet tank Spherical tank 	Anchoring of components <ul style="list-style-type: none"> Anchored components (AC) Unanchored components (UC)
Pumping Plants (OIL04) <ul style="list-style-type: none"> Centrifugal Reciprocating 	
Pipelines (OIL05) <ul style="list-style-type: none"> Gathering System (from wellhead to treatment plant, low pressure and diameter pipelines) Transportation System (from treatment plant to distribution systems, high pressure and large diameter pipelines) Distribution System (from regulator stations to the city, low pressure and small-diameter pipelines) 	<ul style="list-style-type: none"> Location : Buried/Elevated Material type <ul style="list-style-type: none"> Cast Iron (CI) Ductile Iron (DI) Asbestos Cement (AC) PVC (PVC) PEAD, , , steel Material strength Diameter: $\phi 75$, $\phi 100$, $\phi 150$, $\phi 200$, $\phi 400$, $\phi 500$ Wall thickness Type of connection: Rubber gasket, lap-arc welded, heat fusion. Arc or oxyacetylene-gas welds, screwed, mechanical restrained Pressure classification: Low/High Design flow One way feed/Bi-directional feed
SCADA System (OIL06)	

Table 3.9 SYNER-G Taxonomy for natural gas network

CATEGORY	SUB-CATEGORY
Production and Gathering Facility (GAS01) <ul style="list-style-type: none"> Onshore Production Facilities (Production Field) Offshore Production Facilities (Marine-water Platforms) Gathering Facilities 	<ul style="list-style-type: none"> Oil and gas pools and wells (oil, gas and condensate wells) Radial line Trunk line
Treatment Plant (GAS02) <ul style="list-style-type: none"> Amine Process NGL Fractionation Water Removal 	<ul style="list-style-type: none"> Absorber Regenerator Accessory equipment (re-boiler, pumps, condenser, valve, reflux drum, etc.) Fractionating column Accessory equipment (re-boiler, reflux drum, condenser, etc.) Regenerator Contactator Accessory equipment (Absorption/ Adsorption Towers)
Storage Tanks (GAS03) <ul style="list-style-type: none"> Underground Storage Facilities Storage Tanks for Liquefied Natural Gas- LNG (including pipes and electric components) 	<ul style="list-style-type: none"> Depleted gas reservoirs Aquifers Salt caverns <p>Anchoring of components</p> <ul style="list-style-type: none"> Anchored components (AC) Unanchored components (UC)

CATEGORY	SUB-CATEGORY
Stations (GAS04) <ul style="list-style-type: none"> • Compression Stations <ul style="list-style-type: none"> ○ Turbine ○ Motor ○ Engine ○ Scrubber ○ Filter • Metering/Pressure Reduction Stations <ul style="list-style-type: none"> ○ Equipment for monitoring and managing • Regulator Stations • Metering Stations 	
Pipelines (GAS05) <ul style="list-style-type: none"> • Gathering System (from wellhead to treatment plant, low pressure and diameter pipelines) <ul style="list-style-type: none"> ○ Location : Buried/Elevated ○ Material type: PVC, PEAD, cast iron, ductile iron, steel ○ Material strength ○ Diameter: $\phi 75$, $\phi 100$, $\phi 150$, $\phi 200$, $\phi 400$, $\phi 500$ ○ Wall thickness ○ Type of connection: Rubber gasket, lap-arc welded, heat fusion. Arc or oxyacetylene-gas welds, screwed, mechanical restrained ○ Pressure classification: Low/High ○ Design flow ○ One way feed / Bi-directional feed • Transportation System (from treatment plant to distribution systems, high pressure and large diameter pipelines) • Distribution System (from regulator stations to the city, low pressure and small-diameter pipelines) 	
SCADA System (GAS06)	

Table 3.10 Summary of the proposed fragility functions for elements of gas and oil systems

Element	Methodology	Classification	Intensity measure
Pipelines	ALA (2001) Empirical	Pipe material, joint type, soil type and pipe diameter	PGV
	ALA (2001) Expert judgment/ Empirical	Pipe material, joint type	PGD
Storage tanks	HAZUS (2004)	Anchored or unanchored components	PGA
Processing facilities	HAZUS (2004)	Generic station, Anchored or unanchored components	PGA
	SRMLIFE (2007)	Greek typology	PGA

3.3.3 Water and waste-water networks

Water and waste water systems are generally prone to damage from earthquakes even under moderate levels of shaking. Furthermore, as experienced during past earthquakes, seismic damage to water system elements can cause extended direct and indirect economic losses, while environmental pollution is the main result of waste water network failures.

The main damages in both systems were observed in pipes; secondarily in pumping stations, tanks, lift stations and water/waste-water treatment plants. The pipeline damages can mainly be attributed to permanent ground deformation. Rigidity of the pipe body, connection type, age and corrosion are some of the factors that influence the seismic response of water and waste-water system elements.

The typological features and classification considered in SYNER-G are summarized in Table 3.11 and Table 3.12 and the proposed fragility curves are summarized in Table 3.13. The selection is based on a validation study that has been performed for the 1999 Düzce (Turkey) and the 2003 Lefkas (Greece) earthquakes.

Table 3.11 SYNER-G Taxonomy for water supply network

CATEGORY	SUB-CATEGORY
Source (WSN01) <ul style="list-style-type: none"> • Springs • Rivers • Natural Lakes • Impounding Reservoirs • Wells (Shallow/Deep) (Anchored/Unanchored Sub-components)	<ul style="list-style-type: none"> ○ Electric power ○ Electric equipment ○ Well pump ○ Building
Treatment Plant (WSN02) <ul style="list-style-type: none"> • Small • Medium • Large (Anchored/Unanchored Sub-components)	<ul style="list-style-type: none"> ○ Electric power ○ Electric equipment ○ Chlorination equipment ○ Sediment flocculation ○ Basins ○ Baffles ○ Paddles ○ Scrapers ○ Chemical Tanks ○ Elevated pipe ○ Filter gallery
Pumping Station (WSN03) <ul style="list-style-type: none"> • Small • Medium • Large (Anchored/Unanchored Sub-components)	<ul style="list-style-type: none"> ○ Electric power ○ Equipment ○ Vertical/horizontal pump ○ Building

CATEGORY	SUB-CATEGORY
Storage Tanks (WSN04) <ul style="list-style-type: none"> • Closed Tanks • Open Cut Reservoirs 	<ul style="list-style-type: none"> ○ Material type: wood, steel, concrete, masonry ○ Capacity: small, medium, large ○ Anchorage: yes/no ○ Position: at grade, elevated by columns or frames) ○ Type of roof: RC, steel, wood ○ Seismic design: yes/no ○ Construction type: elevated by columns, built “at-grade” to rest directly on the ground, build “at grade” to rest on a foundation, concrete pile foundation ○ Presence of side-located inlet-outlet pipes ○ Volume: height, diameter ○ Thicknesses ○ Operational function: full, nearly full, less than full
Pipes (WSN05)	<ul style="list-style-type: none"> ○ Location: buried/elevated ○ Type: continuous/segmented ○ Material (type, strength): ductile iron, steel, PVC (acrylonitrile-butadienestyrene/ABS), polyethylene/PE, reinforced plastic mortar/RPM, resin transfer molding/RTM- asbestos-cement pipes, cast iron, concrete, clay ○ Type of joints: rigid/flexible ○ Capacity: diameter ○ Geometry: wall thickness ○ Type of coating and lining ○ Depth ○ History of failure ○ Appurtenances and branches ○ Corrosiveness of soil conditions ○ Age ○ Pressure
Tunnels (WSN06)	<ul style="list-style-type: none"> ○ Construction technique ○ Liner system ○ Geologic conditions
Canals (WSN07) <ul style="list-style-type: none"> • Open cut or built up using levees • Reinforced, unreinforced liners or unlined embankments 	<ul style="list-style-type: none"> ○ Material: wood, steel, concrete ○ Appurtenances and branches location ○ Age of construction ○ Geometrical characteristics: width, depth, capacity ○ Section: orthogonal, trapezoid, etc. ○ Inclination
SCADA System (WSN08)	

Table 3.12 SYNER-G taxonomy for waste-water network

CATEGORY	SUB-CATEGORY
Treatment Plant (WWN01) <ul style="list-style-type: none"> • Small • Medium • Large (Anchored/Unanchored Sub-components)	<ul style="list-style-type: none"> ○ Electric power ○ Electric equipment ○ Chlorination equipment ○ Sediment flocculation ○ Chemical Tanks ○ Elevated pipe ○ Building
Pumping (Lift) Station (WWN02) <ul style="list-style-type: none"> • Small • Medium • Large (Anchored/Unanchored Sub-components)	<ul style="list-style-type: none"> ○ Electric power ○ Equipment ○ Vertical/horizontal pump ○ Building
Pipes (WWN03)	<ul style="list-style-type: none"> ○ Location: buried/elevated ○ Type: continuous/segmented ○ Material (type, strength): ductile iron, steel, PVC (acrylonitrile-butadienestyrene/ABS), polyethylene/PE, reinforced plastic mortar/RPM, resin transfer molding/RTM- asbestos-cement pipes, cast, iron, concrete, clay ○ Type of joints: rigid/flexible ○ Capacity: diameter ○ Geometry: wall thickness ○ Type of coating and lining ○ Depth ○ History of failure ○ Appurtenances and branches ○ Corrosiveness of soil conditions ○ Age ○ Pressure
Tunnels (WWN04)	<ul style="list-style-type: none"> ○ Construction technique ○ Liner system ○ Geologic conditions
SCADA System (WWN05)	

Table 3.13 Summary of the proposed fragility functions for water and waste water elements

Element	Methodology	Classification	Intensity measure
Water sources	SRMLIFE, 2003-2007	Anchored/ unanchored components Seismic design of building	PGA
Water treatment plants	SRMLIFE, 2003-2007	Anchored components	PGA
Pumping stations	SRMLIFE, 2003-2007	Anchored/ unanchored components Seismic design of building	PGA
Storage tanks	ALA, 2001	Anchored RC tanks at grade Unanchored RC tanks at grade Open reservoirs with or without seismic design code Buried RC tanks	PGA, PGD
Canals	ALA, 2001	Unreinforced liners or unlined Reinforced liners	PGV, PGD
Water and Waste water pipelines	O'Rourke and Ayala (1993) Honneger and Eguchi (1992)	Pipe material	PGV, PGD
Water and Waste water tunnels	Same as roadway tunnels		
Waste-Water treatment plant	SRMLIFE, 2003-2007	Anchored/ unanchored components Seismic design of building	PGA
Lift stations	SRMLIFE, 2003-2007	Anchored/ unanchored components Seismic design of building	PGA

3.4 FRAGILITY CURVES FOR TRANSPORTATION INFRASTRUCTURES

Transportation systems include roadway, railway and subway networks, port and airport systems and infrastructures. Each system is actually a complex network of various components like bridges, roads, tunnels, embankments, retaining walls, slopes in case of roadway system or wharfs, cranes, buildings, utility systems, and tanks in case of harbour. Experience from past earthquakes reveals that some of these elements are quite vulnerable, while their damage could be greatly disruptive due to the lack of redundancy, the lengthy repair time or the rerouting difficulties. For example, the disruption to the road network can strongly affect the emergency efforts immediately after the earthquake or the rebuilding and other business activities in the following period. A typical paradigm is the port of Kobe after the strong Great Hansin earthquake (M7.1, 1995) that has lost almost 50% of its annual income, despite the enormous retrofitting works.

The complexity of elements at risk, their variability from one place and one country to another, and until recently, the lack of well-documented damage and loss data from strong earthquakes and the spatial variability of ground motion, make the vulnerability assessment of each particular component and of the network as a whole, a quite complicated problem. In addition to the spatial extension of transportation networks, the interactions with other systems and the inherent uncertainties in seismic hazard and vulnerability estimates, make the risk assessment of transportation networks indeed a complex and challenging issue.

The main typological features, damage states and parameters of the proposed fragility functions are given for roadway bridges, roadway and railway elements, and harbour infrastructures. In this chapter the parameters, damage states and plots of the fragility curves are given for each element. For further details, the reader is referred to SYNER-G Deliverables 3.6 (Fardis et al. 2011), 3.7 (Kaynia et al. 2011a), 3.8 (Kaynia et al. 2011b) and 3.9 (Kakderi et al. 2010) and Reference Report 2 (Hancilar and Taucer 2013).

3.4.1 Roadway and railway bridges

As shown in Table 3.14 different categories have been identified to describe bridges, such as the material, characteristics of the deck, spans, pier-deck connection, etc. A hierarchy is used for some categories where additional information might or might not be available. For example, when the material is concrete, the user may or may not know whether it is reinforced or pre-stressed, thus the definition of such second parameter is optional.

Table 3.14 SYNER-G Taxonomy for bridges

CATEGORY	SUB-CATEGORY
Material (MM1) <ul style="list-style-type: none"> Concrete (C) Masonry (M) Steel (S) Iron (I) Wood (W) Mixed (MX) 	Material (MM2) <ul style="list-style-type: none"> Reinforced concrete (RC) Pre-stressed reinforced concrete (PC) Unreinforced masonry (URM) Reinforced masonry (RM) High strength concrete (HSC) Average strength concrete (ASC) Low strength concrete (LSC) Adobe (A) Fired brick (FB) Hollow clay tile (HC) Stone (S) Lime mortar (LM) Cement mortar (CM) Mud mortar (MM) Concrete masonry unit (CMU) Autoclaved aerated concrete (AAC) High % of voids (H%) Low % of voids (L%) Regular Cut (Rc) Rubble (Ru)

Type of Deck (TD1) <ul style="list-style-type: none">Girder bridge (Gb)Arch bridge (Ab)Suspension bridge (Sb)Cable-stayed bridge (Csb)Moveable bridge (Mb)	Type of Deck (TD2) <ul style="list-style-type: none">Solid slab (Ss)Slab with voids (Sv)Box girder (B)Modern arch bridge (MA)Ancient arch bridge (AA)Precast beams with concrete topping (Pbc)Steel beams with concrete topping (Sbc)	Deck characteristics (DC) [Here the width of the deck is explicitly given if known]
Deck Structural System (DSS) <ul style="list-style-type: none">Simply supported (SSu)Continuous (Co)		
Pier to deck connection (PDC) <ul style="list-style-type: none">Not Isolated (monolithic) (NIs)Isolated (through bearings) (Is)Combination (Com)	<ul style="list-style-type: none">Fixed bearings (Fb)Elastomeric bearings (Eb)Sliding bearings (Sb)Seismic isolation/dissipation devices (SeisD)	
Type of pier to deck connection (TC1) <ul style="list-style-type: none">Single-column pier (ScP)Multi-column piers (McP)	Number of piers for column (NP) [Here the number of piers for column is explicitly given if known]	
Type of section of the pier (TS1) <ul style="list-style-type: none">Cylindrical (Cy)Rectangular (R)Oblong (Ob)Wall-type (W)	Type of section of the pier (TS2) <ul style="list-style-type: none">Solid (So)Hollow (Ho)	Height of the pier (HP) [Here the height of piers is explicitly given if known]
Spans (Sp) <ul style="list-style-type: none">Single span (Ssp)Multi spans (Ms)	Spans characteristics (SC) <ul style="list-style-type: none">Number of spans (Ns) - [Here the number of spans is explicitly given if known]Span length (SL) - [Here the length of spans is explicitly given if known]	
Type of connection to the abutments (TCa) <ul style="list-style-type: none">Free (F)Monolithic (M)Isolated (through bearings, isolators) (Isl)	<ul style="list-style-type: none">Free transverse translation (Ftt)Constrained transverse translation (Ctt)Fixed bearings (Fb)Elastomeric bearings (Eb)Sliding bearings (Sb)Seismic isolation/dissipation devices (SeisD)	
Skew (Sk) <ul style="list-style-type: none">StraightSkewed	[Here the skew angle is explicitly given if known]	
Bridge Configuration (BC) <ul style="list-style-type: none">Regular or semi-regular (R)Irregular (IR)		

Foundation Type (FT) <ul style="list-style-type: none"> • Shallow foundation (SF) • Deep foundation (DF) 	<ul style="list-style-type: none"> • Single pile (Sp) • Multiple piles with pile cap (Mpc) • Multiple piles without pile cap (Mp)
Seismic Design Level (SDL) <ul style="list-style-type: none"> • No seismic design (design for gravity loads only) (NSD) • Low-code (LC) • Medium-code (MC) • High-code (HC) 	

The bridge typology is defined using the label between brackets for each parameter within a given category.

Example:

MM1-MM2/TD1-TD2-DC/DSS/PDC/TC1-NP/TS1-TS2-HP/Sp-SC/TCa/Sk/BC/FT/SDL

More than one label can be used per category, separated by a dash. For example, a concrete bridge made up of pre-stressed reinforced concrete would be C-PC, whereas a bridge with cylindrical and solid cross-section piers would be Cy-So. Not all categories need to be defined due to the fact that information about the structure might be missing. In this case, for the categories where information is unknown, an X symbol is used. A couple of examples follow:

- C-RC/Gb-B/SSu/Nis/McP-2/R-Ho-10/Ms-3/M/IR/SD: Reinforced concrete bridge with box girder, simply supported non-isolated deck with 2-column rectangular hollow piers; 3-span deck monolithically connected to the ground; with irregular pier configuration and seismically designed.
- C-RC/Gb-B-X/X/NIs/X/W-X-X/X-X/X/X/X: Reinforced concrete bridge with box girder and deck monolithically connected to wall-type piers.

The proposed taxonomy has been set up with a modular structure, a new and different approach in categorizing and classifying bridges. Such flexible structure, which easily enables the future addition of other categories and sub-categories, as well as different features to existing ones, can be used to describe a considerable number of different bridges. This will cater for the consideration of different kinds of European bridges.

As an example for four reinforced concrete bridge classes, Fig. 3.7 depicts the mean curve and the individual fragility functions, while Table 3.15 gives the mean and coefficient of variation (c_v) of the lognormal parameters of the fragility functions (i.e. logarithmic mean and logarithmic standard deviation).

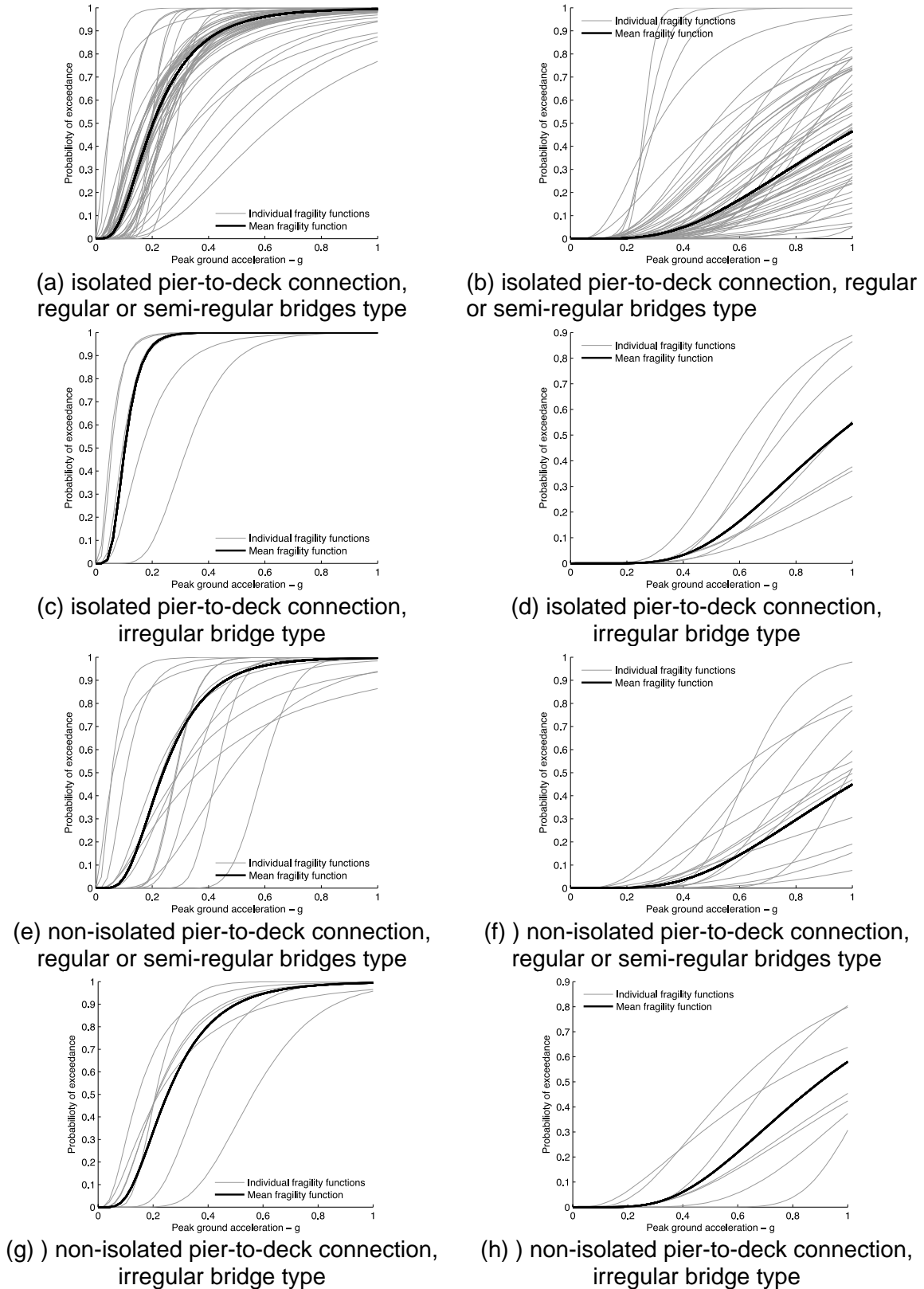


Fig. 3.7 Mean and individual fragility curves for (left column) minor damage limit state and (right column) collapse limit state, for reinforced concrete bridges. (a, b, c, d) isolated pier-to-deck connection and (e, f, g, h) for non-isolated pier-to-deck connection. (a, b, e, f) regular or semi-regular bridges type and (c, d, g, h) irregular bridge type.

Table 3.15 Mean and c_v of lognormal fragility parameters for reinforced concrete, isolated pier-to-deck connection, regular or semi-regular bridges type

Reinforced concrete bridge					
Bridge type		Minor Damage		Collapse	
		Logarithmic mean, μ_1	Logarithmic standard deviation, σ_1	Logarithmic mean, μ_2	Logarithmic standard deviation, σ_2
Isolated pier-to-deck connection, Regular or Semi-Regular	Mean	-1.593	0.611	0.052	0.587
	c_v (%)	27	33	1267	31
Isolated pier-to-deck connection, Irregular	Mean	-2.272	0.423	-0.055	0.468
	c_v (%)	32	54	358	27
Non-isolated pier-to-deck connection, Regular or Semi-Regular	Mean	-1.432	0.512	-0.070	0.546
	c_v (%)	50	56	673	40
Non-isolated pier-to-deck connection, Irregular	Mean	-1.378	0.538	-0.106	0.522
	c_v (%)	32	37	251	42

A computational module has been constructed for the design of a specific bridge according to relevant parts of Eurocodes 2 and 8 (with the associated analyses and any required analysis-design iterations) and the development of the fragility curves. The module is computationally very efficient and works in an automated way, once the design parameters are specified. Incorporated into a broader computational environment for the vulnerability assessment of systems, the module can provide the fragility curves for individual RC bridges of a wide variety of types.

3.4.2 Roadway networks

The typological features and classification considered in SYNER-G are summarized in Table 3.16. The proposed fragility functions for road elements are outlined in Table 3.17.

Table 3.16 SYNER-G Taxonomy for roadway Network

CATEGORY	SUB-CATEGORY
Bridges (RDN01) See Table 3.14	
Tunnels (RDN02)	<ul style="list-style-type: none"> ○ Construction method: bored or mined, cut-and-cover, immersed ○ Shape: circular, rectangular, horseshoe, etc. ○ Depth: surface, shallow, deep ○ Geological conditions: rock/alluvial ○ Supporting system: concrete, masonry, steel, etc.
Embankments (road on) (RDN03)	<ul style="list-style-type: none"> ○ Geometrical parameters of the construction, i.e. slope angle, height ○ Soil conditions ○ Water table
Trenches (road in) (RDN04)	<ul style="list-style-type: none"> ○ Geometrical parameters of the construction, i.e. slope angle, height ○ Soil conditions ○ Water table
Slopes (road on or running along) (RDN05)	<ul style="list-style-type: none"> ○ Geometrical parameters of the construction, i.e. slope angle, height ○ Soil conditions ○ Water table
Road pavements (ground failure) (RDN06)	<ul style="list-style-type: none"> ○ Number of traffic lanes
Bridge abutments (RDN07)	<ul style="list-style-type: none"> ○ Geometry of the abutment i.e. height, width ○ Soil conditions of foundation ○ Fill material behind the abutment

Table 3.17 Summary of the proposed fragility functions for road elements

Element	Methodology	Classification	Intensity measure
Urban tunnels in alluvial	SYNER-G Numerical analysis	Ground type: B, C, D (EC8) Circular (bored) Rectangular (cut and cover)	PGA
Other tunnels	ALA, 2001 Empirical	Rock or Alluvial/ Cut and Cover Good or poor to average construction and conditions	PGA
Embankment (road on)	SYNER-G Numerical analysis	Ground type: C, D (EC8) Height: 2.0, 4.0 m	PGA
Trenches (road in)	SYNER-G Numerical analysis	Ground type: C, D (EC8) Height: 2.0, 4.0 m	PGA
Bridge abutments	SYNER-G Numerical analysis	Ground type: C, D (EC8) Height: 6.0, 7.5m	PGA
Slopes	SAFELAND Expert judgement/ Empirical	yield coefficient, k_y earthquake magnitude	PGA
Road pavements	HAZUS Expert judgement	2 traffic lanes (Urban roads) ≥ 4 traffic lanes (Major roads)	PGD

3.4.3 Railway networks

Railway tracks are categorized as earth structures; therefore, a main typological feature is the soil type, which characterizes either a construction or its foundation and surrounding material. Different soil classification systems are available based on various soil properties. The soil classification provided by Eurocode 8 is used in this study.

The track is a fundamental part of the railway infrastructure; it consists of elements with different material that transfer static and dynamic loads to the foundation soil. The classical railway track consists of rails and sleepers supported on ballast. The ballast bed rests on a sub-ballast layer which forms the transition layer to the formation. The rails and sleepers are connected by fasteners. These components and other structures such as switches and crossings are all considered parts of the track.

The other railway elements (tunnels, embankments, trenches, slopes and bridge abutments) present similar features as the roadway elements (see previous section).

The description and classification of the other railway elements is similar to the corresponding roadway elements. The classification considered in SYNER-G is summarized in Table 3.18. The proposed fragility functions for road elements are outlined in Table 3.19.

Table 3.18 SYNER-G Taxonomy for railway network

CATEGORY	SUB-CATEGORY
Bridges (RWN01)	
See Table 3.14	
Tunnels (RWN02)	<ul style="list-style-type: none"> Construction method: bored or mined, cut-and-cover, immersed Shape: circular, rectangular, horseshoe, etc. Depth: surface, shallow, deep Geological conditions: rock/alluvial Supporting system: concrete, masonry, steel, etc.
Embankments (track on) (RWN03)	<ul style="list-style-type: none"> Geometrical parameters of the construction, i.e. slope angle, height Soil conditions Water table
Trenches (track in) (RWN04)	<ul style="list-style-type: none"> Geometrical parameters of the construction, i.e. slope angle, height Soil conditions Water table
Slopes (track on or running along) (RWN05)	<ul style="list-style-type: none"> Geometrical parameters of the construction, i.e. slope angle, height Soil conditions Water table
Tracks (RWN06)	<ul style="list-style-type: none"> Steel rails Sleepers (ties): wooden, steel, concrete, twin block Support ballast
Bridge Abutments (RWN07)	<ul style="list-style-type: none"> Geometry of the abutment i.e. height, width Soil conditions of foundation Fill material behind the abutment
Stations (RWN08)	<ul style="list-style-type: none"> Passenger buildings Track exchanges Control houses Maintenance buildings Warehouses

Table 3.19 Summary of the proposed fragility functions for railway elements

Element	Methodology	Classification	Intensity measure
Urban tunnels in alluvial	SYNER-G Numerical analysis	Ground type: B, C, D (EC8) Circular (bored) Rectangular (cut and cover)	PGA
Other tunnels	ALA (2001) Empirical	Rock or Alluvial/ Cut and Cover Good or poor to average construction and conditions	PGA
Embankment (tracks on)	SYNER-G Numerical analysis	Ground type: C, D (EC8) Height: 2.0, 4.0 m	PGA
Trenches (tracks in)	SYNER-G Numerical analysis	Ground type: C, D (EC8) Height: 2.0, 4.0 m	PGA
Bridge abutments	SYNER-G Numerical analysis	Ground type: C, D (EC8) Height: 6.0, 7.5m	PGA
Slopes	SAFELAND Expert judgement/ Empirical	yield coefficient, k_y earthquake magnitude	PGA
Railway tracks	SYNER-G Expert judgement	all	PGD

3.4.4 Harbour elements

Port transportation systems are vital lifelines whose primary function is to transport cargos and people. They contain a wide variety of facilities for passenger operations and transport, cargo handling and storage, rail and road transport of facility users and cargoes, communication, guidance, maintenance, administration, utilities, and various supporting operations.

In a port system, the following elements are considered in SYNER-G:

- waterfront structures;
- cargo handling and storage components;
- infrastructures:
 - buildings (sheds and warehouses, office buildings, maintenance buildings, passenger terminals, traffic control buildings);
 - utility systems (electric power system, water system, waste-water system, natural gas system, liquid fuel system, communications system, fire-fighting system);
 - transportation infrastructures (roadway system, railway system, bridges).

Important typological features of port components include:

- Waterfront structures. The basic typological parameters are their geometry, section type, construction material, foundation type, existence and type of anchorage. Types of backfill and foundation soil, along with the existence of rubble foundation are

determinant factors of their seismic behaviour (Ichii, 2003). A more exhaustive typology is provided by Werner (1998) and PIANC (2001).

- Cargo handling and storage components. The basic typological parameter is the existence of anchorage. They could also be classified according to the cargo capacity and cargo type. When considering interactions between port components, their power supply type, foundation type and position are also important typological features. A more detailed typology is provided in Werner (1998).

The typological features and classification of port facilities considered in SYNER-G are summarized in Table 3.20. For the classification of buildings, utility systems and transportation infrastructures, the reader is referred to the respective sections. The proposed fragility curves for harbour elements are outlined in Table 3.21 (see also Kakderi et al. 2010).

Table 3.20 SYNER-G Taxonomy for harbour elements

CATEGORY	SUB-CATEGORY
Waterfront Components (HBR01)	
<ul style="list-style-type: none"> • Gravity Retaining Structures (along the waterfront, quay walls/piers) 	<ul style="list-style-type: none"> ○ Concrete block walls ○ Massive walls ○ Concrete caissons ○ Cantilever structures ○ Cellular sheet pile structures ○ Steel plate cylindrical caissons ○ Crib-work quay walls
<ul style="list-style-type: none"> • Sheet Pile Wharves 	<ul style="list-style-type: none"> ○ Sheet pile ○ Pile ○ Fill-soil foundation
<ul style="list-style-type: none"> • Piers 	<ul style="list-style-type: none"> ○ Deck slabs ○ Pile caps: wood, steel or concrete (with or without batter piles)
<ul style="list-style-type: none"> • Mooring and Breasting Dolphins 	
<ul style="list-style-type: none"> • Breakwaters 	<ul style="list-style-type: none"> ○ Gravity structure ○ Piled structure ○ Rubble mound
Earthen Embankments (HBR02)	
<ul style="list-style-type: none"> • Hydraulic Fills • Native Soil Materials 	<ul style="list-style-type: none"> ○ Native soils ○ Rock and sand dike with back land fills ○ Bulkheads ○ Sea walls ○ Breakwaters

CATEGORY	SUB-CATEGORY
Cargo Handling and Storage Components (HBR03) <ul style="list-style-type: none"> • Cranes • Tanks • Other Cargo Handling and Storage Components (cargo) 	<ul style="list-style-type: none"> ○ Rail, tire and track mounted gantry and revolver cranes ○ Mobile cranes ○ Crane foundations ○ Power supply systems ○ Anchored/unanchored ○ Above grade and partially buried ○ Tank foundations ○ Containment berms ○ Port equipment (stationary or mounted on rails) ○ Structural systems used for material handling ○ Transport (cranes, conveyors, transfer towers and stacker/reclaimer equipment) ○ Tunnels and pipelines ○ Temporary transitional storage and containment components
Buildings (HBR04) <ul style="list-style-type: none"> • Sheds and Warehouses • Office Buildings • Maintenance Buildings • Passenger Terminals • Control and Clock Towers • Older Buildings 	<ul style="list-style-type: none"> ○ Braced in one or two directions ○ Concrete walls ○ Masonry/metallic siding ○ Single/multi-storey ○ Steel/Timber/Concrete/Masonry ○ Braced in one or two directions ○ Concrete walls ○ Masonry/metallic siding ○ Concrete/Masonry/Steel/Wood ○ Unreinforced masonry ○ Non-ductile concrete ○ No seismic design

CATEGORY	SUB-CATEGORY
Liquid Fuel System (HBR05) <ul style="list-style-type: none"> Fuel storage tanks Buildings Pump equipment Piping Backup power 	
Communication System (HBR06) <ul style="list-style-type: none"> Buildings Communication equipment Backup power 	

Table 3.21 Summary of the proposed fragility functions for harbour elements

Element	Methodology	Classification	Intensity measure
Waterfront structures	HAZUS Expert judgment	One class	PGD
Waterfront structures	Kakderi and Pitilakis (2010) Numerical analysis	Wall height h ($>$ and $\leq 10\text{m}$) Soil foundation conditions (V_s values) (soil types B and C according to EC8)	PGA
Cargo handling and storage components	HAZUS Expert judgment	Stationary (anchored) and rail-mounted (un-anchored) cranes	PGA, PGD
Liquid fuel system	SRMLIFE (2003-2007) Fault-tree analysis	Anchored/ unanchored equipment With/ without back-up power Building with low/ medium/ high seismic code design	PGA
Liquid fuel system	SRMLIFE (2003-2007) Fault-tree analysis	Facilities with buried tanks	PGD
Communication system	SRMLIFE (2003-2007) Fault-tree analysis	Anchored components Low-rise/ mid-rise building Low/ high seismic code design	PGA

3.5 FRAGILITY CURVES FOR CRITICAL FACILITIES

3.5.1 Health care facilities

Hospital facilities belong to the category of the so-called “complex-social” systems: *complex* because, from an engineering point of view, these systems are made of many components of different nature that jointly contribute to provide an output which is the medical services; *social*, because hospitals provide a fundamental assistance to citizens in every-day life and

their function becomes of paramount importance in the case of a disaster. The system taxonomy for hospitals is illustrated in Fig. 3.8.

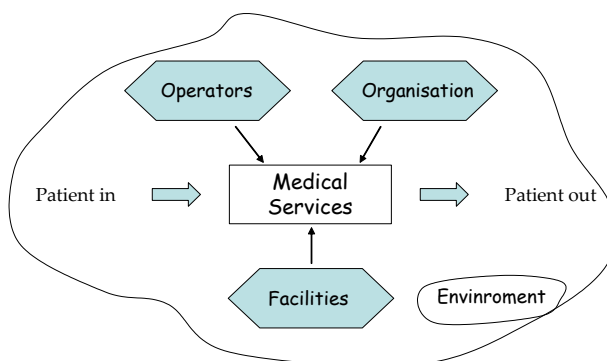


Fig. 3.8 System taxonomy of a hospital

At the core of the system there are the **medical services**, which consist of standardized procedures established to guarantee an adequate treatment of patients. The medical services are delivered to patients by a joint contribution of the three “active” components of the system:

- The facility (**physical component**) where the medical services are delivered. The physical component of a hospital system consists of *structural elements* and *non-structural elements* (architectural elements, basic contents and equipment). While the former are critical to preserve the life-safety of the building occupants, the latter are fundamental to preserve the hospital functionality.
- The **operators**, which are the doctors, nurses and in general whoever plays an active role in providing medical care.
- The **organisation**, which is responsible of setting up the adequate conditions so that the medical services can be delivered. In general, this is up to the hospital management through the development, the implementation and the supervision of the standardized procedures.

The **environment** includes all external influences to the functioning of a hospital system, which encompasses such diverse factors as cultural background and soil properties. It acts on all the “active” components both directly, through characteristics such as accessibility, soil conditions, etc., and indirectly, through social context, economic pressures, standards, educational system, etc.

The performance assessment of a hospital system is a task significantly more demanding with respect to the assessment of “simple” systems such as residential buildings or bridges. In fact, for a correct evaluation of the system performance, contributions of all components, and their interactions, have to be appropriately accounted for.

The taxonomy derived for a health-care facility is presented in Table 3.22.

Table 3.22 SYNER-G Taxonomy for health-care facilities

CATEGORY	SUB-CATEGORY
Organisational Component (HCS01)	
Human Component (HCS02)	
Physical Component (HCS03)	
<ul style="list-style-type: none"> • Structural Elements (HCS03-1) • Non-structural Elements (HCS03-2) • Architectural Elements (HCS03-3) • Basic Installations (HCS03-4) • Basic Installation: Medical Gas (HCS03-5) • Basic Installation: Power System (HCS03-6) • Basic Installation: Water System (HCS03-7) • Basic Installation: Elevators and Conveying System (HCS03-8) • Building Contents (HCS03-9) 	<ul style="list-style-type: none"> ○ Force mechanisms ○ Deformation mechanisms ○ Drift sensitive ○ Acceleration sensitive ○ Differential displacement sensitive ○ Walls (internal and external) ○ Ceilings ○ Windows, doors, glazing ○ Generation (electrical generator, water tank, gas tank) ○ Distribution (pipes for water, waste-water, gas, fuel and electrical conduits) ○ Oxygen (bottle, cylinders) ○ Nitrogen (cylinders) ○ Supply line ○ Equipments ○ Transformation station (medium voltage-MV and low voltage-LV) ○ Emergency generator (UPS and EPG) ○ Transmission lines ○ Distribution stations ○ Supply (city water and tanks) ○ Equipments (electric power, electric pumps and boilers) ○ Piping ○ Motor (power and engine) ○ Counter weights ○ Doors ○ Guide rails ○ Furnishings ○ Medical, office and industrial equipments ○ General supplies ○ Shelves etc.

A hospital system is made of five components: *human*, *organizational*, *physical*, *environmental* and *medical services*. The medical services that have to remain operative after the seismic event in order to guarantee the adequate treatment of patients and victims are classified as *essential* medical services.

The seismic risk for a hospital system is measured by the comparisons between treatment demand and capacity:

$$HTD(IM) = \zeta S_2 / (S_1 + S_1 S_2 + S_2) C(IM) \varepsilon_{cas} N_{pop} \quad (3.3)$$

$$HTC(IM) = \alpha \beta \gamma_1(IM) \gamma_2(IM) / t_m \quad (3.4)$$

The analysis of the *human*, the *organizational*, the *environment* and the *medical services* components consists in:

- verifying that the hospital is provided of all the *essential* medical services;
- assessing the quality of the emergency plan;
- verifying the existence of adequate resources to put into effect the emergency plan;
- assessing the quality of the human component and the availability of the operators to put in practice the emergency plan;
- examining the environment where the hospital is located that affects the number and the typology of victims.

The following data/information is derived:

- (1) estimates of the coefficients α and β in Eq. (3.3);
- (2) identification of the hospital areas where the essential medical services are housed;
- (3) fault-tree of the hospital system and fragilities for all the relevant elements at risk;
- (4) estimate of the casualty model parameters $C(IM)$ and of the severity indexes of the event, S_1 and S_2 in Eq. (3.3).

The numerical analysis of the *physical* component is carried out by a probabilistic procedure. It provides the number of functioning operating theatres, γ_1 , and the system-survival Boolean function, γ_2 , in Eq. (3.4). The “survival condition” of the physical component is expressed as a function of the performance of the medical services, making a distinction between the *essential* medical services and basic medical services (all the others): the operational performance level is required for the former, a life-safety performance level for the latter. The fault-tree technique is employed for the determination of the state of the system as a function of the state of its elements (see also Pinto et al. 2011b).

3.5.2 Fire-fighting systems

Fire is a common consequence of large earthquakes in urban and industrial areas. Fire-fighting activities can be prevented due to damages in the water or other (e.g. roadway) networks after large earthquakes. On the other hand, fire following earthquake is an extremely variable phenomenon, due to variability in the number of ignitions and in the extent of fire-spread from each ignition.

The fire-fighting system plays a major role in the management of crisis situations. It comprises not only the fire stations, pipeline network and fire faucets (either separate or

dependent on the water supply system), but also a whole crisis management system (special units, fire fighters, etc).

Usually fire-fighting system is part of a water system consisting of the same pipelines and storage tanks. In the case it is a separate network, it is usual that the storage tanks are made of steel, and the pipes are made of PVC. It is more common to find separate fire-fighting systems in small/confined areas with known needs, such as harbours, airports or hospitals and not in large urban areas.

For fire-fighting buildings the typological categories proposed in the respective part of this report can be used, while for the other elements the typologies described in water supply system can be applied.

The Taxonomy for fire-fighting systems proposed by the SYNER-G project is given in Table 3.23.

Table 3.23 SYNER-G Taxonomy for fire-fighting system

CATEGORY	SUB-CATEGORY
Fire-fighters Stations (FFS01)	
<ul style="list-style-type: none"> Buildings 	
Pumping Stations (FFS02)	
<ul style="list-style-type: none"> Small Medium Large (Anchored/Unanchored Sub-components)	<ul style="list-style-type: none"> Electric power Equipment Vertical/horizontal pump Building
Storage Tanks (FFS03)	
<ul style="list-style-type: none"> Closed Tanks Open Cut Reservoirs 	<ul style="list-style-type: none"> Material type: wood, steel, concrete, masonry Capacity: small, medium, large Anchorage: yes/no Position: at grade, elevated by columns or frames) Type of roof: RC, steel, wood Seismic design: yes/no Construction type: elevated by columns, built “at-grade” to rest directly on the ground, build “at grade” to rest on a foundation, concrete pile foundation Presence of side-located inlet-outlet pipes Volume: height, diameter Thicknesses Operational function: full, nearly full, less than full
Fire-hydrant (FFS04)	
	<ul style="list-style-type: none"> Pressure Demand Operational: yes/no
Pipelines (FFS05)	
	<ul style="list-style-type: none"> Location: buried/elevated Type: continuous/segmented Material (type, strength): ductile iron, steel, PVC (acrylonitrile-butadienestyrene/ABS),

CATEGORY	SUB-CATEGORY
	<p>polyethylene/PE, reinforced plastic mortar/RPM, resin transfer molding/RTM- asbestos-cement pipes, cast, iron, concrete, clay</p> <ul style="list-style-type: none"> ○ Type of joints: rigid/flexible ○ Capacity: diameter ○ Geometry: wall thickness ○ Type of coating and lining ○ Depth ○ History of failure ○ Appurtenances and branches ○ Corrosiveness of soil conditions ○ Age ○ Pressure

The fragility functions for fire-fighting systems' elements (pipes, storage tanks, pumping station, fire-station buildings) are described in previous sections (e.g. water and waste-water network, buildings). The functionality of fire-faucets can be estimated taking into account the connectivity with water system failures.

For pipes, storage tanks and pumping stations the proposed curves are the ones for water and waste-water systems elements. For fire-station buildings, the curves proposed for RC and masonry building types in Europe could be used.

It is noted that the fragility of fire-fighting system is closely connected with the possible fires just after the earthquake. The interaction between the road closures and the serviceability of water network with the fire-fighting system (if it is not separate from water system) is also essential.

3.6 CONCLUSIONS

3.6.1 Fragility functions for reinforced concrete and masonry buildings

The review of existing fragility curves for buildings shows a variety of methodologies, damage states, damage and intensity measures. It also becomes clear that existing taxonomies could leave out a large number of characteristics that could be used to distinguish the seismic performance of buildings. Hence, a modular classification scheme was developed. This collapsible and expandable scheme gives the flexibility to describe a building with as much information as can be collected, and allows one to expand the taxonomy when more detailed information is available, for example, by adding new categories or sub-categories so as to describe all types of buildings.

The main outcome of the project is a set of fragility functions for the most important typologies in Europe, which are stored into the Fragility Function Manager. This dynamic tool was used for the harmonisation of the fragility curves and for the estimation of the associated uncertainty in their mean and standard deviation values. For simplicity, fragility curves were harmonised for the yielding and ultimate damage states, as it is difficult to compare the functions for the intermediate ones.

New fragility curves were developed for RC frame and wall-frame buildings designed according to Eurocode 2 alone or for the three ductility classes of Eurocode 8. The curves were established point-by-point, from the probability that the (random variable) demand for given intensity measure exceeds the (random variable) capacity and consider shear failures, which are normally ignored in analytical fragility studies. New fragility curves, accounting for out-of-plane failure and behaviour, were developed for stone masonry buildings.

A further contribution of SYNER-G is towards the quantification of the epistemic uncertainty in fragility functions for buildings. A methodology was developed and implemented in a software tool that can be used for other elements at risk.

3.6.2 Fragility functions for utility networks

A modern electric power network (EPN) is a complex interconnected system designed to generate, transform and transfer electric energy from generating units to various locations. Based on the review of the main recent works on fragility functions of EPN components, standard damage scales for micro- and macro-components were proposed together with the most appropriate fragility functions for the components that are of interest in SYNER-G.

The existing fragility curves for pipelines, storage tanks and support facilities within natural gas and oil networks were collected and reviewed. Existing fragility curves developed in the USA are mainly empirical, while those developed in Europe are based on numerical or fault-tree analysis. The most appropriate functions were selected based on their ability to cover all the important elements and typologies in Europe.

Water and waste-water systems are complex systems, prone to damage – even for moderate earthquakes – which may result in extended direct and indirect losses and possibly in pollution of the environment. The most appropriate functions were proposed based on comparison to observed damage.

3.6.3 Fragility functions for transportation infrastructures

Experience from past earthquakes reveals that transportation infrastructures are quite vulnerable and their damage can be greatly disruptive for the whole network due to lack of redundancy, lengthy repair time or re-routing difficulties.

The existing fragility curves for road and railway bridges were reviewed, stored in the Fragility Function Manager and used to identify the key parameters of a new taxonomy. It is noted that few studies exist on the seismic fragility of European bridges, and for this reason, the fragility curves developed for bridges in other parts of the world are often adjusted for use in Europe. Except for a few recent studies, shear failure of the piers is often disregarded in existing fragility studies. New fragility curves were produced for road and railway bridges with continuous deck, monolithically connected to the piers or supported on elastomeric bearings, where the damage states are defined by the flexural and shear failure modes together with the deformation of the deck and the bearings.

Road and railway elements, such as tunnels, embankments, road pavements, slopes, trenches, railway tracks and bridge abutments, are earth structures and thus directly affected by the local soil conditions. Based on the review of the existing fragility curves, it was decided to develop new curves for urban tunnels in alluvial, embankments/trenches and bridge abutments. The effects of soil type and ground motion characteristics were taken into

account by using different soil profiles and seismic input motions. The response of the soil profiles was calculated through 1D equivalent linear analyses and the non-linear response of the soil-structure system was calculated through 2D quasi-static or dynamic analyses.

The existing fragility functions for railway elements are limited and are mainly based on data for road elements. New fragility curves were developed based on those for road elements and considering appropriate threshold values for the definition of the damage states.

Damage to waterfront structures is usually attributed to ground failure, while damage to cargo handling and storage components is due to ground shaking. Existing fragility curves have been developed based on expert judgement, numerical or fault-tree analysis. Among them, the most appropriate for the European typologies were selected. The HAZUS curves for quay walls were found compatible with the damage after the 2003 Lefkas earthquake.

3.6.4 Fragility functions for critical facilities

Hospital facilities are complex systems comprising several components (human, organizational, physical, environmental and medical services), each including a large variety of elements. Their behaviour has been studied, but capacity models and fragility curves are not available for all of them. A general methodology for the evaluation of the “probability of failure” of hospital systems has been proposed. It uses the fault-tree technique to establish the relationship between the state of the elements and the state of the system and a probabilistic approach to account for the large uncertainties characterising most of the quantities that contribute to the system response. Uncertainties are related, among others, to the external hazard, the evaluation of the structural response, the knowledge of system properties, the modelling of the capacities, and definition of damage levels. It is noted that each hospital is practically a prototype, as the layout is totally facility-dependent, and for this reason, a detailed analysis is necessary for each system.

Fire-fighting systems are normally part of water systems and utilize the same pipelines and storage tanks. Therefore, the same fragility curves are proposed for the elements at risk that belong to the two systems. Similarly, the fragility curves for buildings may be used for the buildings within fire-fighting systems.

4 Socio-economic vulnerability and losses

The current state-of-the-art in earthquake engineering produces reasonably accurate estimates of physical damage to buildings and infrastructure systems as well as reasonable estimates of the repair and replacement costs associated with this type of damage. However, poor linkages between damage to physical systems and resultant social and economic consequences remain a significant limitation with existing earthquake loss estimation models. One of the main aims in SYNER-G, was to develop a unified approach for modelling socio-economic impacts caused by earthquake damage which integrates social vulnerability into the physical systems modelling approaches. In SYNER-G, social losses (e.g., displaced population, shelter needs, health impacts) are computed as an integrated function of hazard intensity, systemic vulnerability of physical systems and the social vulnerability of the population at risk. This way of conceptualizing the integrated framework emphasizes the importance of understanding the interrelations between physical and social systems. In other words, how direct physical losses can potentially aggravate existing vulnerabilities in society and how vulnerabilities in society can ultimately lead to greater impacts from physical damage and losses. For more details on the integrated approach for social losses assessment the reader is referred to SYNER-G Reference Report 5 (Khazai 2013).

Key outputs and scientific achievements of SYNER-G include:

- Development of a new semi-empirical Casualty Model: methodology, implementation and validation.
- Development of a new Displaced Population Model: methodology, implementation and validation.
- Development of harmonized, evidence-based socio-economic vulnerability and capacity indicators for Europe reflecting populations at risk of being displaced or in need of shelter.
- Development of harmonized, evidence-based socio-economic vulnerability and capacity indicators for Europe reflecting populations at risk of aggravated health impacts.
- Development of integrated GIS-based transportation accessibility models to shelter sites and healthcare facilities for effective emergency response.
- Development of a new multi-criteria decision model for the assessment of post-earthquake shelter demand.
- Development of a new multi-criteria decision model for the assessment of post-earthquake health impact.
- Development of an open source software tool and to capture post-disaster shelter needs decisions and interactions.

The integrated approach proposed in SYNER-G (Fig. 4.1) provides a framework to link the degree of damage and performance of inter-related physical systems to vulnerabilities and coping capacities in society to assess: (1) Impacts on displaced populations and their shelter

needs, and (2) Health impacts on exposed populations and their health-care needs. Furthermore, non-availability of lifeline networks (roads, pipelines, electricity and water supply) have important consequences on the recovery process and contribute to increased social disruptions within shelter and health sectors. The impact of disruptions of the transportation system and utility systems on shelter and health systems is investigated. Emphasis in SYNER-G is placed on the early emergency relief and recovery period where the rapid provisioning of food, water, shelter and emergency healthcare services are the most important interventions to keep people alive and safe. Thus, the focus was on integrating models of social impact with loss estimation models for use in short-term emergency response planning.

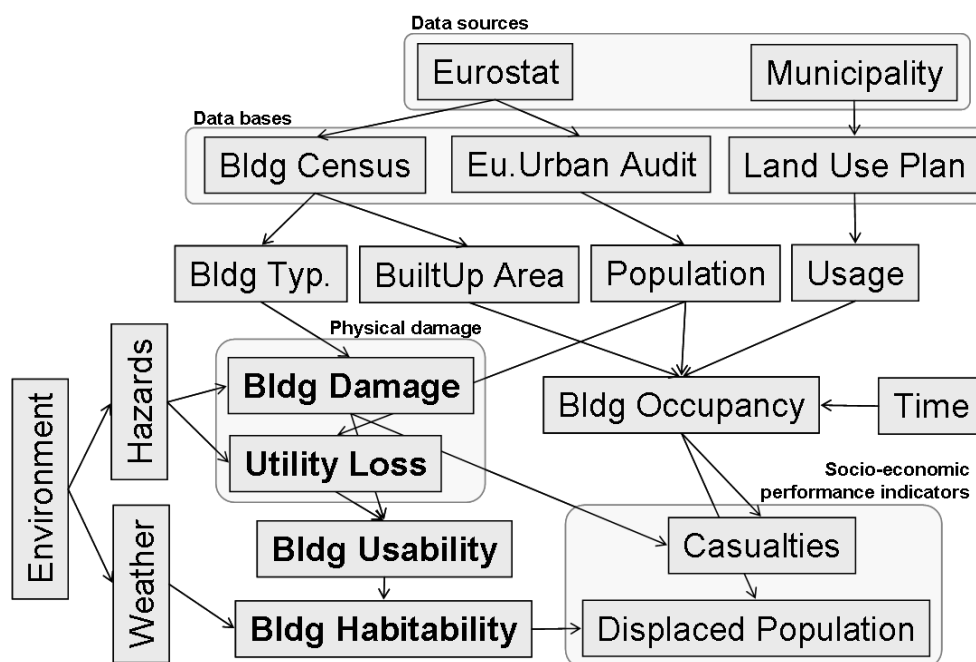


Fig. 4.1 Integrated evaluation of physical and socio-economic performance indicators

4.1 SHELTER NEEDS MODEL

Disaster displacement is a complex and dynamic process. Relationships between severely damaged and destroyed buildings and displaced persons after earthquakes in 457 earthquakes from 1900 to 2012 show a departure from linear relationships (assumed in state-of-the-art earthquake loss estimation models) representing coupled interactions between environmental, physical and socio-economic processes (Fig. 4.2).

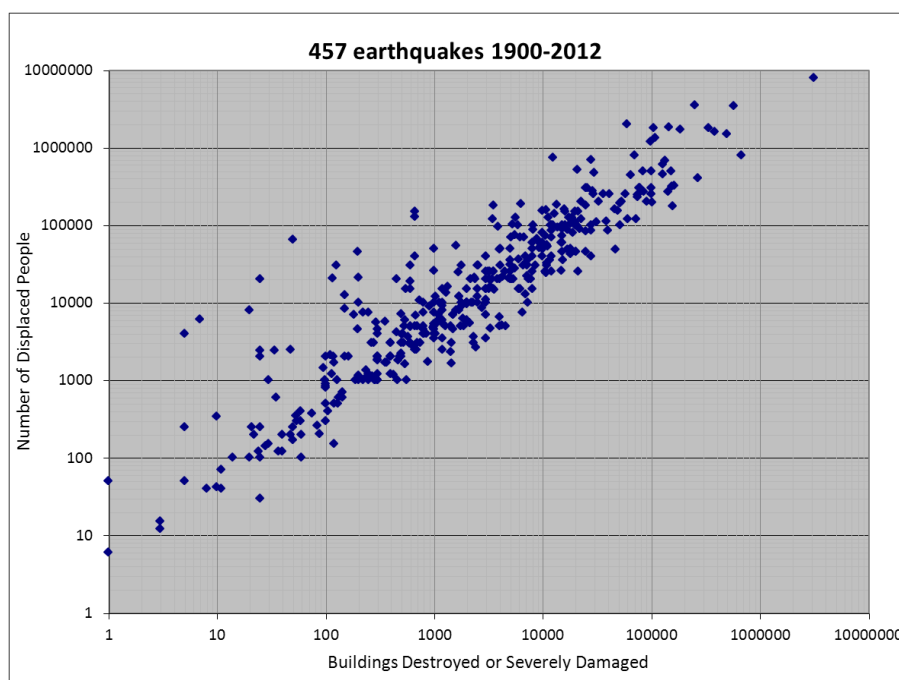


Fig. 4.2 Relationship between severely damaged and destroyed buildings and displaced persons after earthquakes (n = 457 earthquakes from 1900-2012 from the CATDAT database in Khazai 2013).

A new approach was developed for modelling emergency shelter demand by integrating shelter-seeking logic models into a systemic seismic vulnerability analysis and earthquake loss estimation software tool. Thus, the shelter model in SYNER-G provides a new advancement to shelter estimation methodology through three types of key inputs: (1) the “habitability” of buildings (defined by a households tolerance to the loss of power, gas and water for different levels of building damage and weather conditions) to provide information that can be used as a better determinant in influencing the decision of populations to evacuate than building damage alone; (2) GIS-based shelter accessibility analysis as an input to the shelter seeking model; and (3) complex socio-economic factors which represent the decision to evacuate and seek public shelter. These three inputs are combined into a dynamic shelter model which simulates a households' decision-making and considers physical, socio-economic, climatic and spatial factors in addition to modelled building damage states. The shelter model is implemented in the EQVis platform to provide stakeholders an interactive framework in decision-making process for shelter planning and preparedness.

The integrated shelter needs model developed in SYNER-G is based on a multi-criteria decision theory (MCDA) framework which allows the bringing together of parameters influencing the physical inhabitability of buildings, with social vulnerability (and coping capacity) factors of the at-risk population to determine as well as external factors to determine the desirability to evacuate and seek public shelter. As shown in Fig. 4.3, the multi-criteria framework can be described schematically as composed of the two main criteria: overall population at risk of being displaced after an earthquake (DPI), and the proportion of this population likely to seek public shelter (SSI). Subsequently, the total demand for public shelter for a particular location (i.e., city district) can be described as a

product of the population at risk of being displaced (related to the occupants in uninhabitable buildings and their desire to evacuate or not) and a set of indicators determining the population likely to seek public shelter.

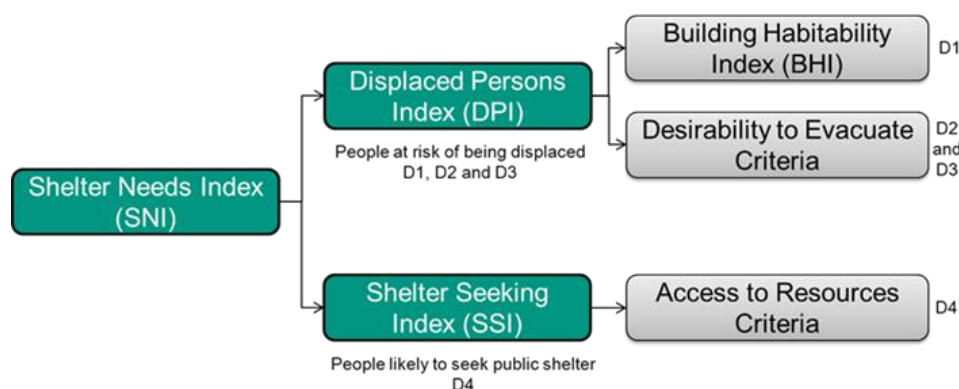


Fig. 4.3 Multi-criteria decision model for computing Shelter Needs Index (SNI)

To operationalize the shelter model, appropriate indicators from the EU Urban Audit Database have been selected using principal component analysis combined with expert judgment. Vulnerability factors deduced from the EU Urban Audit have been validated by applying the model using data from the M 6.3 earthquake that struck L'Aquila, Italy in April 2009. Fig. 4.4 shows how the modeling approach can be used to capture the actual shelter demand conditions (given as the observed number of people in shelter camps normalized by total population in different Mixed Operations Centres (COM) which had the overall coordinating role in their own territories for all rescue and shelter provision operations after the L'Aquila earthquake. Additionally, the shelter model was implemented in Thessaloniki where the systemic analysis for building and utility losses were brought together with socio-economic factors related to desirability to evacuate and seek shelter as "Hot Spots" for shelter needs using an interactive decision-support tool (Fig. 4.5).

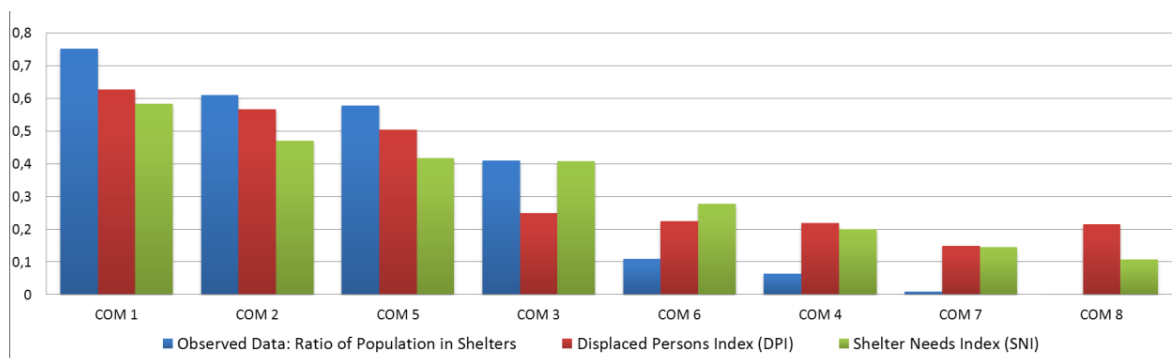


Fig. 4.4 Ratio of actual population in shelters (Observed data) shown against the ranking of displaced persons and shelter needs in the 8 COMs after the 2009 L'Aquila earthquake

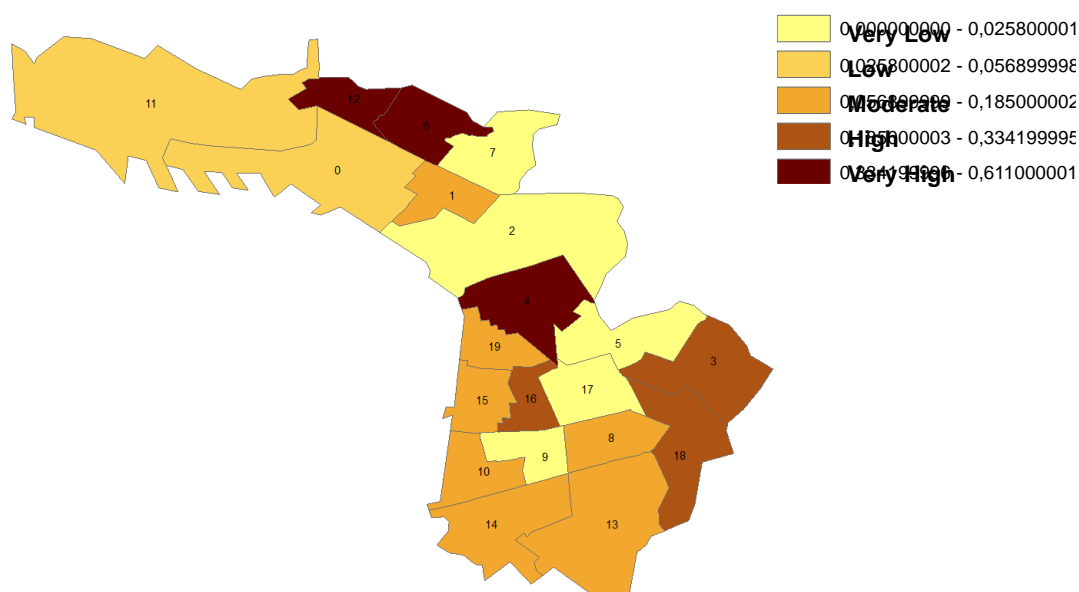


Fig. 4.5 Ranking of Shelter Needs Index (SNI) for sub-city districts of Thessaloniki

4.2 HEALTH IMPACT MODEL

Similar to the shelter needs model, the health impact model presents a new method for integrating social vulnerability in modeling health impacts caused by earthquake damage. The health impact model is a function of casualties (number of dead and injured) produced by an earthquake and a number of impact factors that can aggravate health impacts further. First, a semi-empirical casualty model was developed in SYNER-G using a database for historic earthquake casualties collected for two large Italian earthquakes: Irpinia 1980, 214 municipalities and Friuli 1976, 26 municipalities. To link social impacts of health and health-care services to a systemic seismic vulnerability analysis, a multi-criteria decision model has been developed and appropriate social indicators for individual health impacts and for health care impacts were identified based on literature research, and tested using available European statistical data. The impact factors indicators developed are based on the following criteria: 1) social vulnerability factors which affect vulnerability and post-earthquake health of at-risk populations (e.g. demographic characteristics such as age, education, occupation and employment); 2) baseline health status factors (e.g. health expenditures, health care access, mortality, morbidity); 3) hospital treatment capacity factors and 4) environmental health factors (such as residential crowding, sanitation, etc.). The results were used to develop a health impact model that describes the processes and links between socio-demographic, environmental, epidemiological and health behaviour parameters to increased short-term health impacts. Furthermore, healthcare systems parameters are integrated in a healthcare capacity model to assess secondary impacts on the overall health care delivery to the affected population.

5 Systemic vulnerability specification

Based on the general methodology developed within the project, each of the four systems considered in SYNER-G (Buildings and aggregates, Gehl et al. 2011; utility networks, Esposito and Iervolino 2011b, Argyroudis et al. 2011, Pinto et al. 2011c; transportation networks, Pinto et al. 2012a; critical facilities, Pinto et al. 2012b) has been specified according to the features composing the SYNER-G approach:

- Taxonomy of the components within the system.
- Solving algorithms used to assess the system's performance.
- Nature of the interactions with components from other systems.

5.1 GENERAL SPECIFICATION

5.1.1 Taxonomy of components within each system

Following the framework of the general SYNER-G methodology, each class of systems is composed of sub-classes that are used to describe the various types of components, based on the geographical extent and their function within the system:

- Cell classes are used to define inhabited areas (i.e. Buildings System) and contain information on buildings typologies, population or soil occupation policy.
- All network-like systems (i.e. Water Supply, Electric Power, Gas Network and Road Network) contain two types of sub-classes (Edges and Points), which are further subdivided in specific classes, according to the role played by the component within the system: network nodes can be stations, pumps, reservoirs, sources, distribution nodes, etc.
- For critical facilities such as components of the Health-Care System, they are modelled as point-like objects.

Each of the sub-classes is specified with their characteristic attributes and methods, depending on the type of system considered. For instance, initial properties of the objects may include geographic location, area, length, soil type, typology, associated fragility, capacity, connectivity with other components (for networks), etc. Once the simulation is running, the specific methods update the object properties, such as damage states, losses within each cell or remaining connectivity.

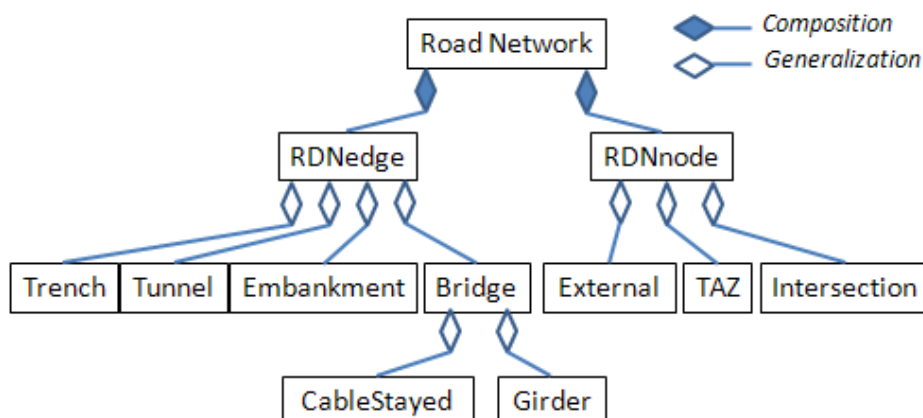


Fig. 5.1 Example of a specified UML diagram for the Road Network System

5.1.2 System evaluation and performance indicators

The way the performance of each system is assessed is also addressed in the work package. Three main types of solving algorithms are considered in the SYNER-G approach:

- Connectivity analysis: this approach removes the damaged components from the network and it updates the adjacency matrix accordingly, thus giving the nodes or areas that are disconnected from the rest of the system. This approach is used for all utility networks (water, electricity, gas) and the road transportation system.
- Capacitive analysis: for utility networks, graph algorithm can be used to optimize capacitive flows from sources (e.g. generators, reservoirs) to sinks (i.e. distribution nodes), based on the damages sustained by the network components (from total destruction to slight damages reducing the capacity).
- Fault-tree analysis: this type of approach aims to evaluate the remaining operating capacity of objects such as health-care facilities. The system is broken up into structural, non-structural or human components, each one of them being connected with logic operators.

Performance indicators, at the component or the system level, depend on the type of analysis that is performed: connectivity analysis gives access to indices such as the connectivity loss (measure of the reduction of the number of possible paths from sources to sinks). On the other hand, capacitive modelling yields more elaborate performance indicators at the distribution nodes (e.g. head ratio for water system, voltage ratio for electric buses...) or for the whole system (e.g. system serviceability index comparing the customer demand satisfaction before and after the seismic event).

5.1.3 Interdependencies

Three types of interactions between systems are considered within SYNER-G:

- “Demand” interactions: they correspond to a supply demand from a given component to another system. For instance, the presence of densely populated cells in the vicinity of a given distribution node (e.g. from a water supply or electric power system) will generate a substantial demand on the supply system. Another example could be

the number of casualties that will put a strain on the treatment capacity of health-care facilities.

- Physical interactions: they are associated with exchanges of services or supplies between systems, like the supply of potable water to inhabited cells, the supply of transportation capacities by roads or the supply of power to various network facilities (e.g. water pumps) by electric generators.
- Geographical interactions: they are involved when two components are located in the same area and when the damage of one of them is directly influencing the physical integrity of the second one. For instance, the collapse of buildings in city centres can induce the blockage of adjacent roads due the debris accumulation.

The interactions between systems that are treated in the framework of SYNER-G are listed in the table below: D stands for Demand, P for Physical and G for Geographical interactions.

Table 5.1 Interactions between systems considered in SYNER-G

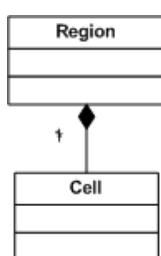
	BDG	EPN	WSS	GAS	RDN	HBR	HCS	FFS
<i>Buildings</i>	BDG		D	D	D	D G		D
<i>Power</i>	EPN	P		P	P		P	P
<i>Water</i>	WSS	P					P	P
<i>Gas</i>	GAS	P					P	P
<i>Roads</i>	RDN	P					P	P
<i>Harbour</i>	HBR							
<i>Hospitals</i>	HCS					D		
<i>Fire Sys.</i>	FFS							

It should be noted that the “demand” interactions are considered as static, since they are estimated only once, in order to avoid the presence of any feedback loops that would introduce dynamic systems, which are left of the SYNER-G scope. As a result, this table of interdependencies governs the order in which each system has to be computed during the simulation runs, in order to maintain a straightforward analysis scheme.

5.2 DESCRIPTION OF THE CONSIDERED SYSTEMS

5.2.1 Building and aggregates

Taxonomy



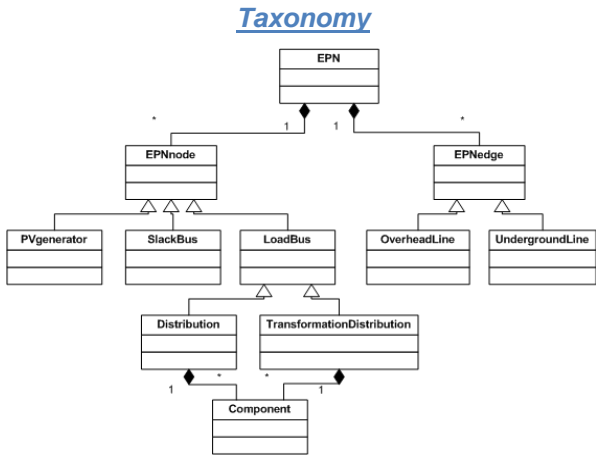
Performance indicators

cell/city/region

Nb of yielding buildings
Nb of collapsed buildings
Utility losses
Accessibility losses
Habitability

5.2.2 Utility Networks

5.2.2.1 Electrical power Network



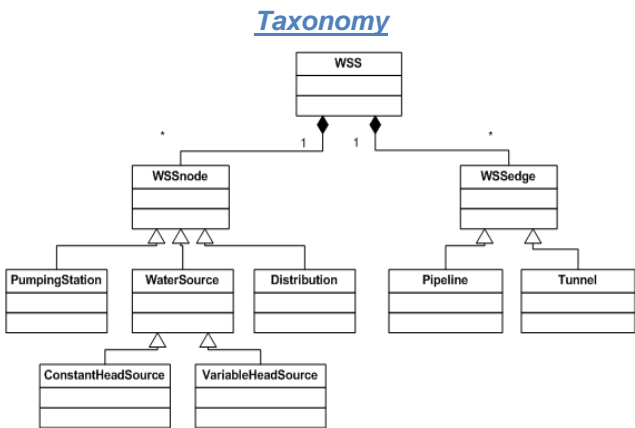
Analysis

- **Connectivity**
- **Serviceability**

Performance indicators

- **Component:**
Voltage ratio
power ratio
connectivity
- **System:**
Average ratios
Connectivity loss

5.2.2.2 Water and waste water network



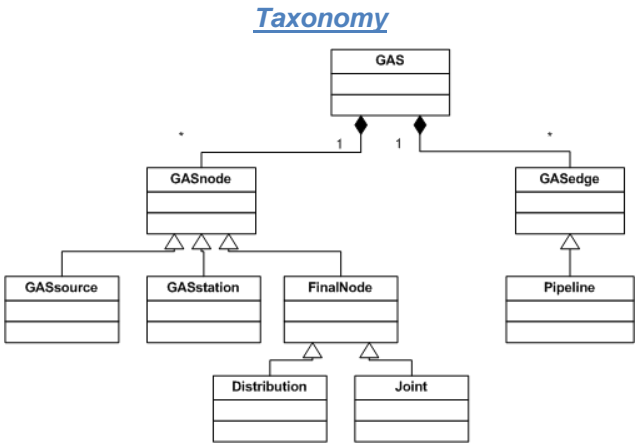
Analysis

- **Connectivity**
- **Serviceability**

Performance indicators

- **Component:**
Head Ratio
Damage Consequence Index
Upgrade Benefit Index
- **System:**
Average Head Ratio
System Serviceability Index

5.2.2.3 Gas and oil Network



Analysis

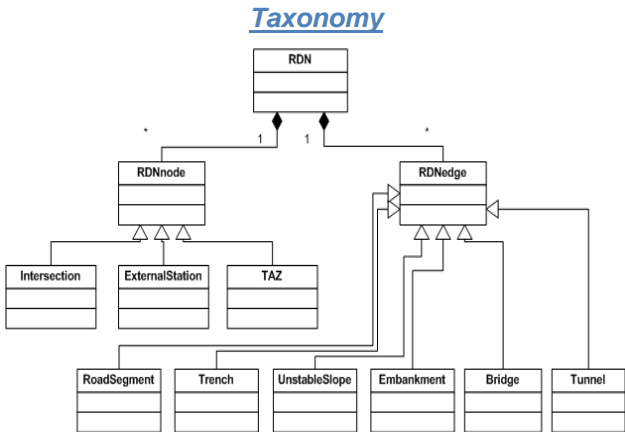
- **Connectivity**
- **Serviceability**

Performance indicators

- Component:
Head Ratio
Damage Consequence Index
Upgrade Benefit Index
- System:
Average Head Ratio
System Serviceability Index

5.2.3 Transportation network

5.2.3.1 Road network

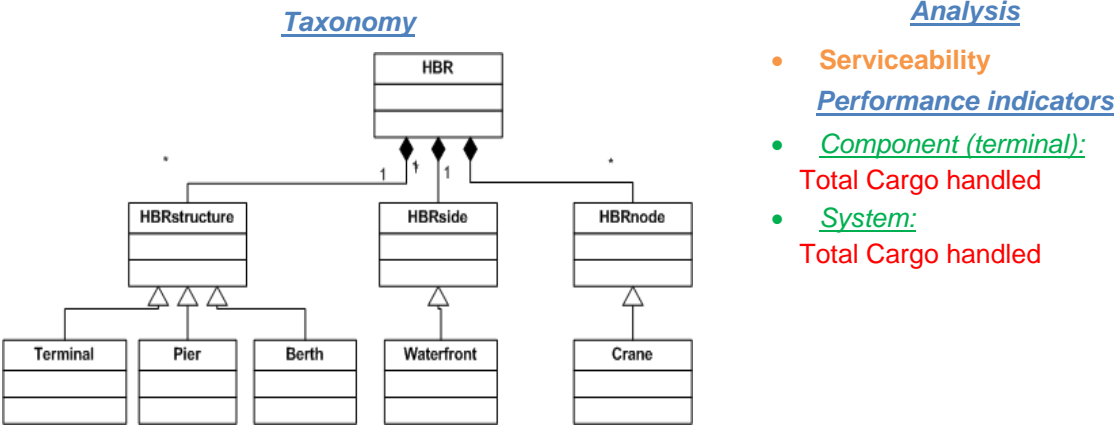


Analysis

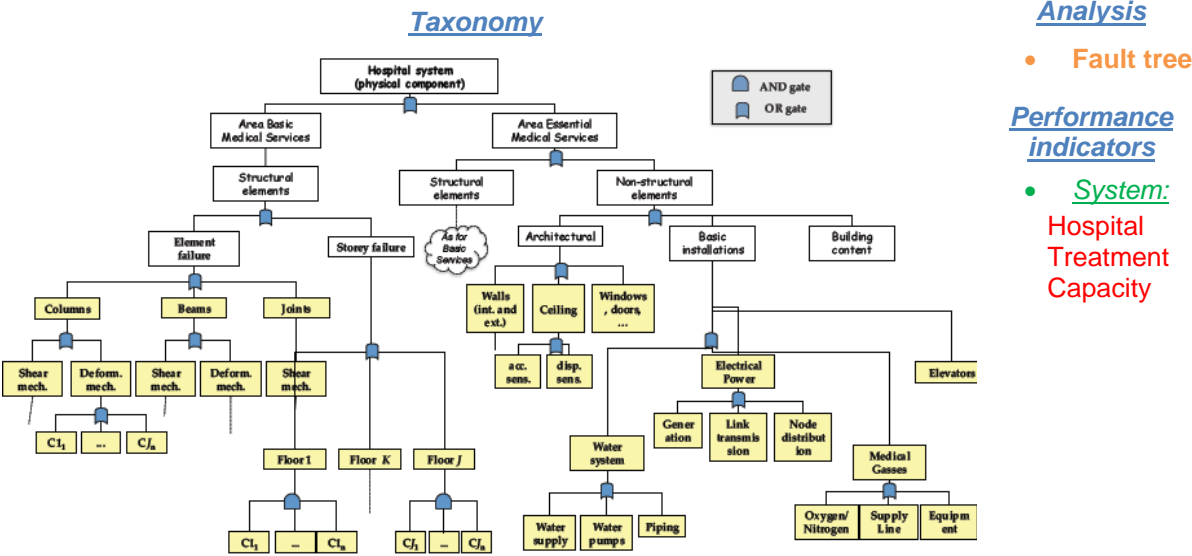
- **Connectivity**
- Performance indicators
 - Component (Traffic Analysis Zone):
Connectivity
 - System:
Simple Connectivity Loss
Weighted Connectivity loss

5.2.4 Critical Facilities

5.2.4.1 Harbour facilities



5.2.4.2 Health care system



6 SYNER-G toolbox and web portal

A comprehensive tool box has been developed (**EQvis**) containing several pre and post-processing tools as well as other plug-ins such as the **prototype software** (OOFIMS), the Fragility Manager Tool, the MCDA software for modelling shelter needs and health impact (Fig. 6.1). The product EQvis (European Earthquake Risk Assessment and Visualisation Software) is an open source product that allows owners, practicing engineers and researchers the realistic risk assessment on systemic level (Fig. 6.2). It has been based on the similar pre and post-processing modules of MAEviz (see Schäfer and Bosi 2013 for more information).

The field of analyses that can be performed with EQvis is very large, e.g. Hazard Computation, Structural Damages, Functionalities, Repair Cost Estimations, Cost Benefit Analyses, Utility Network Damages, Multi Attribute Utility Analyses, Shelter Needs, Social Vulnerability, Temporary Housing, etc.

The Fragility Manager Tool offers the user to combine certain fragility functions and store them directly on the platform and use them. The platform can take the fragility curves for all buildings and bridges and assign them to all the objects correctly. In the next step different analyses can be computed.

Socio-economic analysis tools delivered another plug-in: The socio-economic module. The connection between the OOFIMS module and the socio-economic module was computed and the output was again done through GIS data format.

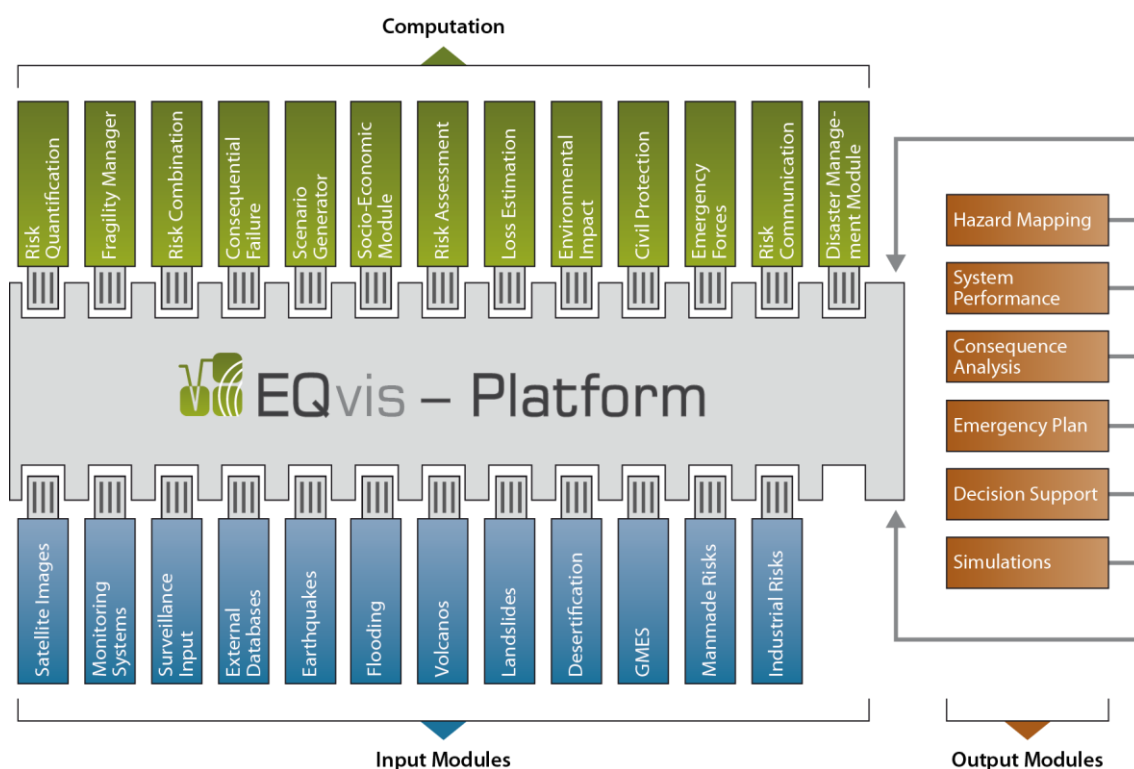


Fig. 6.1 The plug-in based structure of the software

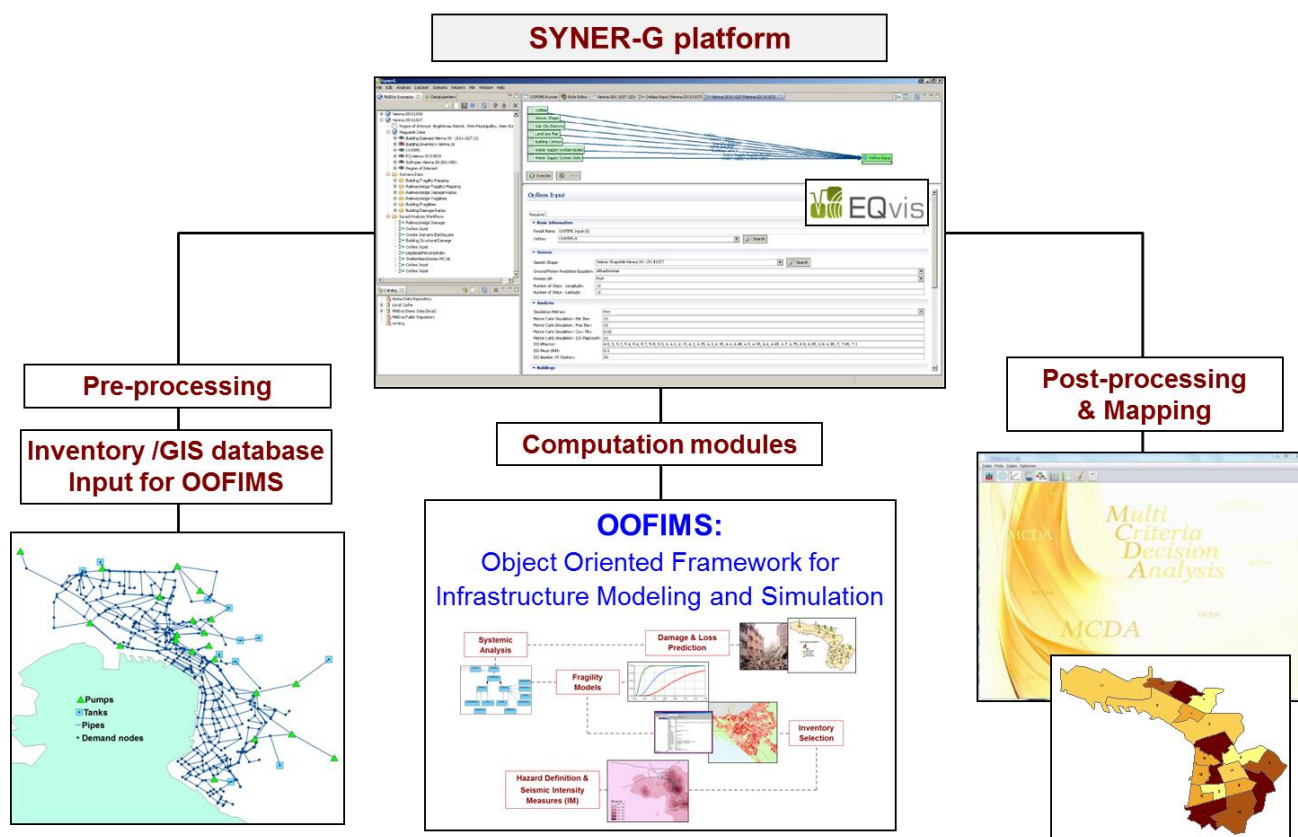


Fig. 6.2 Layout of the SYNER-G platform

7 Pilot studies and application of SYNER-G methodology

7.1 INTRODUCTION

This report presents, in a synthetic way the application of the SYNER-G methodology and tools to the selected case studies at urban level (city of Thessaloniki in Greece, city of Vienna in Austria) and regional level (gas network of L'Aquila in Italy, transportation network in South Italy, electric power network in Sicily) as well as in complex infrastructures (hospital facility and health-care regional system in Italy, harbour of Thessaloniki in Greece) accounting for inter- and intra-dependencies among infrastructural components.

The object-oriented paradigm (OOP) has been adopted for the purpose of modeling the infrastructure and the seismic hazard. Within the OOP the problem is described as a set of *objects*, characterized in terms of *attributes* (or *properties*) and *methods*, that interact with each other. Objects are *instances* (concrete realizations) of *classes* (abstract models, or *templates* for all objects with the same set of properties and methods). The SYNER-G prototype software includes an object-oriented representation of a subset of all the systems in the taxonomy.

This report is related to other SYNER-G reference reports and deliverables, which are needed for a comprehensive understanding of the applications (e.g. Pitilakis and Argyroudis 2013; Kaynia et al. 2011; Gehl et al. 2011; Franchin et al. 2011; Pinto et al. 2011c; Weatherhill et al. 2011b; Franchin et al. 2011; Pinto et al. 2012a,b among others).

7.2 THE CASE STUDIES

The following case studies have been chosen for the application and validation in terms of applicability of the SYNER-G methodology and tools:

City of Thessaloniki in North Greece, located in a high seismicity area. The study area covers the municipality of Thessaloniki which is divided in 20 Sub City Districts as defined by Eurostat and Urban Audit approach (Fig. 7.1). The case study includes the following elements: building stock (BDG), road network (RDN), water supply system (WSS) and electric power network (EPN). The networks are comprised by the main lines and components and cover the wider Metropolitan area. The internal functioning of each network is simulated and a connectivity analysis is performed. Moreover, specific interdependencies between systems are considered: EPN with WSS (electric power supply to pumping stations), RDN with BDG (road blockage due to building collapses), BDG with EPN and WSS (displaced people due to utility loss). An accessibility analysis to hospital facilities and shelter areas considering the damages in RDN is also performed and a shelter demand analysis based on a multi-criteria approach is applied.

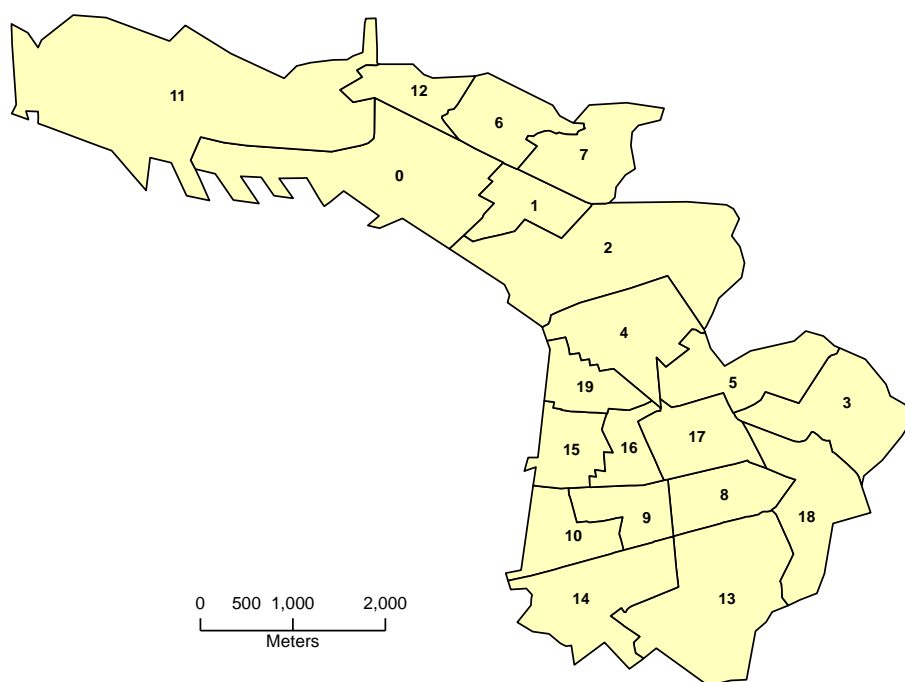


Fig. 7.1 Sub-city districts (SCD) of Thessaloniki study area as defined by Urban Audit

City of Vienna in Austria, located in a low seismicity area. The region of interest for the case study is the Brigittenau district, which is the 20th district of Vienna (Fig. 7.2). A specific building identification procedure has been formulated to identify and inventory buildings that were considered in the case study. Both deterministic and probabilistic analyses have been performed. The EQvis software is used for the deterministic analysis, while the SYNER-G OOFIMS runner performed the probabilistic analysis including buildings, water supply system, road and electric power network with specific interdependencies between them.



Fig. 7.2 The city of Vienna with the part of the 20th district

The gas system of L'Aquila in Italy. The medium-pressure portion of the L'Aquila gas system was selected (Fig. 7.3). It is characterized by 3 M/R stations, 209 Reduction Groups, and pipelines at medium pressure, either made of steel or high density polyethylene. The network is comprised of 602 nodes and 608 links. A connectivity analysis is performed considering ground shaking and ground failure due to landslides.

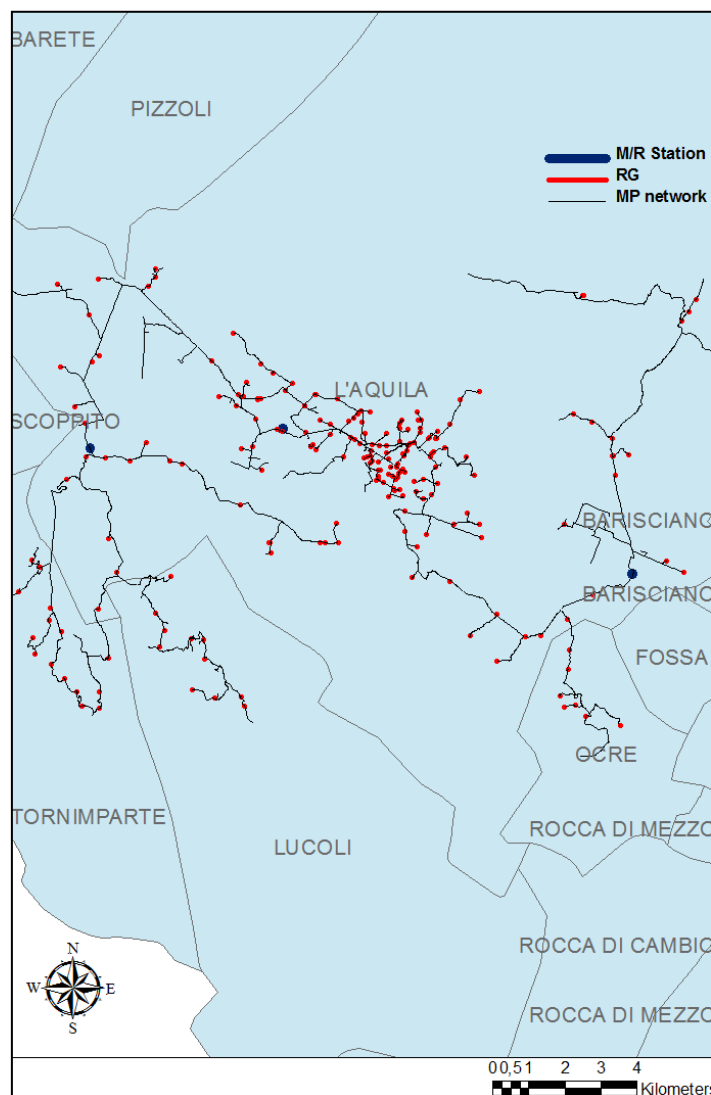


Fig. 7.3 Case study of L'Aquila gas system

The road network in Calabria region, Southern Italy. A data reduction process was performed in order to remove the irrelevant components at the regional scale. A pure connectivity analysis is performed considering 2,861 nodes and 5,970 edges of the network (Fig. 7.4). The seismic hazard is modeled through 20 faults taken from the Italian DISS database.

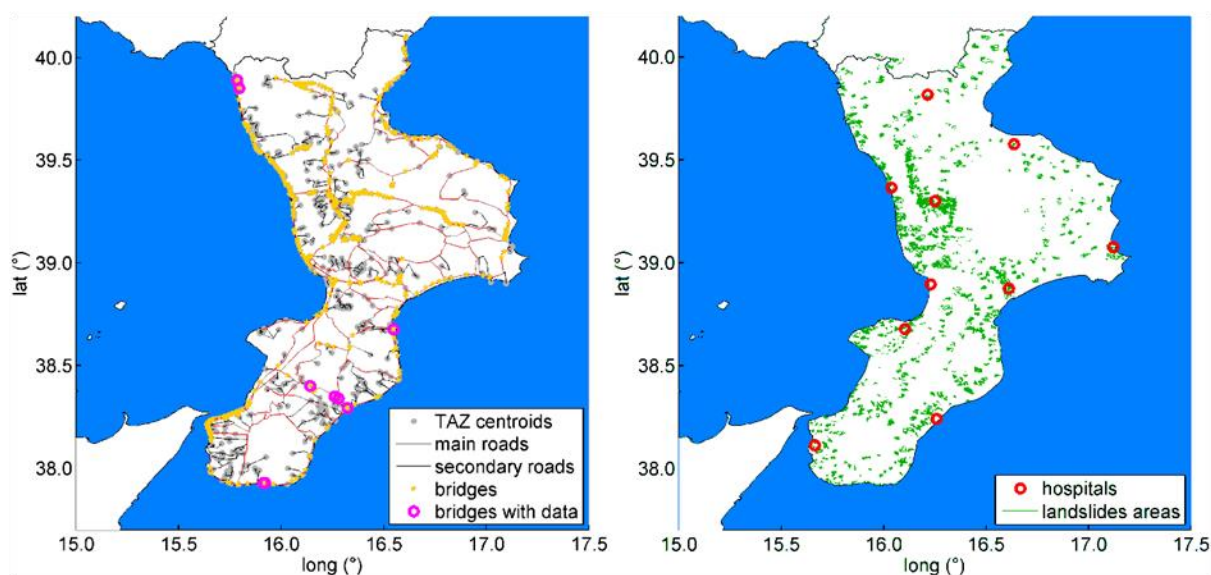


Fig. 7.4 Calabria region road network topology (left) and location of hospitals and landslides areas (right)

The electric power network of Sicily. A capacitive study is performed, with power flow analysis that follows the analysis of short-circuit propagation, in which circuit breakers are active components playing a key role in arresting the short-circuit spreading. The substations are not modeled as vulnerable points (Fig. 7.5); their full internal logic is modeled to account for partial functioning. The network is composed of 181 nodes and 220 transmission lines.

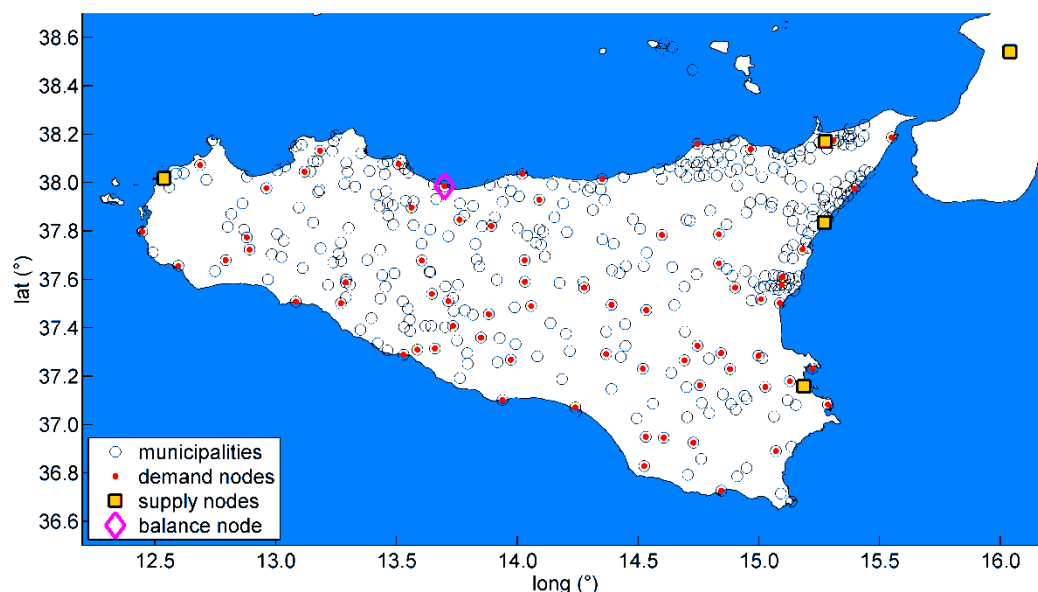


Fig. 7.5 Position of municipalities and EPN nodes in Sicily case study

Hospital facility and health-care regional system in Italy. The response of a regional health-care system depends on the hospital's performance but also on other factors, among which the response of the road network is of primary importance. In this case study the main goal is to forecast the expected impact in terms of: a) victims that cannot be hospitalised; b) hospitals that cannot provide medical care to the victims; c) city/villages that are not served by a functioning hospital within a "reasonable" distance. A hypothetical region with an

infrastructure (system of systems) composed of a road network (RDN) and a health care system (HCS) was examined (Fig. 7.6).

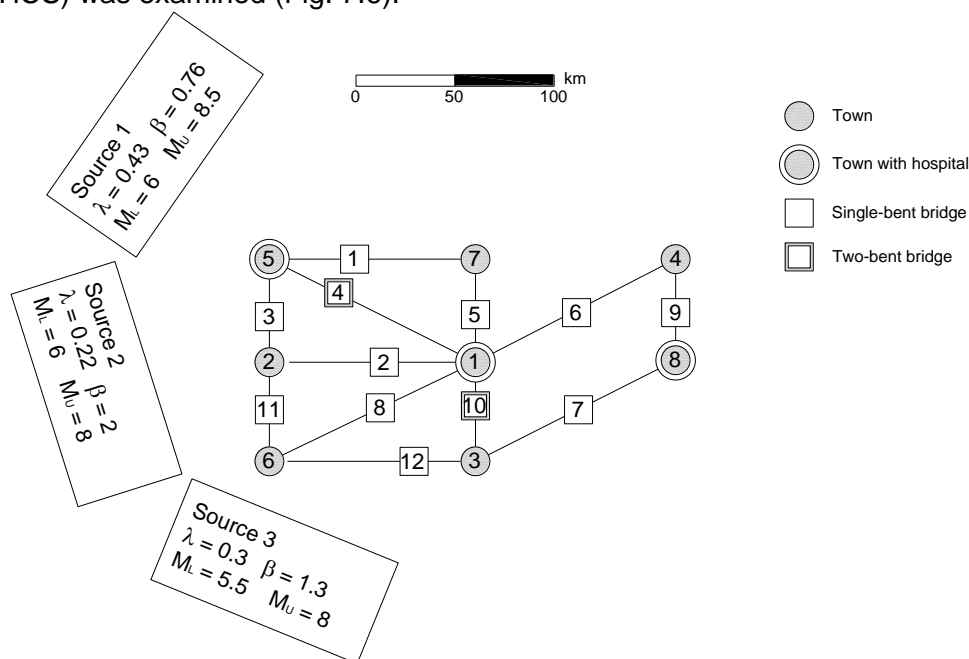


Fig. 7.6 The hypothetical study area

The vulnerability assessment is based on a representative large medical centre located in south Italy which should be able to provide all the “essential” medical services required to take care of the victims of a natural disaster under emergency conditions. The facility consists of a main body composed of two separate RC buildings connected by two tower structures (Fig. 7.7). The vulnerability of the facility is evaluated by non-linear dynamic analyses taking into account the response of structural as well as non-structural elements.

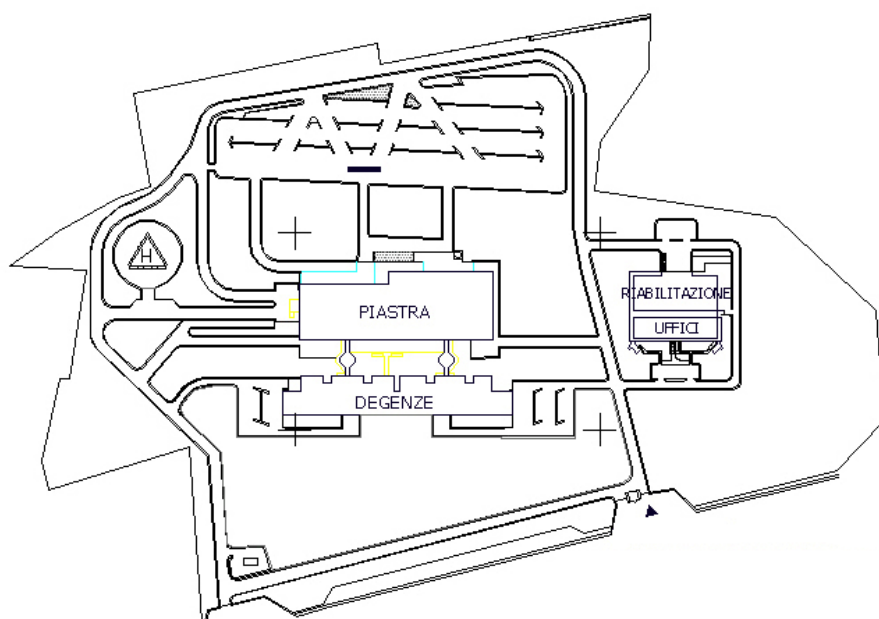


Fig. 7.7 General plan of the examined hospital system

The harbour of Thessaloniki. The assessment of the systemic vulnerability of Thessaloniki's port is performed. The port covers an area of 1,550,000 m² and trades approximately 16,000,000 tons of cargo annually, having a capacity of 370,000 containers and 6 piers with 6,500m length (Fig. 7.8). In the case study, waterfront structures, cargo handling equipment, power supply system, roadway system and buildings are examined. In particular, for the systemic analysis, waterfront structures of a total 6.5 km length, 48 crane-nodes and two Terminals (one container and one bulk cargo) are considered. The interactions accounted for in the analysis are the supply of EPN to cranes and the road closures due to building collapses.



Fig. 7.8 Thessaloniki's port

Table 7.1. Summary of elements at risk in each case study

Network	Vulnerable Components	Nodes	Edges	Comments
City of Thessaloniki				
BDG	buildings	27,738 buildings (92% R/C, 8% masonry)	-	20 SCDs, buildings, 2,630 building blocks, population: 376,589 (municipality), 790,824 (city) population
RDN	roads, bridges	594 (15 external nodes, 127 TAZ's centroids, 452 simple intersections)	674 (60 bridges)	
EPN	substations	30 (1 generator/	29 lines	

		transformation substation, 8 transmission/transformation substations, 21 demand nodes)		
WSS	pipelines	477 (437 demand nodes, 21 pumping stations, 11 tanks)	601 (24 diameter values between 500-3,000mm, construction materials: asbestos cement, cast iron, PVC, welded steel)	
City of Vienna/ Deterministic analysis				
BDG	buildings	550 (30% R/C, 70% masonry)	-	Brigittenau district (20th district of Vienna)
RWN	tunnels, bridges	34 bridges, 21 tunnels	-	
RDN	roads, bridges	67 bridges, 9617 road segments	-	
City of Vienna/ Probabilistic analysis				
BDG	Buildings	550 (30 % R/C, 70 % masonry)	-	3 SCDs, 11 Building Census, population: 35402
RDN	roads	101 (9 TAZ's centroids, 4 external nodes, 88 simple intersections)	161	
WSS	pipelines	110 (107 demand nodes, 3 tanks)	108 (4 diameter values: 1600, 1200, 800 and 500mm, construction material: cast iron)	
EPN	substations	109 (2 generators, 5 transmission/transformation substations, 102 demand nodes)	107 lines	
The gas system of L'Aquila in Italy				
GAS	pipelines, M/R stations	602 (3 sources, 209 Reduction Groups, 390 joints)	608	Both TGD and PGD hazards
The road network in Calabria region, Southern Italy				
RDN	road segments (landslides and co-seismic rupture)	2861 (422 TAZ's centroids and simple intersections)	5970 (bridge/road segments and main/secondary	10 health care facilities are considered

	bridges (ground shaking)		roads)	
The electric power network of Sicily				
EPN	micro-components in substations (ground shaking)	181 (1 balance node, 5 supply nodes, 175 demand nodes)	199 overhead transmission lines (26 HV, 160 MV, 13 LV), 21 lines with transformer	390 municipalities fed
Hospital facility and health-care system in Italy				
	RDN (ground shaking)	12 bridges, 8 TAZs		
	HCS (ground shaking)	3 hospitals		
The harbour of Thessaloniki				
HRB	cranes waterfronts (ground shaking and ground failure)	72 (48 cranes, 24 pier edges)	17 (waterfront – gravity type)	
EPN	substations	75 (1 generator, 8 transmission substations, 17 distributions substations, 49 demand nodes)	74 lines	
BDG	buildings (ground shaking)	88 buildings (72% R/C, 9% URM, 19% Steel)	-	4 building blocks
RDN	road segments (ground failure)	7 (4 TAZ's centroids, 3 simple intersections)	5 (road segments)	

7.3 FRAGILITY CURVES

The fragility curves used in the applications are summarized in Table 7.2 for each vulnerable component. The fragilities curves are compiled and described in Reference Report 4 (Kaynia 2013).

Table 7.2 Fragility curves used in the case studies

System	Component	Classification	IM Type	Fragility curves
Thessaloniki case study				
EPN	transmission stations	open, mixed and closed-type with low level of building seismic design	PGA	SRM-LIFE (2003-2007)
WSS	pipelines	pipe material and diameter, joint type, soil type	PGV, PGD	ALA (2001)
BDG	RC buildings masonry buildings	see Table 7.3 , Table 7.4	PGA	see SYNER-G report D6.1 (Argyroudis et al. 2013)
RDN	bridges	see Table 7.5	PGA	see SYNER-G report D6.1 (Argyroudis et al. 2013)
	road pavements	urban roads (2 lanes)	PGD	NIBS (2004)
	roads (blockage due to buildings collapses)	road-building distance, building height	PGA	SYNER-G (Gehl et al. 2011)
Vienna case study				
BDG	RC buildings masonry buildings	see Table 7.6		
RDN	road pavements	urban roads (2 lanes), major roads (4 lanes)	PGD	NIBS (2004)
WSS	pipelines	pipe material and diameter, joint type, soil type	PGV, PGD	ALA (2001)
EPN	transmission stations	open, mixed and closed-type	PGA	SRM-LIFE (2003-2007)
L' Aquila case study (gas network)				
GAS	pipes	pipe material, pipe diameter	PGV, PGD	ALA (2001)
	M/R stations	un-anchored compressor stations	PGA	NIBS (2004)
Transportation network in Italy				
RDN	bridges	main road, secondary road	PGA	see SYNER-G report D3.6 (Fardis et al. 2011)
	road pavements	main road, secondary road	PGD	see SYNER-G report D3.7 (Kaynia et al. 2011)
Electric power network in Italy				
EPN	Transformation/ distribution and distribution substations	microcomponents	PGA	see SYNER-G report D3.3 (Pinto et al. 2010)

Hospital facility and health-care system in Italy				
HCS	hospital facility (fault tree analysis)	non structural (architectural elements, basic installations, equipment/contents) & structural elements	PGA	see SYNER-G report D3.10 (Pinto et al. 2011b)
RDN	bridges	single-bent overpasses, two-bent overpasses	PGA	
Harbour of Thessaloniki				
HRB	waterfronts	H>10m, Vs=250m/s H<=10m, Vs=250m/s	PGA, PGD	Kakderi and Pitilakis (2010), NIBS (2004)
	cranes/ cargo handling equipment	non-anchored	PGA, PGD	NIBS (2004)
EPN	distribution substations	low voltage, non-anchored	PGA	NIBS (2004)
	transmission stations	open, mixed and closed-type with low level of building seismic design	PGA	SRM-LIFE (2003-2007)
RDN	road pavements	urban roads (2 lanes)	PGD	NIBS (2004)
BDG	R/C and URM buildings	masonry: urm, stone/brick, low/medium height R/C: structural system, infill walls, building height, level of seismic design	PGA	Kappos et al. (2006)
	steel buildings	steel frame with unreinforced masonry infill walls, low-height	PGA	NIBS (2004)

Table 7.3 Parameters of fragility curves for RC buildings in Thessaloniki

Structural type	Seismic code	Height	Yielding		Ultimate	
			Median (g)	St. deviation	Median (g)	St. deviation
Infilled frames	1959	L	0.25	0.41	0.74	0.26
		M	0.30	0.40	0.57	0.26
		H	0.41	0.40	0.38	0.41
	1984	L	0.23	0.41	1.03	0.44
		M	0.32	0.41	0.96	0.26
		H	0.39	0.43	0.92	1.30
Pilotis	1959	L	0.12	0.41	0.36	0.26
		M	0.12	0.41	0.29	0.26
		H	0.27	0.41	0.29	0.26
	1984	L	0.11	0.41	0.50	0.44
		M	0.14	0.41	0.50	0.32
		H	0.31	0.41	0.66	0.45
Dual	1959	L	0.12	0.49	0.18	0.69
		M	0.15	0.50	0.33	0.51
		H	0.21	0.45	0.24	0.37
	1984	L	0.12	0.50	0.29	0.72
		M	0.15	0.50	0.34	0.39
		H	0.20	0.45	0.50	0.89
	EC8	L	0.09	0.50	0.38	0.41
		M	0.13	0.50	0.41	0.40
		H	0.15	0.50	0.45	0.39

Table 7.4 Parameters of fragility curves for masonry buildings in Thessaloniki

		Median (g)					Standard deviation
		DG1	DG2	DG3	DG4	DG5	All damage grades
Low-rise	Rigid floors	0.02	0.24	0.50	-	-	0.6
	Flexible floors	0.02	0.12	0.24	0.40	0.60	0.6
Mid-rise	Rigid floors	0.04	0.18	0.35	0.55	0.80	0.6
	Flexible floors	0.02	0.06	0.12	0.20	0.36	0.6

Table 7.5 Bridge types in the Thessaloniki study area

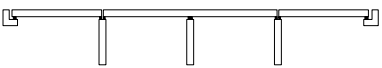
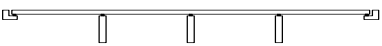

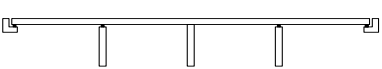
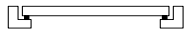
Structural system	Type	Transverse translation at ends	Construction year	Pier Type
 Bearings, deck with expansion joints	B01	free	1984	multi-column
	B02	free	1986	multi-column
	B05	free	1985	multi-column
	B09	free	1990	single-column
	B22	free	1991	multi-column
 Bearings, continuous deck	B03	free	1991	wall
	B06	free	2002	multi-column
	B17	free	1992	wall
	B18	free	1992	wall
 Monolithic connection, continuous deck	B04	restrained	2000	multi-column
	B19	free	2004	wall
 Monolithic connection and bearings, continuous deck	B07	restrained	2003	single-column
	B08	restrained	2003	single-column
	B15	restrained	2002	single-column
	B20	free	1985	wall
	B21	free	1985	wall
 Single-span bridges on bearings	B10	free	1976	-
	B11	free	1985	-
	B12	free	1990	-
	B13	free	1985	-
	B14	free	1987	-
	B16	free	1994	-

Table 7.6 Fragility curves used in Vienna test case for RC and masonry buildings

RC buildings	
Fragility curves	IMT
Borzi et al. 2007-RC - 8 storeys-seismicallydesigned (c = 10 %)	PGA
Borzi et al. 2007-RC - 4 storeys-seismicallydesigned (c = 10 %)	PGA
Erberik 2008 - RC - low rise bare frame LRBR	PGV
Erberik 2008 - RC - mid-rise bare frame MRBR	PGV
Erberik 2008 - RC - mid-rise infilled frame MRIR	PGV
Erberik and Elnashai 2004 – RC flat slab - mid-rise infilled frame MRINF	Sd
Kappos et al. 2003 - RC3.1-HR-HC	PGA
RISK-UE 2003 - RC moment frame-HR-HC-UTCB hybrid approach	Sd
RISK-UE 2003 - RC moment frame - LR-HC-UTCB hybrid approach	Sd
RISK-UE 2003 - RC moment frame - MR-HC-IZIIS approach	Sd
Vargas et al. 2010 - RC - 8 storeys	Sd
Masonry buildings	
Fragility curves	IMT
Borzi et al. 2008 - MA Brick - High percentage voids - 2 storeys	PGA
LESSLOSS 2005-adobe and rubble stone - 8-15 storeys - Lisbon	Sd
RISK-UE 2003 - M12-HR-UNIGE approach	Sd
Borzi et al. 2008 - MA brick-low percentage voids - 4storeys	PGA
RISK-UE 2003 - M12-LR-UNIGE approach	Sd

7.4 SEISMIC AND GEOTECHNICAL HAZARD

Following the specification provided in SYNER-G report D2.13 (Weatherill et al. 2011), the ground motion prediction equation introduced by Akkar and Bommer (2010) is applied for the estimation of the ground motion parameters on rock, while the spatial variability is modeled using appropriate correlation models. For each site of the grid the averages of primary IM from the specified GMPE are calculated, and the residual is sampled from a random field of spatially correlated Gaussian variables according to the spatial correlation model. The primary IM is then retrieved at vulnerable sites by distance-based interpolation and finally the local IM is sampled conditional on primary IM.

To scale the hazard to the site condition different amplification methods are available in the SYNER-G prototype software: Present Eurocode 8 provisions, Eurocode 8 amplification as modified by Pitilakis et al. (2012), NEHRP, Choi&Stewart, context-specific. Depending on the available information for site characterization an amplification method is selected.

For the liquefaction and landslide hazard the modeling approach of HAZUS (NIBS 2004) is adopted for the estimation of the permanent ground displacements, PGD, at the vulnerable sites. A detailed description of the entire hazard model adopted in the methodology and

hence implemented in the SYNER-G prototype software can be found in Franchin et al. (2011) and Weatherhill et al. (2011b).

The main features for the seismic and geotechnical hazard assessment are outlined in Table for each case study. For more information the reader is referred to SYNER-G reference report 6 (Pitilakis and Argyroudis 2013).

Table 7.7 Summary of seismic and geotechnical hazard for the case studies

Case study	Seismic Hazard	GMPE	Soil amplification	Liquefaction susceptibility	Landslide susceptibility
City of Thessaloniki	areaFault: 5 zones/ SHARE project	Akkar and Bommer (2010)	EC8 (A, B, C soil classes)	Very high, moderate, none / HAZUS (NIBS 2004)	no
City of Vienna/ Deterministic analysis	- Neulengbach earthquake (1590), M=6.0 - Method testing, M=7.0	Campbell and Borzognia (2006)	EC8 (A, B, C soil classes)	no	no
City of Vienna/ Probabilistic analysis	areaFault: 4 seismic zones /SHARE project	Akkar and Bommer (2010)	EC8 (A,B,C soil classes)	no	no
The gas system of L'Aquila in Italy	simpleFaultGeometry: Paganica fault Mw=6.3, occurrence rate = 1/ 750	Akkar and Bommer (2010)	Vs30 values/ Akkar and Bommer (2010)	no	classification according to lithological group, slope angle, and ground-water condition, Kc=0.05-0.6g/ HAZUS (NIBS 2004)
The road network in Calabria region, Southern Italy	simpleFaultGeometry: 20 faults/ Italian DISS and SHARE project	Akkar and Bommer (2010)	no soil classification data available	yes/ HAZUS (NIBS 2004)	2089 active landslides areas / HAZUS (NIBS 2004)
The electric power network of Sicily	simpleFaultGeometry: 18 faults/ Italian DISS and SHARE project	Akkar and Bommer (2010)	no soil classification data available, IM values computed on rock	no	no
Hospital facility and health-care system in Italy	areaFault: 3 seismic zones (hypothetical)	Akkar and Bommer (2010)	no	no	no
The harbour of Thessaloniki	areaFault: 5 zones/ SHARE project	Akkar and Bommer (2010)	EC8 (A, B, C soil classes)	very high/ HAZUS (NIBS 2004)	no

7.5.1 City of Thessaloniki, Greece

Different methods are implemented in the SYNER-G tool to compute the different indicators required for the assessment of the building aggregates performances:

All these methods are chained in Fig. 7.9 and described in detail by Gehl et al. (2011).

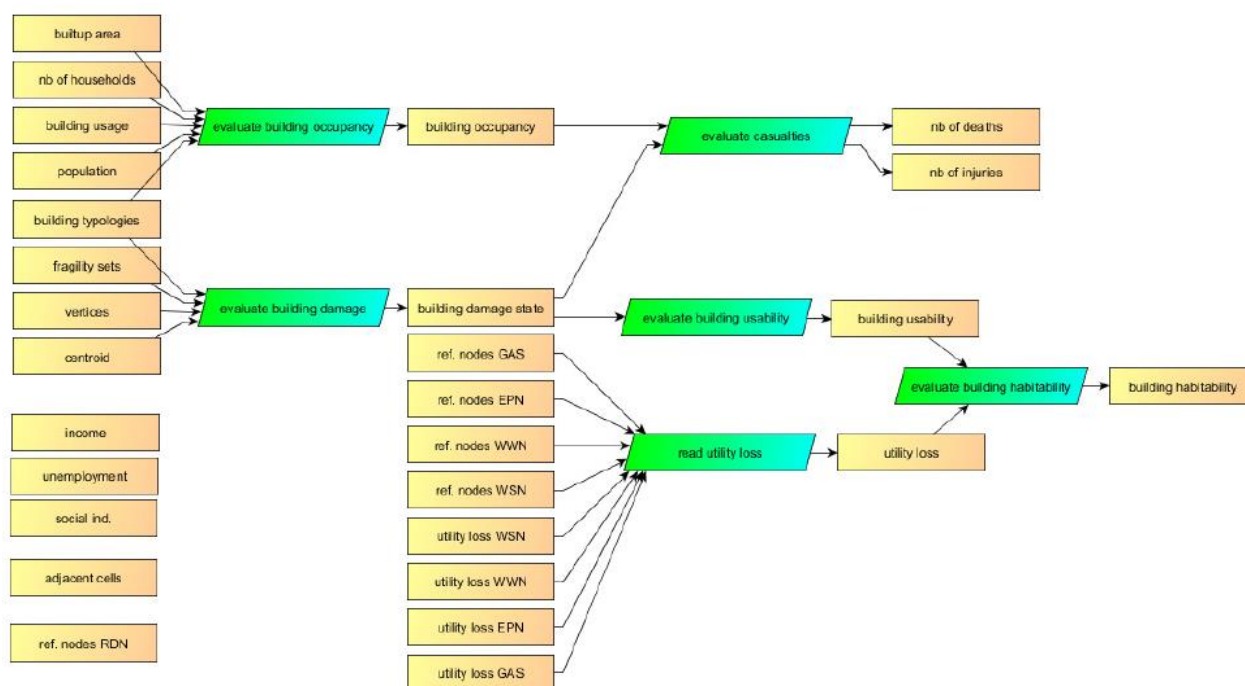


Fig. 7.9 Flowchart of the building class computation

The analysis performed in this application is based on connectivity only. Power flow analysis (see D5.2 Pinto et al. 2011c) could not be applied, since detailed data about the substations layout and their micro- and macro-components are not available. The set of subsystems connecting (1) generator (non-vulnerable) to transmission substations (vulnerable), (2) transmission substations to distribution substations (assumed non-vulnerable in this

application), and (3) distribution substations and demand nodes, are analysed separately, in order to retrieve their functionality (isolated/non-isolated state) of each demand node. Demand nodes (non-vulnerable) are located at the pumping stations of the WSS. The interaction with the WSS is simulated through the connection of WSS pumping stations with the reference EPN load bus (here substation), as an approximation of analysing the whole EPN distribution system. More details are available in D6.1 (Argyroudis et al. 2013) and Reference Report 6 (Pitilakis and Argyroudis 2013).

The electric power network is made up of nodes and edges/lines connecting them. As a consequence, the EPN class is the composition of EPNedge and EPNnode classes, that are both abstract (see section 5.2.2.1). In this connectivity analysis, the first one is the generalization of EPN *Line* (non-vulnerable), while the second one is the generalization of *Generator* (non-vulnerable), *Transmission* substations (vulnerable), distribution *Substations* (vulnerable) and EPN Demand nodes (non-vulnerable).

Water supply system

The WSS class is the composition of WSSnode and WSSlink abstract classes, of which the first is the generalization of the Pipe class, while the second is the generalization of the DemandNode, WaterSource and PumpingStation classes (see section 5.2.2.2). In particular, the WaterSource abstract class is the generalization of the VariableHeadWaterSource and ConstantHeadWaterSource classes. The analysis performed in this application is based on connectivity only.

An important interdependence considered within SYNER-G is between the WSS and EPN, in particular about the electric power supply to the pumping stations. If a pump serving a source node is not fed by the reference EPN node, then the pump itself is considered out of service and the relative WSS node removed from the system for the connectivity analysis.

The list of properties of the WSS class is given in detail in SYNER-G report D5.4 (Argyroudis et al. 2011).

Road network

Similarly to other Network classes, a road network is made up of *nodes* and *links/edges* connecting them. As a consequence, the RDN class is the composition of the *RDNnode* and *RDNedge* abstract classes (see section 5.2.2.3).

Additional developments have been implemented for Thessaloniki case study in order to simulate the road blockage due to collapsed buildings, the road blockage due to collapsed bridges and the aggregation of functionality losses for connectivity evaluation (see also SYNER-G report D6.1, Argyroudis et al. 2013). In particular, the following procedure is adopted to account for the functionality of the RDN edge.

During the simulation, an edge can be in the following states:

- Broken: 0 or 1 (direct physical failure)
- BlockedbyBuilding: 'open', 'open for emergency', 'closed'
- BlockedbyBridge: 0 or 1

These state variables appear in the output attributes of the simulations and they are used to update the adjacency matrix of the RDN class. This matrix represents all working edges that link two nodes by a 0, and the values are 1 otherwise. For each simulation, the values in the adjacency matrix are updated to account for the loss of functionality of some edges (i.e., connectivity analysis). Since here the edge can be disrupted by several causes, the logical

tree presented in Fig. 7.10 is adopted to update the adjacency matrix (i.e., use of an OR gate).

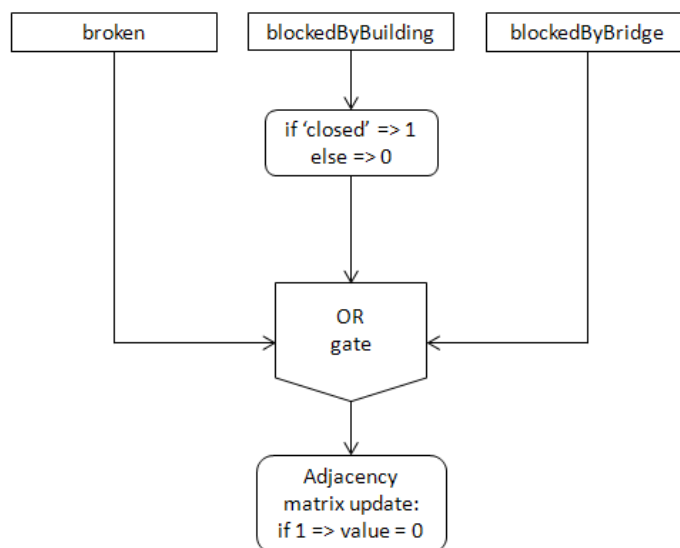


Fig. 7.10 Update procedure of the adjacency matrix

7.5.2 City of Vienna, Austria

The same methods as described in the Thessaloniki case study are applied (section 7.5.1). Gas system (application in L'Aquila, Italy)

For the purpose of the application study, the SYNER-G prototype software was equipped with the GAS class, focusing on the components of a gas distribution system, in order to evaluate seismic performance of the case study (L'Aquila gas distribution network).

The gas distribution system class is modeled as an undirected graph and it is considered a subclass of the Undirected abstract class. The network is comprised of nodes and link/edges based on the class diagram presented in section 5.2.2.3. As consequences it is the composition of GASedge and GASnode abstract classes, of which the first is the generalization of PipeGAS class, while the second is the generalization of GASdemand, GASsource and Joint classes.

The Joint class represents all nodes used to reproduce the geometry of the system. The GASsource class is represented by M/R stations that are used to connect the distribution medium-pressure network to the high-pressure transmission lines and the GASdemand is the generalization of IDU class and Station class. The IDU class represents the node directly connected with customers in the low-pressure network while the Station class is represented by RGs that are considered final nodes when the only medium-pressure network is analyzed.

Each class is characterized by attributes and methods. Attributes refer to properties that describe the whole system and each component. Methods refer to functions used to evaluate the state of the network or of each component of the system.

A detailed description of properties and methods implemented for the case study is available in the SYNER-G report D6.5 (Esposito and Iervolino 2012).

7.5.3 Road network (application in Calabria region, Southern Italy)

The RDN class diagram is given in section 5.2.3.1. The RDN is modeled as a *directed* graph, i.e., a graph in which all edges have a travelling direction, from node i to node j . For this reason, the RDN class is considered as a subclass of the *Directed* abstract class, which in turn is a subclass of the *Network* abstract class.

Similar to other Network classes, a road network is made up of *nodes* and *links/edges* connecting them. As a consequence, the RDN class is the composition of the *RDNnode* and *RDNedge* abstract classes. The first is the generalization of the TAZ, ExternalStation and Intersection classes. A brief explanation of these node typologies is given in Deliverable D5.5 (Pinto et al. 2012a). The *RDNedge* class is the generalization of the RoadSegment, Embankment, Trench, UnstableSlope, RDNTunnel and Bridge classes. The definition of these edge typologies is given in SYNER-G reports D3.6 (Fardis et al. 2011) and D3.7 (Kaynia et al. 2011), where the “road pavement” typology corresponds to the RoadSegment class.

7.5.4 Electric power network (application in Sicily)

The SYNER-G prototype software includes an object-oriented representation of a subset of all the systems in the taxonomy, among which is the electric power network.

The modeling of EPN is based on the class diagram of section 5.2.2.1. In the software, the EPN is modeled as an undirected graph, i.e., a graph in which flow can occur in both directions on all. For this reason, the EPN class is considered as a subclass of the *Undirected* abstract class, that in its turn is a subclass of the *Network* abstract class.

EPN class is the composition of *EPNedge* and *EPNnode* classes, that are both abstract. The first one is the generalization of the OverheadLine and UndergroundLine classes, while the second one is the generalization of the SlackBus, PVGenerator and LoadBus classes. The latter is the generalization of the TransformationDistribution and Distribution classes, both of which are composed of the *Component* abstract class. This latter class is the generalization of eleven classes, one for each micro-component composing the substations.

7.5.5 Hospital facility and regional health-care system (application in Italy)

The system under evaluation is composed of hospitals, area districts and a road network. The road network is deputed to connect districts and hospitals allowing the transportation of injured and sick people. The response of the system depends not only on the performance of each component but also on their mutual interactions.

The consequences on a hospital facility are expressed through the *HTC* index, the number of surgeries that can be operated after the seismic event, which is probabilistically estimated by taking into account not only the physical damages to the building, but also the performance of non-structural elements, the preparedness of the staff and the effectiveness of the emergency procedure.

Damages to the road network, and in particular to bridges, are also included. They affect the capability of transportation of the victims to hospitals, both by a reduction of the travel speed and by the closure to traffic of the collapsed bridges.

The number of victims is evaluated on the basis of demographic data by means of casualty models. The uncertainty in the estimation of victims is introduced in the analysis. Victims are evaluated per area districts, whose spatial extension may vary from a small neighbourhood to a whole town depending on the scale of the study and in the detail of the available information. Among all victims, a classification according to the severity of their condition is made by means of indications from epidemiologic studies (statistical data derived from previous events). The “severely injured” victims that need to be hospitalised are estimated and subdivided in two classes: those that need a surgical treatment, which form the *Hospital Treatment Demand (HTD)*, and those that need a medical care and a bed. Victims that need to be hospitalised are transferred from the origin area districts to a hospital located in the region of study. The analysis is concluded either when all the patients are hospitalised or when all the hospitals in the region are saturated.

The components of the system and the “hospitalisation” model developed for this study are described in some more detail in Pitilakis and Argyroudis (2013).

The system described above can be viewed as a part of the SYNER-G general framework (e.g. Franchin and Cavalieri 2012), where an integrated approach for the assessment of the systemic seismic vulnerability and risk analysis of buildings, lifelines and infrastructures is developed. Damages to building aggregates are not accounted for in the present application; nevertheless, the general framework is comprehensive and can include them, as illustrated in (Cavalieri et al. 2012). It is therefore possible a detailed (and more accurate) estimation of the victims if (enough) data on the built area is known to the analyst.

7.5.6 Harbour (application in Thessaloniki)

Container and bulk cargo movements of ports are simulated. The assumption of discrete type of cargo handling (container or bulk cargo) per terminal is made. The elements studied include piers, berths, waterfront and container/cargo handling equipment (cranes) (see section 5.2.4.1). Waterfronts and cranes are the physical components of the harbour. Piers and berths are structural (functional) elements. Several berths are composing a pier. Each berth is a part of a waterfront designed to serve one ship, and it consists of a portion of a waterfront served by one or more cranes. The berth length is estimated based on the pier’s operational depth. To quantify the capacity of each berth, each crane capacity (lifts per hour / tons per hour) is considered in the evaluation. The main **Performance Indicator (PI)** used is the *total cargo/containers handled in a pre-defined time frame per terminal and for the whole port system*.

An important interdependency considered within SYNER-G is between the cargo handling equipment and Electric Power Network (EPN), in particular for the electric power supply to cranes. Road closures due to potential building collapses are also another important dependency. In this case, the delivering process of cargo/containers from the terminals to the port gates could be hampered.

The functionality of the harbour is assessed through several system-level Performance Indicators (PIs), as evaluated starting from the effects of seismic events (Fig. 7.11). More details, and an analytical description of general outline of the method, are available in Reference Report 6 (Pitilakis and Argyroudis 2013).

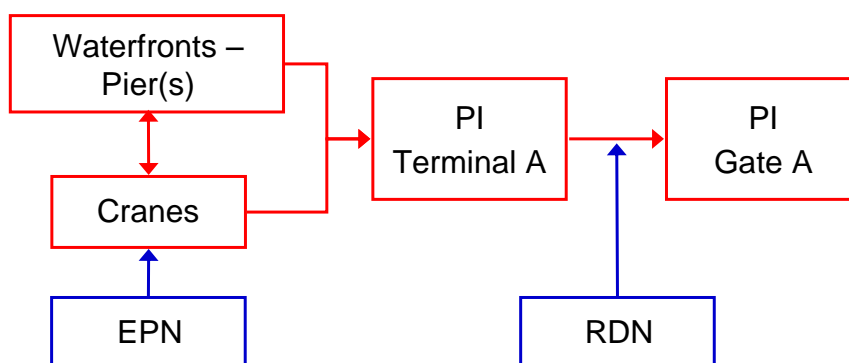


Fig. 7.11 Functionality simulation of port facilities

7.5.7 Summary of systemic vulnerability analysis

In the following table the main features of the systemic analysis for each case study are summarized.

Table 7.8 Systemic analysis for the case studies

Components	Interactions with	Analysis	Performance indicators	Simulation
City of Thessaloniki				
BDG (masonry, RC)	EPN, WSS		yielding & collapsed buildings, deaths, injuries, displaced people	MCS (10,000 runs)
EPN (substations)	-	connectivity	Electric power network Connectivity Loss (ECL)	
WSS (pipes, pumping stations)	EPN	connectivity	Water Connectivity Loss (WCL)	
RDN (road segments, bridges, overpasses)	BDG	connectivity	Simple Connectivity Loss (SCL), Weighted Connectivity Loss (WCL)	
City of Vienna				
BDG (masonry, RC)	EPN, WSS		yielding & collapsed buildings, deaths, injuries, displaced people	MCS (10,000 runs)
RDN (roads)	BDG	connectivity	Simple Connectivity Loss (SCL), Weighted Connectivity Loss (WCL)	
WSS (pipes)	EPN	connectivity	Water Connectivity Loss (WCL)	
EPN (substations)	-	connectivity	Electric power network Connectivity Loss (ECL)	
The gas system of L'Aquila in Italy				
GAS (M/R stations, pipes)	-	connectivity	Connectivity Loss (CL), Serviceability Ratio (SR)	MCS
The road network in Calabria region, Southern Italy				

RDN (roads, bridges)	-	connectivity	System-level: Simple Connectivity Loss (SCL), Weighted Connectivity Loss (WCL) Component-level: Minimum travel time, Terminal Reliability	MCS (20,000 runs), ISS (2,000 runs), ISS-KM (200 runs)
The electric power network of Sicily				
EPN (substations)	-	capacitive study (power flow analysis)	System-level: Connectivity Loss (CL), Power Loss (PL), System Serviceability Index (SSI) Component-level: Voltage Ratio (VR)	MCS (20,000 runs), Importance Sampling (ISS) (2,000 runs), Importance Sampling with k-means clustering (ISS-KM) (200 runs)
Hospitals system at regional scale in Italy				
RDN (bridges)	-	System analysis including vulnerable hospitals and bridges	Casualties (divided in two categories) that are not allocated in hospitals. Maximum hospitalisation travel time. Hospitals seismic risk (probability of not being able to provide the required medical treatments to victims).	MCS (10,000 runs)
Hospital facilities	RDN			
The harbour of Thessaloniki				
Cranes	EPN	port performance analysis	Container Terminals: TCoH = total number of containers handled (loaded and unloaded) per DAY, in Twenty-foot Equivalent Units (TEU) TCoM = total number of containers' movements per DAY, in Twenty-foot Equivalent Units (TEU) (in the whole harbour facility) Bulk cargo terminals TCaH = total cargo handled (loaded and unloaded) per DAY, in tones TCaM = total cargo movements per DAY, in tones (in the whole harbour facility)	MCS (10,000 runs)
Waterfront structures	-			
EPN	-			
Buildings	-			
Road network	BDG			

7.6 RESULTS

In the followings, representative results are given for each case study.

7.6.1 City of Thessaloniki

Electric power network

Fig. 7.12 shows the moving average (mean) curve for ECL as well as the mean+stdv and mean-stdv curves. The jumps present in the plots are located in correspondence of simulation runs/samples in which at least one demand node is disconnected, leading ECL to yield values greater than 0. At the end of the analysis (10,000 runs) the moving average is stabilized. Fig. 7.13 shows the MAF of exceedance for ECL. As an example, the ECL with mean return period $T_m=500$ years ($\lambda=0.002$) is 24%.

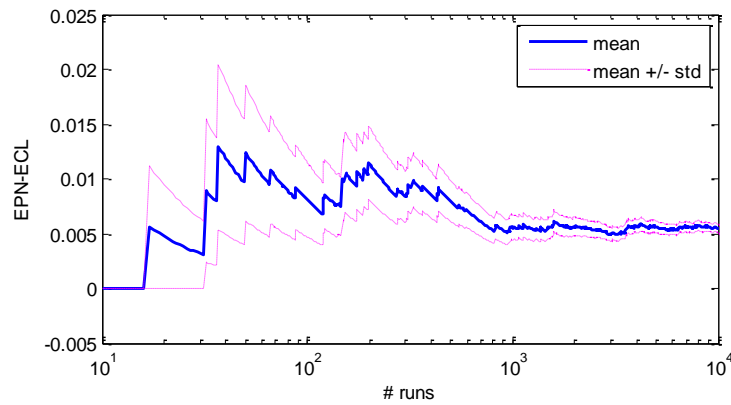


Fig. 7.12 Moving average μ , $\mu+\sigma$, $\mu-\sigma$ curves for ECL

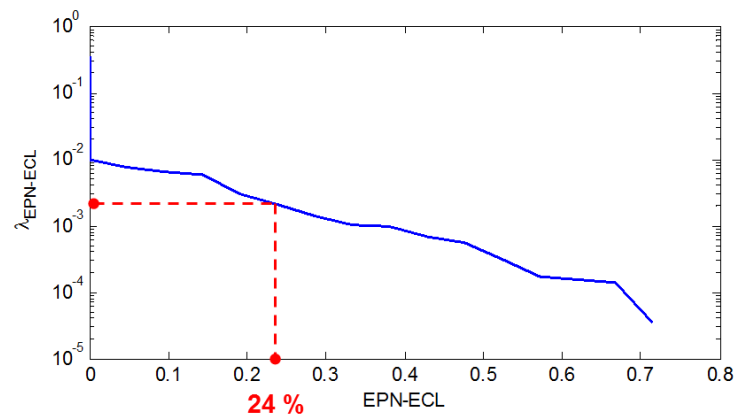


Fig. 7.13 MAF curve for electric power network connectivity loss (ECL)

Fig. 7.14 shows the level of correlation between the ECL and non-functional transmission substations. In this way the most critical components of the network can be defined in relation with their contribution to the connectivity loss of the network. The majority of substations present high levels of correlation near or over 35%. This can be mostly attributed to the low level of redundancy of the network in combination to the substations vulnerability and distribution of PGA in average over all runs of the simulation.

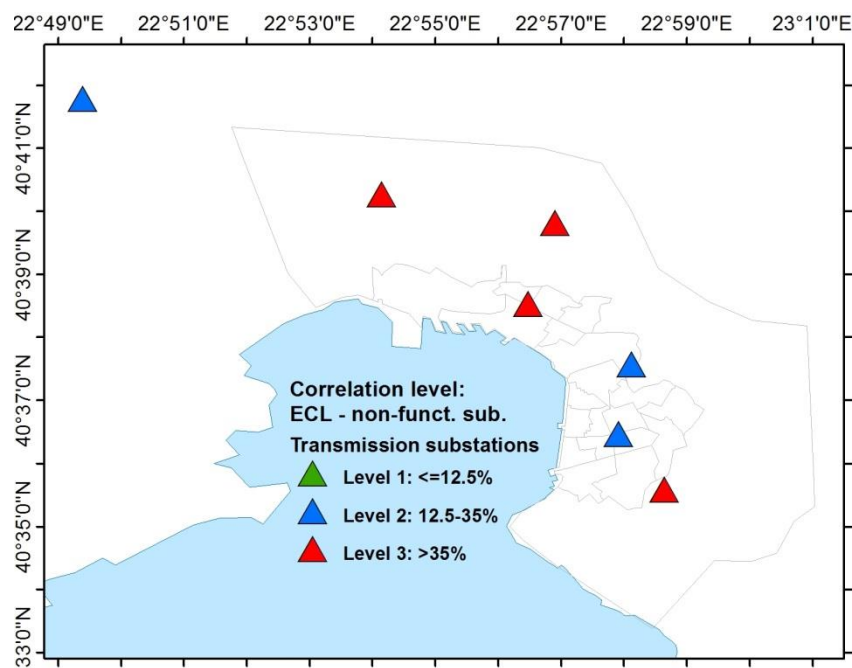


Fig. 7.14 Correlation of non-functional transmission substations to electric power network connectivity loss.

Water supply system

Fig. 7.15 shows the moving average (mean) curve for WCL (Water Connectivity Loss) as well as the mean+stdv and mean-stdv curves. The jumps present in the plots are located in correspondence of simulation runs/samples in which at least one node is disconnected, leading WCL to yield values greater than 0. At the end of the analysis (10,000 runs) the moving average is stabilized. Fig. 7.16 shows the MAF of exceedance for WCL. In the same figure, the estimated MAF of exceedance curve for WCL when the interaction with electric power network is not considered in the analysis is compared. The interaction can be important; as an example the connectivity loss is increased from 1% to 1.8% for $\lambda=0.001$ ($T_m=1000$ years) when the connections of water pumping stations to EPN are included in the analysis.

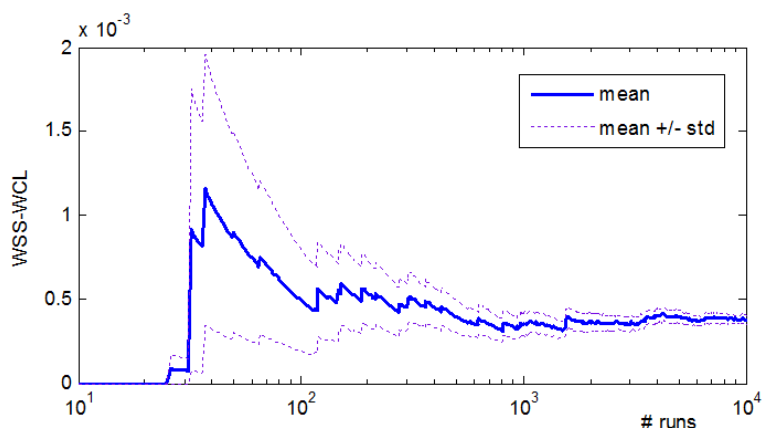


Fig. 7.15 Moving average μ , $\mu+\sigma$, $\mu-\sigma$ curves for WCL

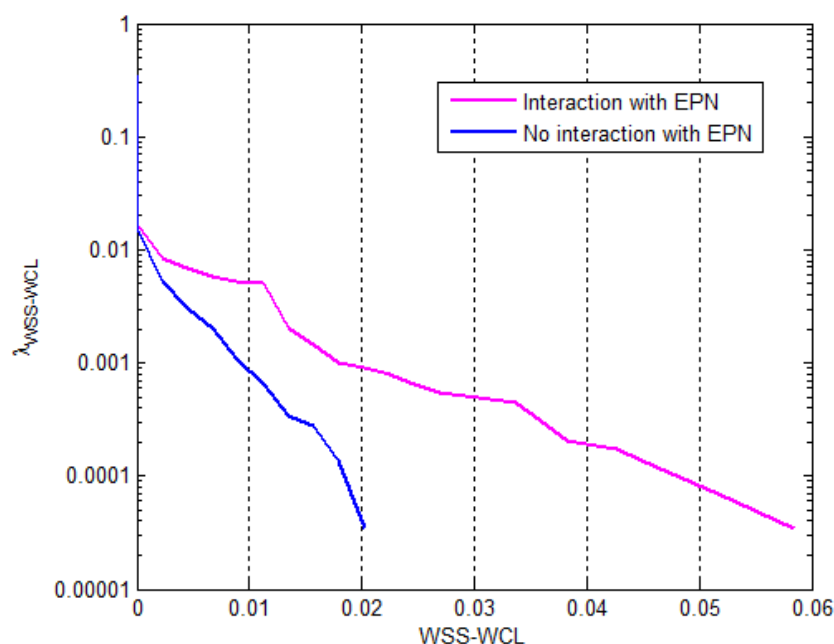


Fig. 7.16 MAF curve for water connectivity loss (WCL) with and without interaction with electric power network (EPN)

Fig. 7.17 shows the level of correlation between the WCL and damages in pipelines as well as the non-functional EPN substations supplying the water pumping stations. The most correlated pipelines are concentrated along the coast where the liquefaction susceptibility is high and therefore damages due to permanent ground displacement are expected. Interestingly, a higher level of correlation is estimated for the EPN transmission substations. The highest value of 80 % is attributed to component in the south east part of the city, where several pumping stations (connected to EPN) are located.

Fig. 7.18 shows the expected distribution of damages for the event with the highest magnitude that corresponds to connectivity loss (WCL=1.4%) with mean return period $T_m=500$ years (0.002 probability of exceedance). Only few broken pipes are observed, while the majority of non-functional pumping stations and not-connected demand nodes are accumulated at the S-SE part of the city.

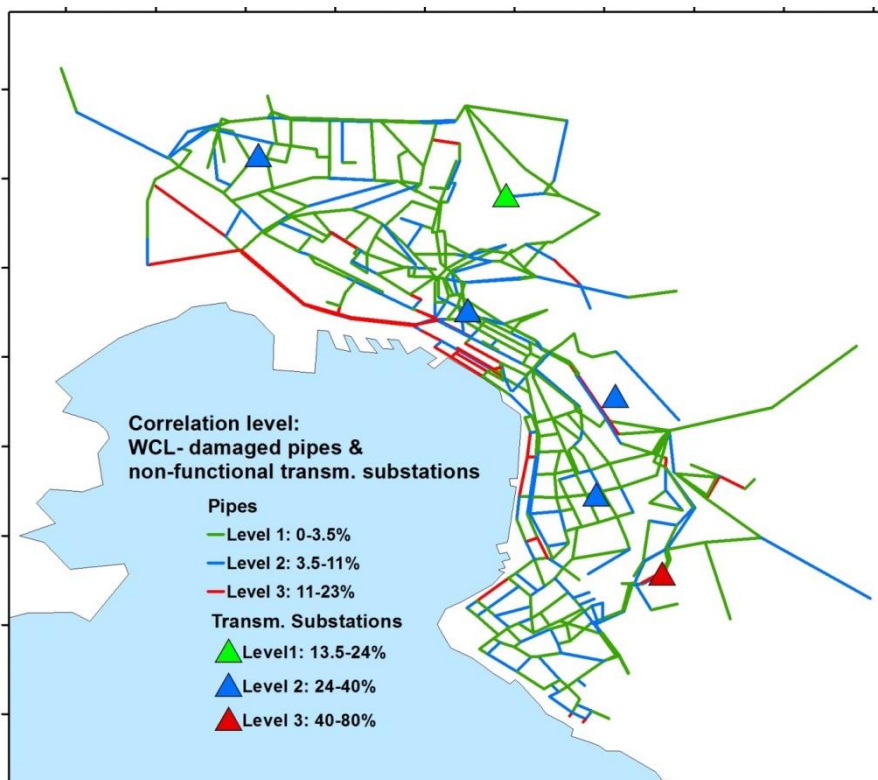


Fig. 7.17 Correlation of damaged pipes and non-functional EPN transmission stations to water network connectivity

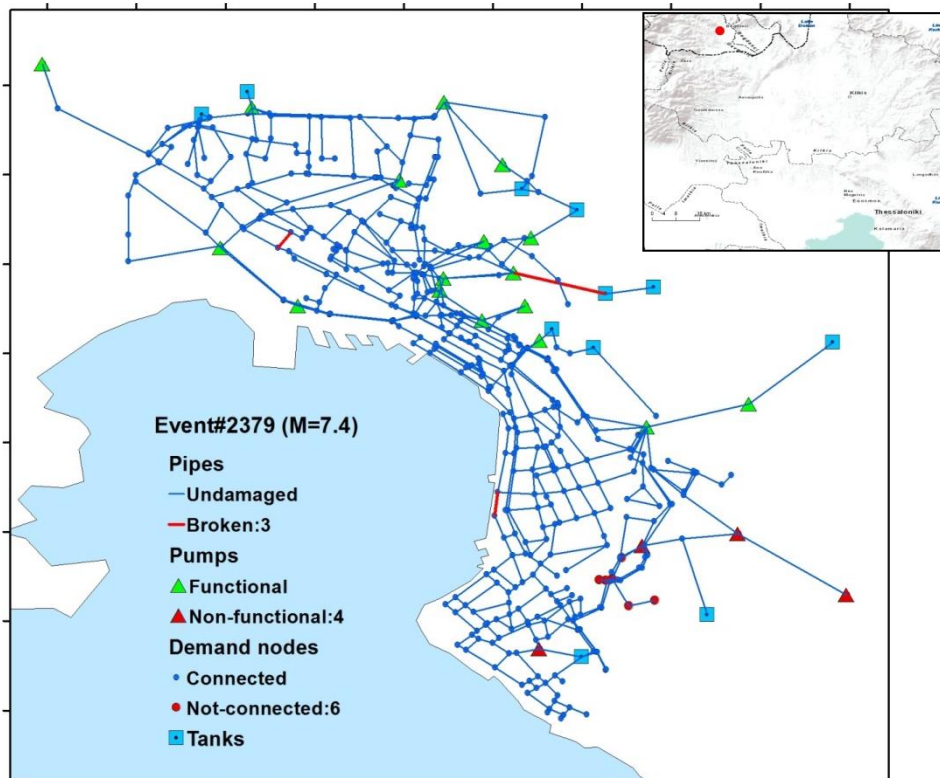


Fig. 7.18 Water supply system damages for an event (#2379, M=7.4, R=72km) that corresponds to WCL with $T_m=500$ years

Buildings

Fig. 7.19 shows the moving average (mean) curves as well as the mean+stdv and mean-stdv curves for expected deaths. The values are given as percentages of the total population (790,824 inhabitants). At the end of the analysis (10,000 runs) the moving average is stabilized with an average value of 4 deaths. This low fatality rate is reasonable in this case as the analysis averages the results over all possible magnitudes and epicentral distances, and the lower magnitude and longer distance events are certainly controlling the output. Similar curves and results are derived for injuries and displaced people (in bad and good weather conditions).

Fig. 7.19 also shows the MAF of exceedance curves for deaths (as percentages of the total population). The expected deaths for $\lambda=0.002$ (mean return period $T_m=500$ years) are 201. The distribution of building damages for an event that corresponds to this return period of deaths is shown in Fig. 7.20. Similar maps can be obtained for casualties and displaced people. For this event, the estimated losses are: 2,248 collapsed and 16,634 yielding buildings, 201 deaths, 492 injuries and 180,000 (in good weather) and 288,000 (in bad weather) displaced people. Fig. 7.21 shows the level of correlation between the damaged WSS and EPN components and the displaced people. It is observed that the correlation is higher with the EPN substations, which highlights the importance of the interaction between EPN loss and habitability.

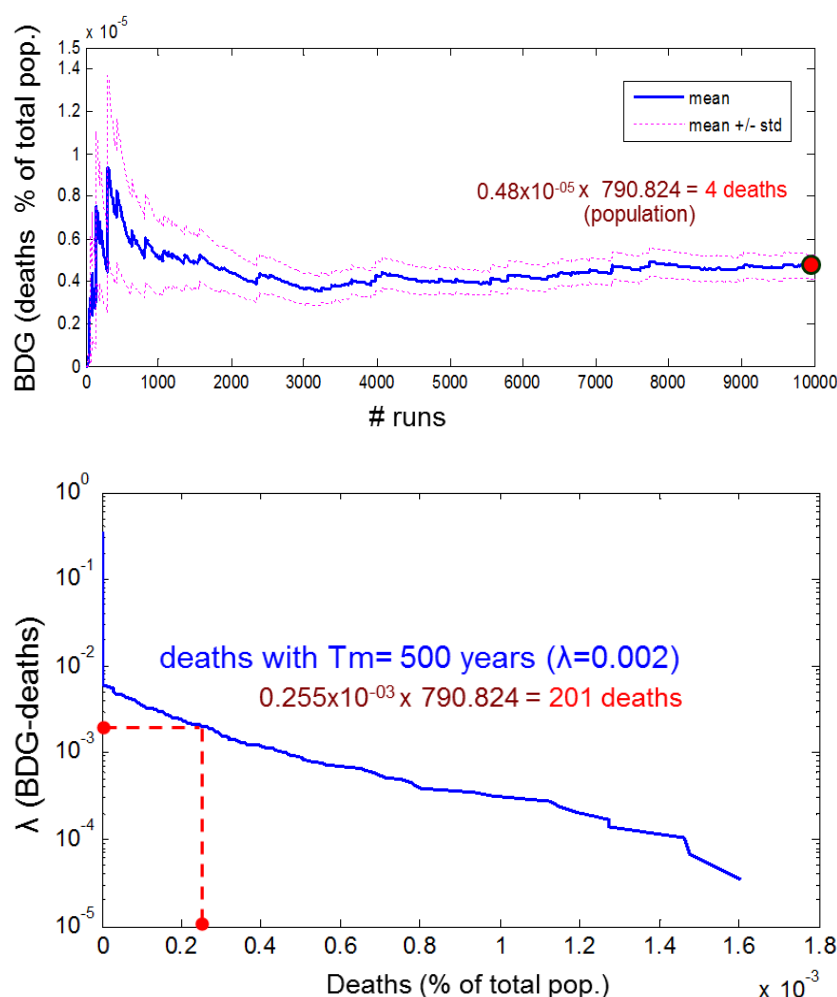


Fig. 7.19 Moving average μ , $\mu+\sigma$, $\mu-\sigma$ curves (up) and MAF curve (down) for deaths

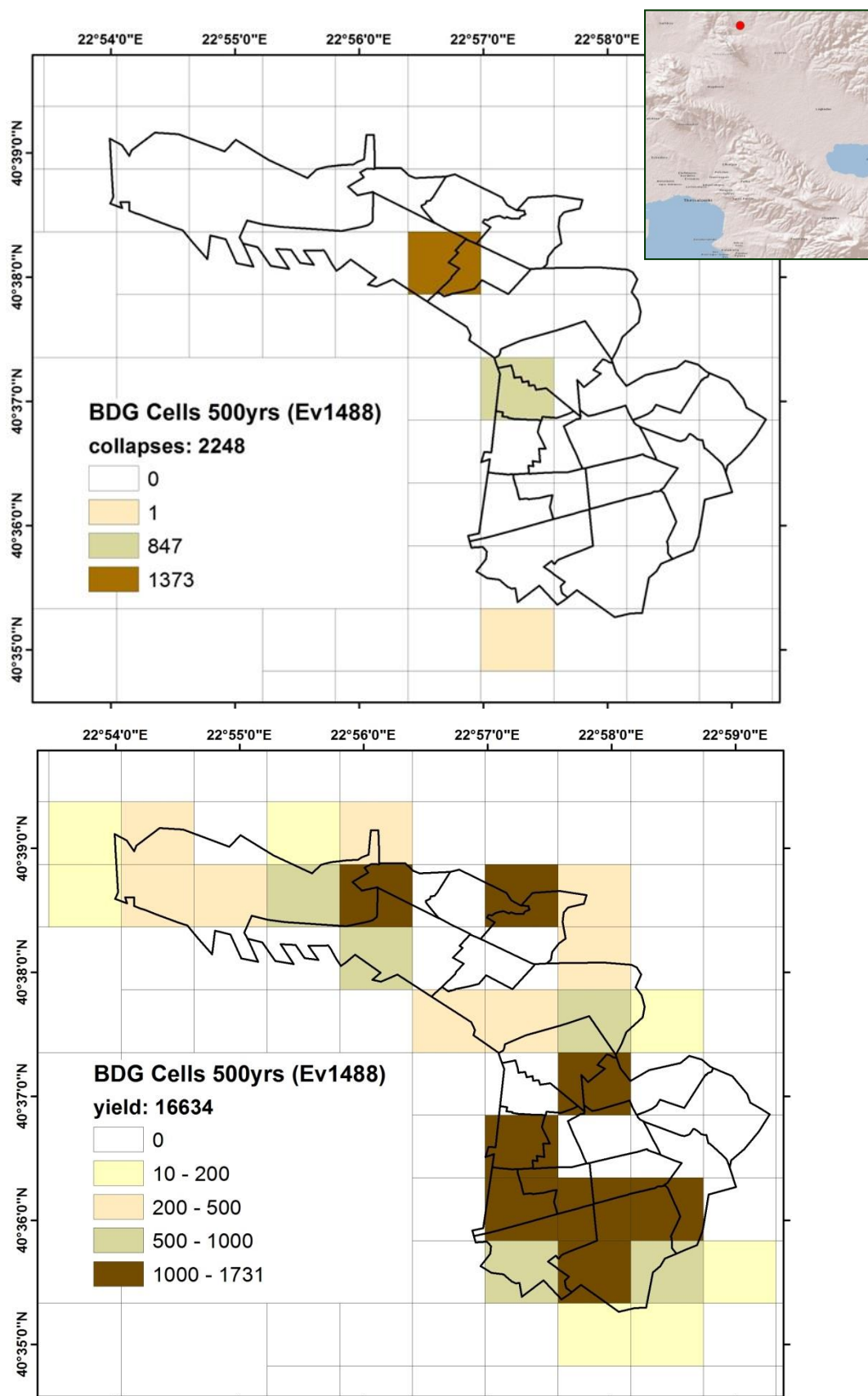


Fig. 7.20 Distribution of estimated damages (collapsed and yielding buildings) into cells of the study area for an event (#1488, M=5.5, R=24 km) that corresponds to death rate with $T_m=500$ years

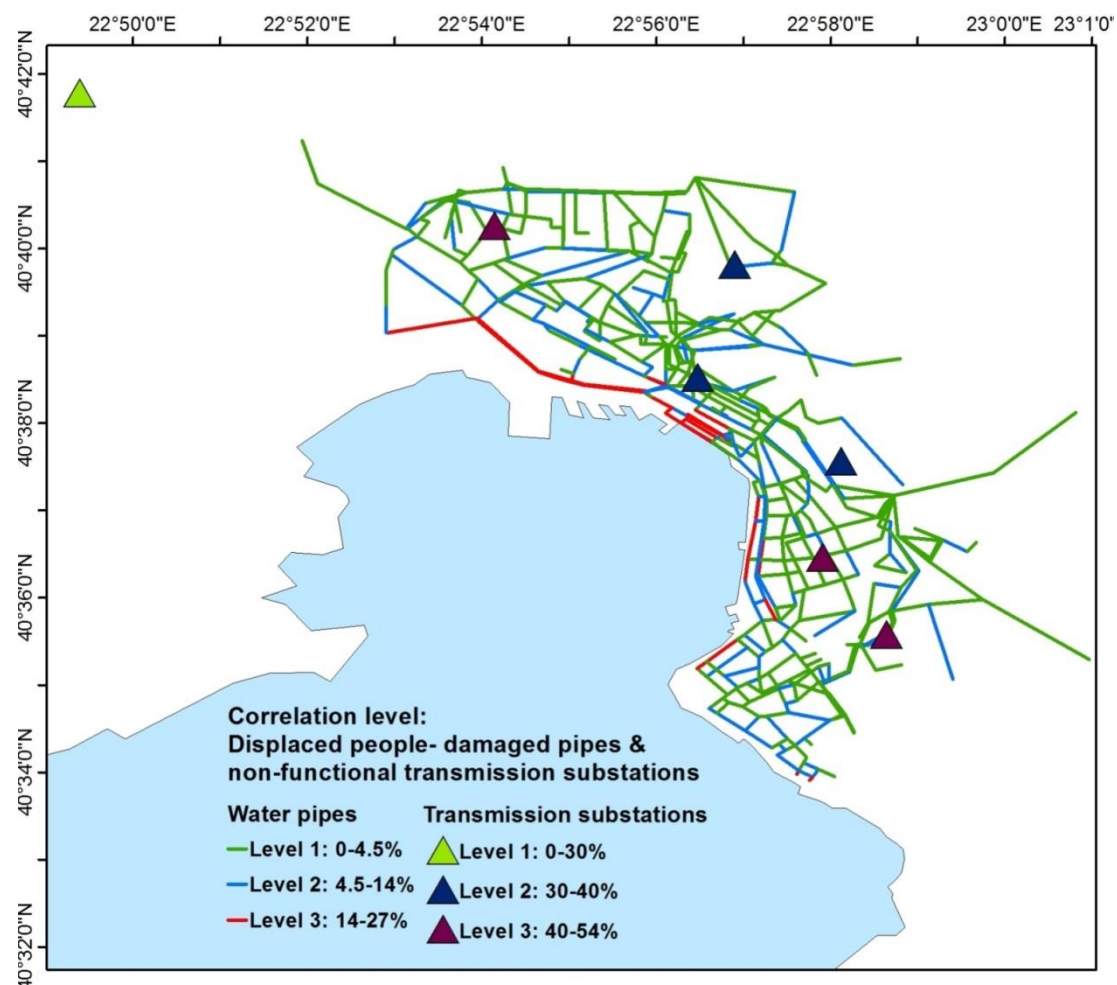


Fig. 7.21 Correlation of damaged EPN and WSS components to displaced people

Roadway network

Fig. 7.22 shows the moving average (mean) curves for SCL (left) and WCL (right), as well as the mean+stdv and mean-stdv curves for the two PIs. The figures indicate that the expected value of connectivity loss given the occurrence of an earthquake is higher for WCL than for SCL, as expected. This is because WCL takes into account not only the existence of a path between two TAZs, but also the increase in travel time due to the seismically induced damage suffered by the RDN. The jumps present in the plots are located in correspondence of simulation runs/samples in which at least one TAZ node is disconnected, leading SCL and WCL to yield values greater than 0. At the end of the analysis (10,000 runs) the moving average is stabilized.

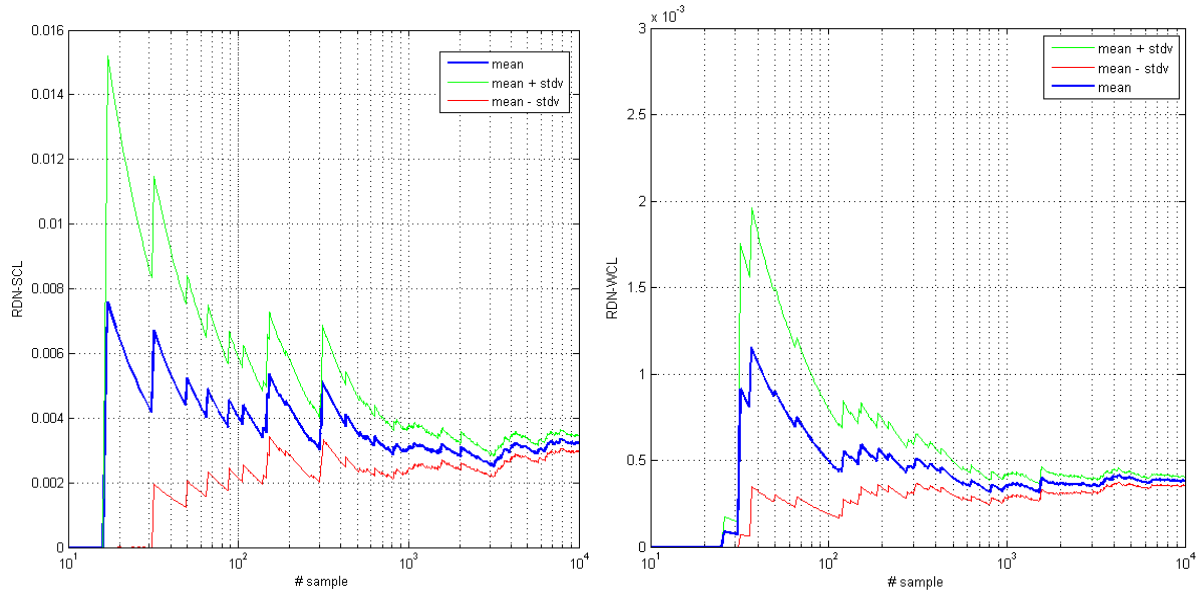


Fig. 7.22 Moving average μ , $\mu+\sigma$, $\mu-\sigma$ curves for SCL (left) and WCL (right).

Fig. 7.23 shows the MAF of exceedance curves for SCL and WCL. As expected, weighting the computation of connectivity loss with the path travel times yields higher values of exceedance frequency. The same figure compares the estimated MAF of exceedance curve for SCL and WCL when the road blockage due to collapsed building is not considered in the analysis. The interaction with building collapses can be important especially for mean return periods of WCL higher than 500 years ($\lambda=0.002$). As an example the connectivity loss is increased from 20% to 33% for $\lambda=0.001$ ($T_m=1000$ years) when the building collapses are included in the analysis.

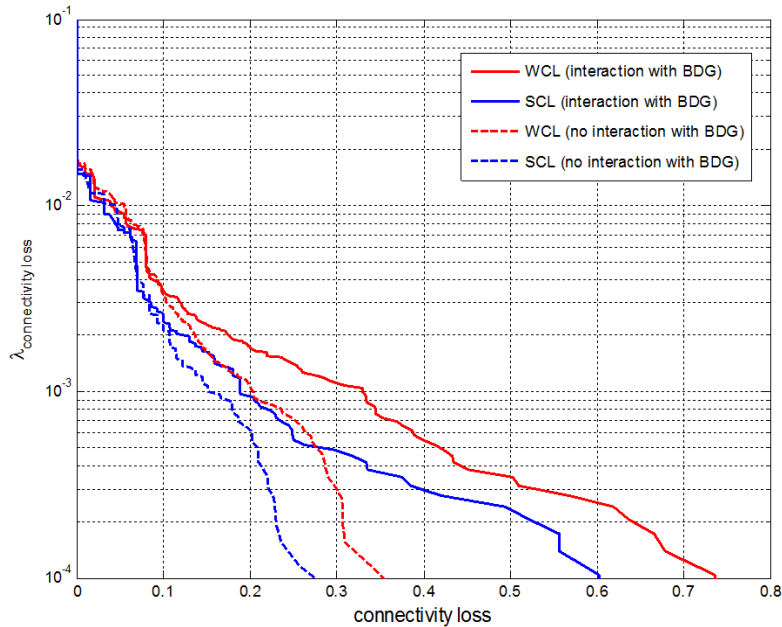


Fig. 7.23 MAF curves for simple (SCL) and weighted (WCL) connectivity loss with and without interaction with building collapses

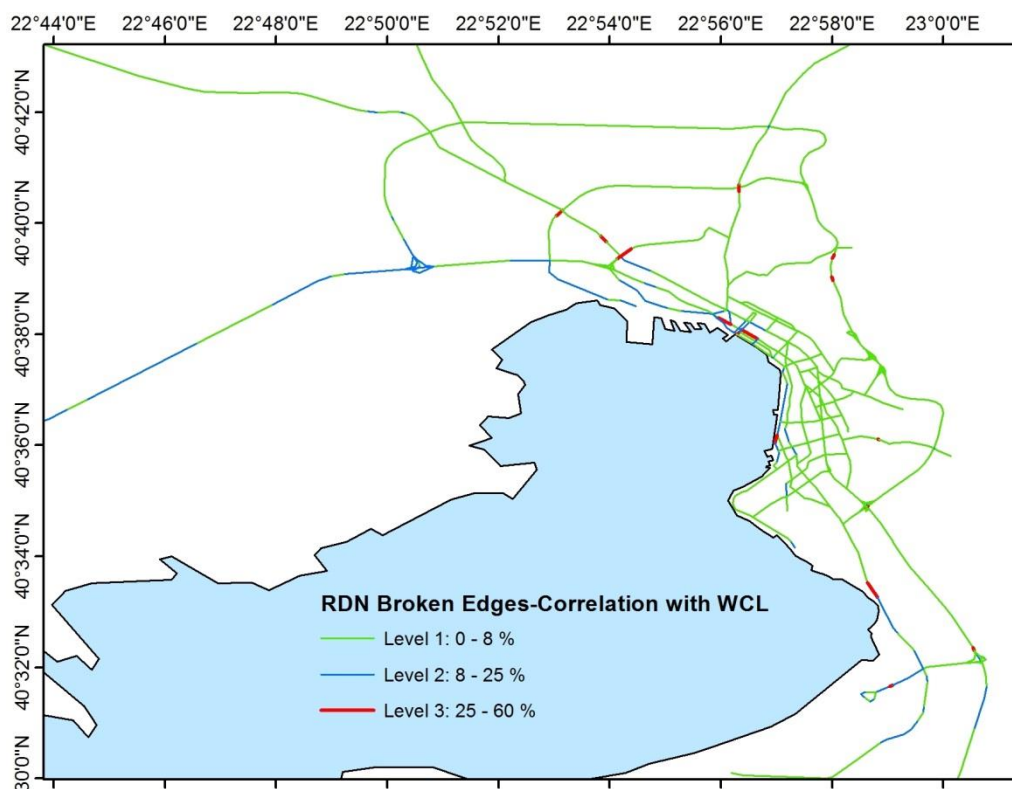


Fig. 7.24 Correlation of broken edges (bridges) to road network connectivity (PI=WCL)

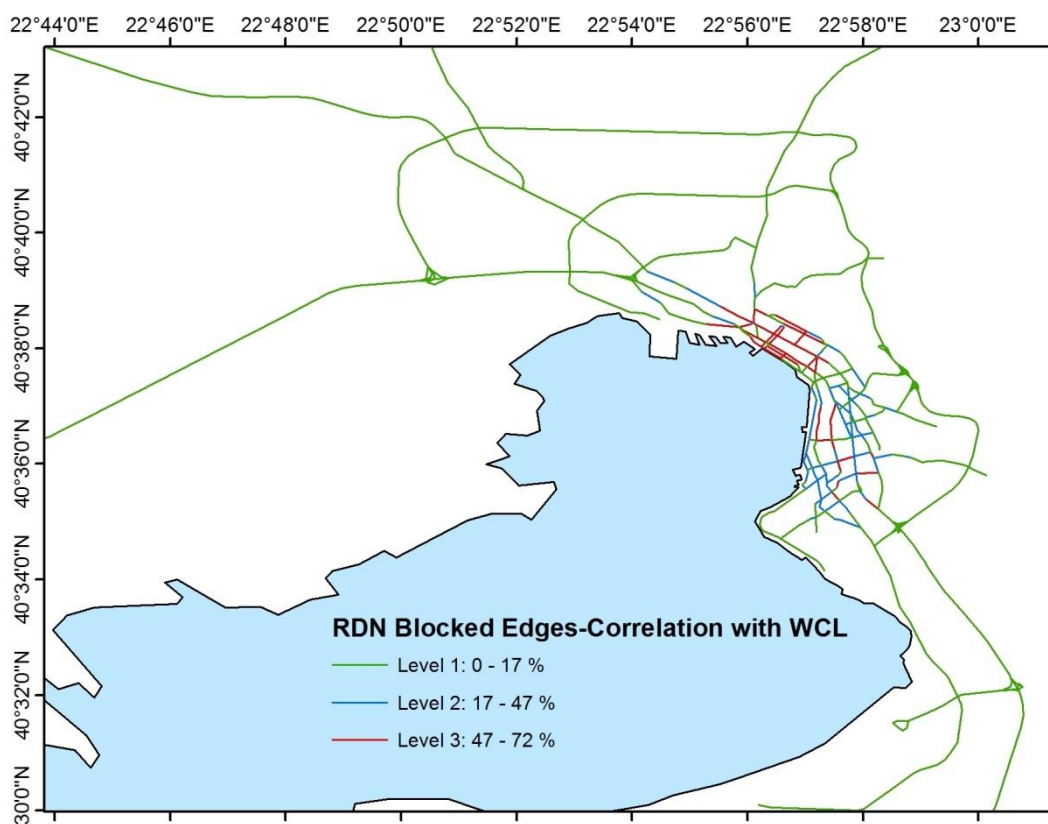


Fig. 7.25 Correlation of blocked by buildings edges to road network connectivity (PI=WCL)

Fig. 7.24 and Fig. 7.25 shows the level of correlation between the WCL and the distribution of damages in bridges and road blockages respectively. In this way the most critical segments can be defined in relation with their contribution to the connectivity loss of the network. The highest risk of bridge failure is related with structures of high vulnerability (old, simple span bridges) and high values of PGA. The most correlated blocked roads are mainly in the historical center of the city, where the vulnerability of buildings is higher and the road to building distance is shorter. Several road segments in the city center and the SE part of the study area present a medium correlation due to building collapses. Few roads near the coast which are subjected to ground failure to liquefaction are also highly correlated to the network connectivity.

Shelter demand analysis

The estimated damages and losses for buildings, utility and road networks are used as input to the integrated shelter need model developed in SYNER-G. In particular, a Shelter Needs Index (SNI) is estimated for each one of the 20 Sub City Districts (Fig. 4.4) based on: a) the displaced people estimates for bad and good weather conditions, which are a function of the building damages (BDG) and the utility losses (WSS and EPN), b) the desirability of people to evacuate and c) their access to resources. Criteria b) and c) are evaluated based on indicators from the Urban Audit survey (e.g. age, family status, unemployment rate, education level etc).

Accessibility analysis

The estimated damages and losses of the road network provided input for the accessibility modeling to shelters and hospital facilities using isochrone-based and zone-based techniques. An example is given in Fig. 7.26, where the accessibility to health facilities is estimated using the results of RDN over all runs.

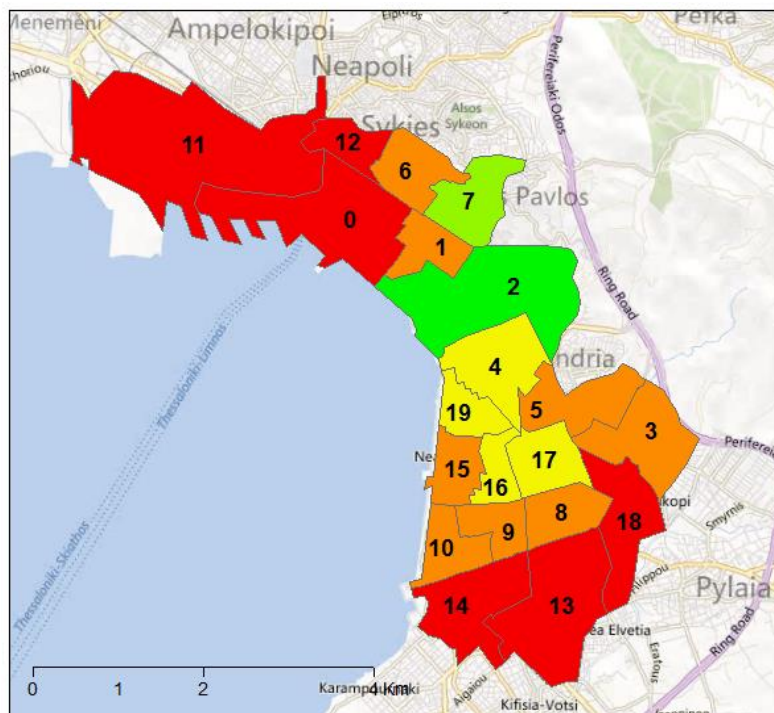


Fig. 7.26 Accessibility to hospitals for Thessaloniki SCDs (zone based technique)

7.6.2 City of Vienna

In the output of OOFIMS calculation the case study area is subdivided into cells and calculations are performed for each cell. Cell dimension is approximately 100x100 m.

The results reported below refer to the case which interdependency is considered among the water supply system and the electric power network. In particular in what follows the data obtained by averaging the results of each run over the total number of runs are reported. This implies that damage level (for buildings, roads, water supply system, and electric power network) spans in the range 0-1, while deaths and injured average (being obtained as sum of affected persons divided by 10,000) can have different range.

Buildings

Fig. 7.27 and Fig. 7.28 present respectively the damage distribution and the affected persons in the area of interest. Biggest damage level and death/injured persons are mainly concentrated in the south zone of the district where there are almost only masonry buildings.

Analyzing the mean annual frequency of exceedance and the moving average (Fig. 7.29) one can obtain 24 deaths with 500 years mean return period and 4 deaths as average over all runs. From similar plots it is resulted that the expected injuries for a 500 years return period are around 67 and in average the injuries are around 11 persons.

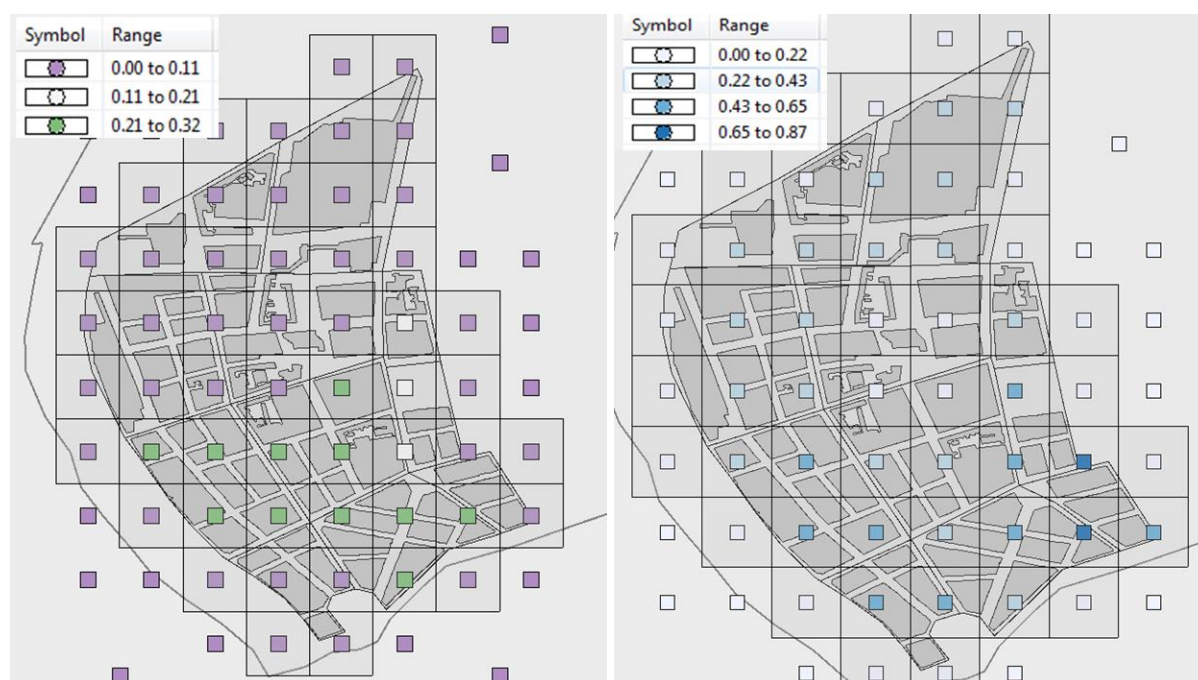


Fig. 7.27 Average building collapse (left) and building yielding distribution (right)

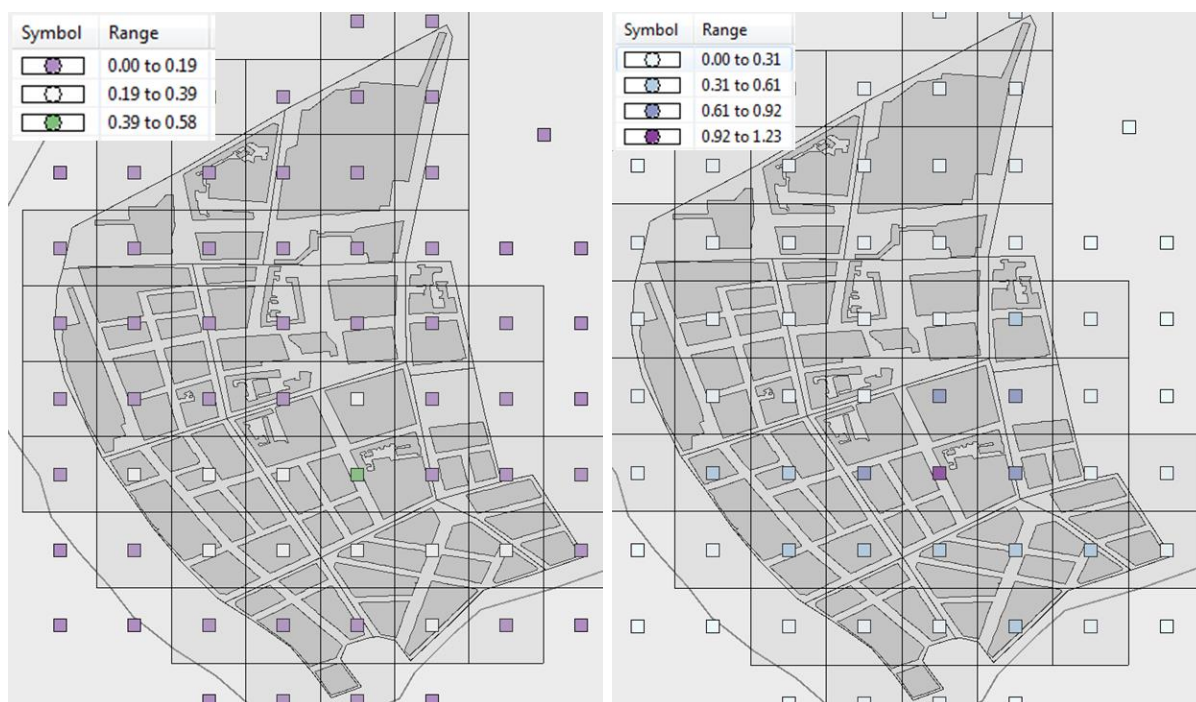


Fig. 7.28 Average death (left) and injured (right) distribution

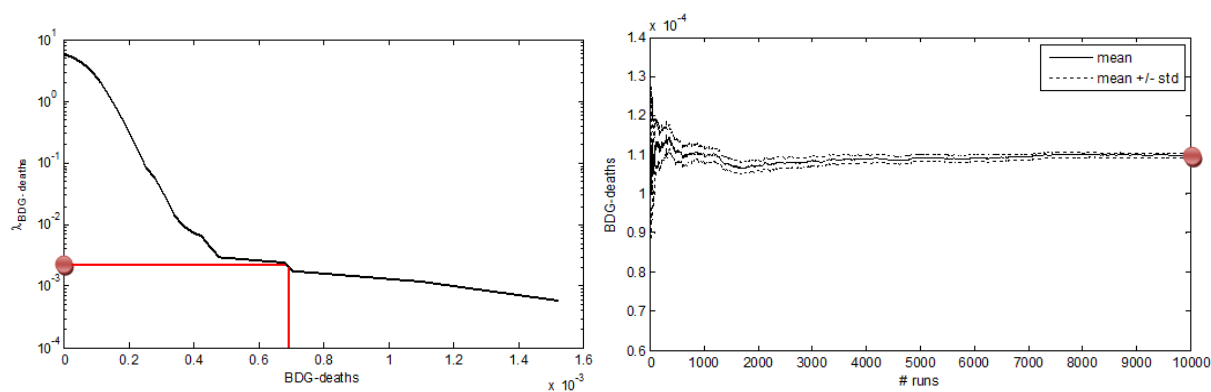


Fig. 7.29 Mean annual frequency of exceedance and moving average (death persons)

Roads

Analysis of the roads damage has shown that blocked as well as unusable ones are concentrated in the proximity of collapsed buildings (Fig. 7.30).

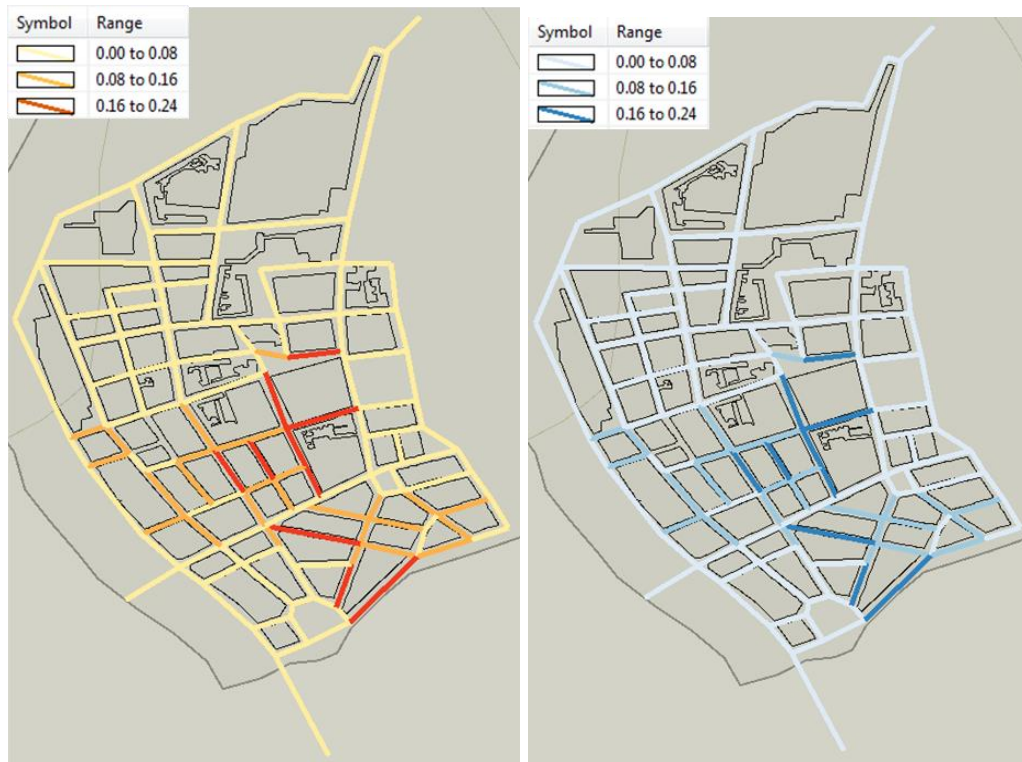


Fig. 7.30 Average blocked roads (left) and unusable ones (right)

Water supply system

Pipes and nodes of the water supply system results to be slightly affected from the earthquake and average level of damage is negligible (Fig. 7.31).

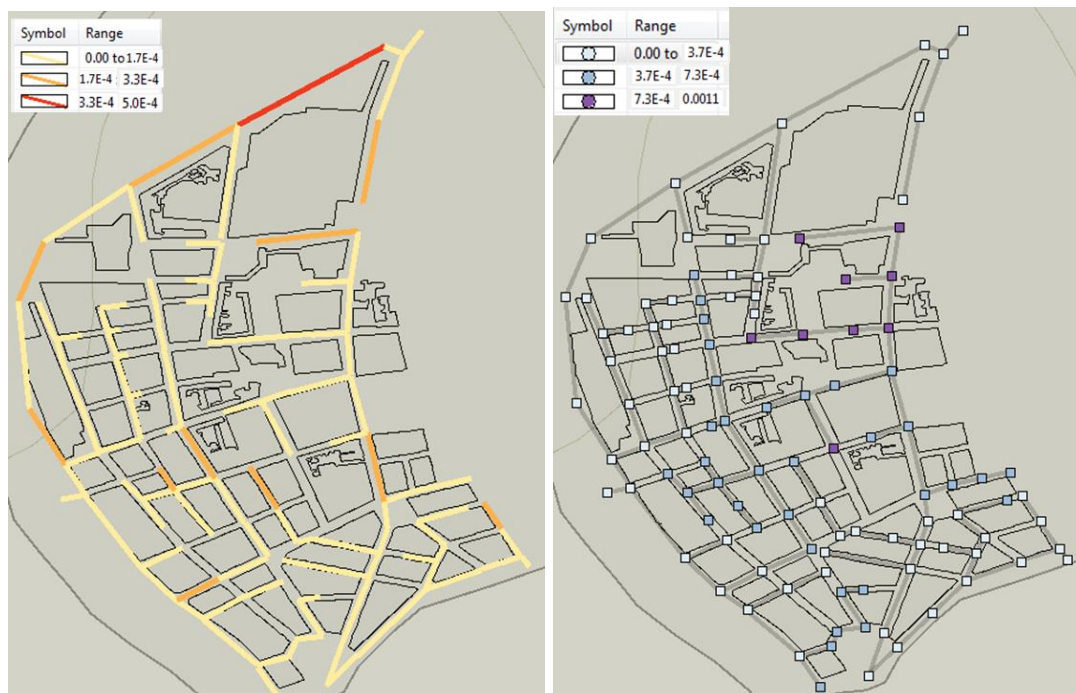


Fig. 7.31 Pipes broken (left) and non-functional nodes (right)

Selected scenario

Among the 10,000 runs, a particular scenario has been selected as an example. It presents a 5.4 magnitude earthquake located in the south-east of Vienna, at a distance of approximately 50 km from Brigittenau district. The selected scenario is considered meaningful since it is in the proximity of the tectonic zone of the Austrian region more prone to seismicity.

Fig. 7.32 and Fig. 7.33 present respectively the distribution of collapsed and yield buildings, death and injured persons and displaced persons in case of good and bad weather conditions. Deaths distribution is in accordance with the collapsed buildings. Major damaged are registered, as in the averaged results, in the south of the district where mainly masonry buildings are present. Similar maps are produced for displaced people.

Table 7.9 Data from the selected event for Vienna case study

Selected event: 278 M = 5.39 Hypocenter: 17.0071, 48.0789 Depth: 10 km			
EPN - Broken Transmission Stations	0	BDG - Deaths	4
EPN - Non functional demands	10	BDG - Injuries	19
WSS - Broken pipe	0	BDG - Collapse	4
WSS - Non functional demands	0	BDG - Yield	27
RDN - Broken	0	BDG - Displaced (GW)	1400
RDN - Blocked	11	BDG - Displaced (BW)	2411



Fig. 7.32 Number of buildings collapsed (left) and yield (right) for the selected event of M = 5.4



Fig. 7.33 Number of deaths (left) and injured (right) persons for the selected event of $M = 5.4$

Road damage confirms the tendency already identified in the analysis of the average damage with blocked and unusable roads mainly located in the south of the district. The selected scenario does not produce any damage to the water supply system. This is expected considering that the average damage level obtained before was negligible. Table 7.9 reports the summary of damage caused by the selected event.

7.6.3 Gas system in L'Aquila, Italy

A Monte Carlo Simulation (MCS) was carried out in order to evaluate the probability of exceeding a predefined level u of performance, given the occurrence of an earthquake on the fault. This probability was computed empirically using the MCS approach as follows:

$$\hat{P}(PI > u) = \frac{1}{n} \cdot \sum_{j=1}^n I(pi_j > u) \quad (7.1)$$

where pi_j is the performance indicator level corresponding to the simulation j , n is the total number of simulations and $I(pi_j > u)$ is an indicator function which equals 1 if $pi_j > u$ and 0 otherwise. The number of runs of the simulation was defined in order to yield stable estimates of the probability of exceeding the considered PI.

Results indicate that the expected value of connectivity loss given the occurrence of an earthquake is 0.65, i.e., it is expected that the average reduction in the ability of demand nodes to be connected to M/R stations is of 65%. While for the SR indicator, it is expected that 68% of demand nodes receive gas accounting for the importance level related to the nominal flow of the demand nodes. Fig. 7.34 shows the probability of exceedance (complementary cumulative distribution function, ccdf) of the two PIs.

In order to evaluate the contribution of some components of the risk on the performance of the network, some variables computed during each run of the simulation were stored and analyzed. In particular regarding hazard, the percentage of sites vulnerable to PGD (i.e., the ratio between the number of pipes where a PGD greater than 0 was occurred and the number of pipes located on sites potentially subjected to landslide) were saved, while in order to study the effects of the performance state of the components of the network, the number of broken pipes³ and damaged M/R stations were analyzed.

In the following figures (Fig. 7.35 and Fig. 7.36) histograms and scatter plots of these variables with respect to the two performance indicators are shown.

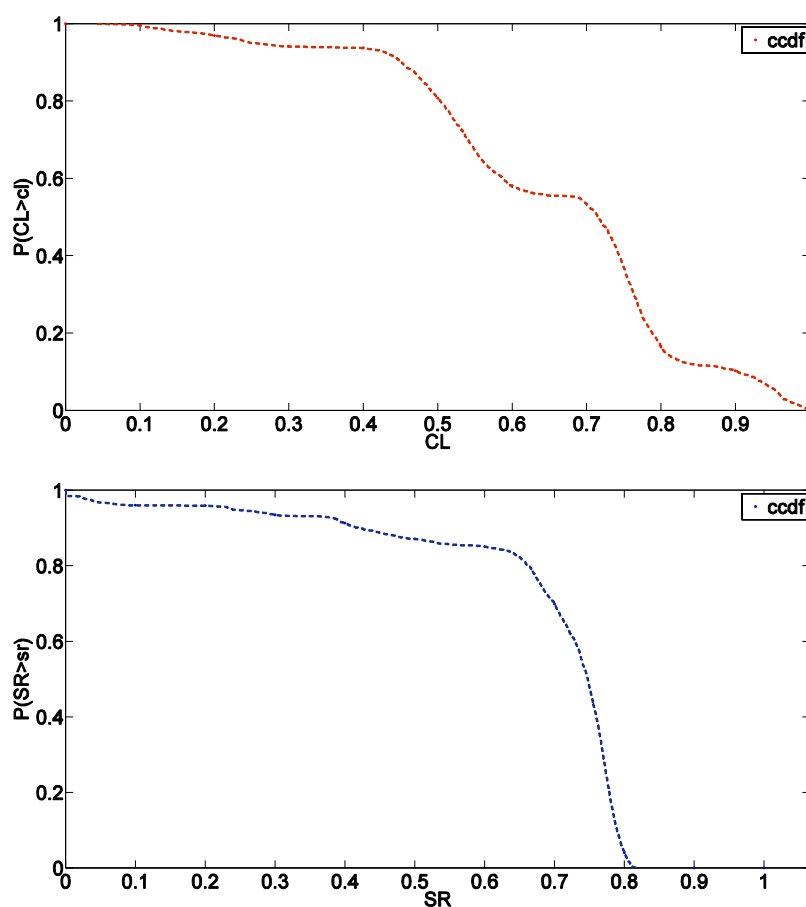


Fig. 7.34 Ccdf and confidence bounds for CL (top) and SR (bottom)

Correlation coefficients between these variables and performance indicators were also computed in order to evaluate possible linear dependences. As shown in the previous figures it seems that the number of damaged M/R stations is better correlated with the two PIs.

³ Note that pipes do not share the same length.

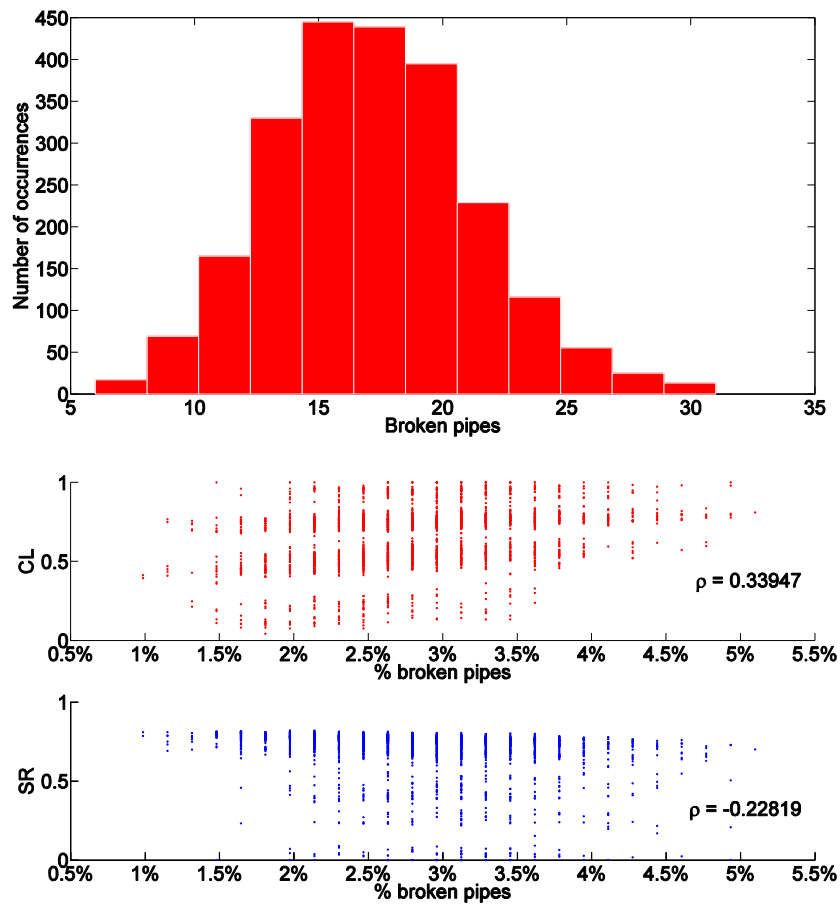


Fig. 7.35 Histograms of broken pipes in the simulations (top) and scatter plots of PIs with respect to percentage of broken pipes (bottom)

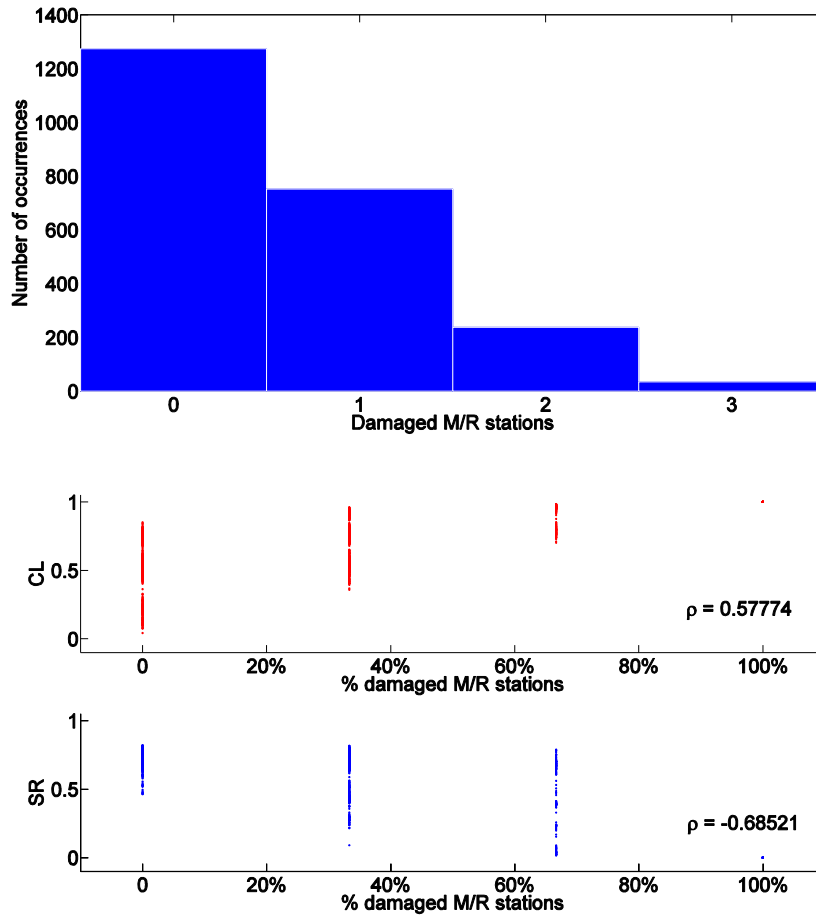


Fig. 7.36 Histograms of damaged M/R stations in the simulations (top) and scatter plots of PIs with respect to percentage of damaged M/R stations (bottom)

An efficient procedure to investigate the values of variables that contribute most to given values of the network's performance is disaggregation. Disaggregation of seismic performance, in fact, allows identifying the values of some variables providing the largest causative contribution to the risk given exceedance or occurrence of specified values of the performance indicator. The aim is to evaluate the probability of a variable (X), that is supposed to have an influence on the final performance, conditional to the occurrence of the performance indicator as expressed below:

$$P[X | u_1 < PI \leq u_2] = \frac{P[X, u_1 < PI \leq u_2]}{P[u_1 < PI \leq u_2]} \quad (7.2)$$

Therefore, the distribution of the number of broken pipes, damaged M/R stations and the percentage of pipes vulnerable to PGD conditional to the occurrence of the two PIs to ten intervals (equally spaced and ranging from 0 to 1) were computed and shown in Fig. 7.37, Fig. 7.38 and Fig. 7.39.

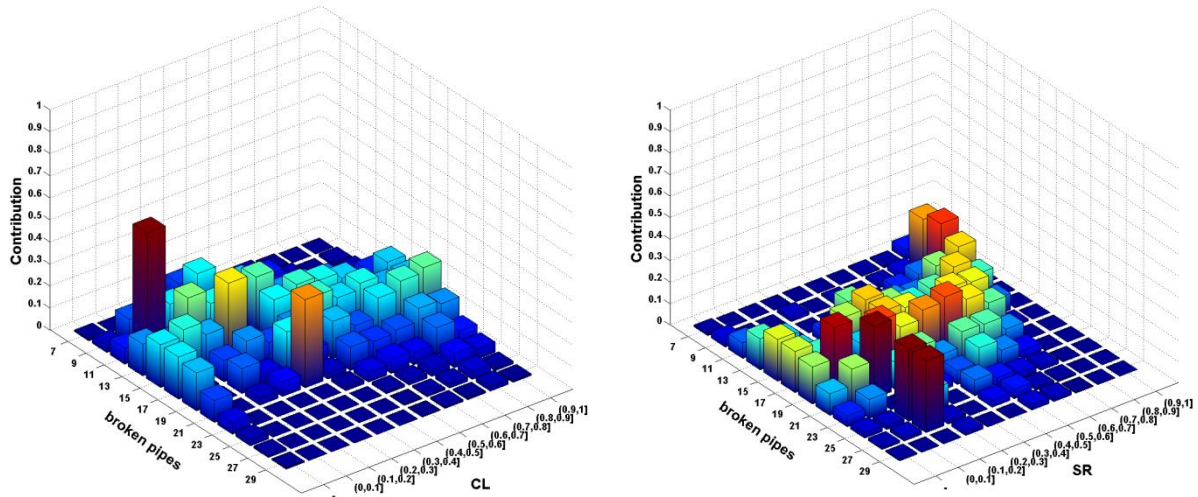


Fig. 7.37 Relative frequency of the number of broken pipes conditional to CL (left) and SR (right)

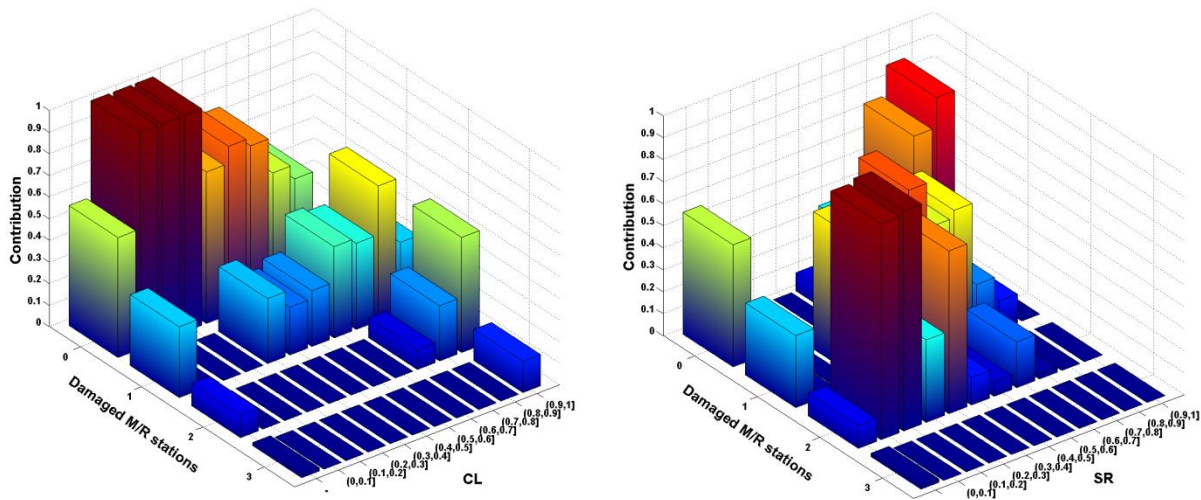


Fig. 7.38 Relative frequency of the number of damaged M/R stations conditional to CL (left) and SR (right)

Moreover, for each interval of the two PIs, the bars on the right side of the conditional distribution of the damaged M/R stations taper differently than the bars on the left side; i.e., the conditional distributions are asymmetric. In particular, the distribution of damaged M/R stations conditional to large losses (high values of CL and low values of SR) results skewed to the left, i.e., the mode is in correspondence of a high number of damaged M/R stations while the distribution of damaged sources conditional to high level of serviceability (low values of connectivity loss) results skewed to the right and the mode is in correspondence of a number of damaged M/R stations equal to zero. Regarding other variables, the distributions of number of broken pipes, and percentage of pipes vulnerable to PGD, conditional to the performance of the network are somewhat flat (Fig. 7.37 and Fig. 7.39).

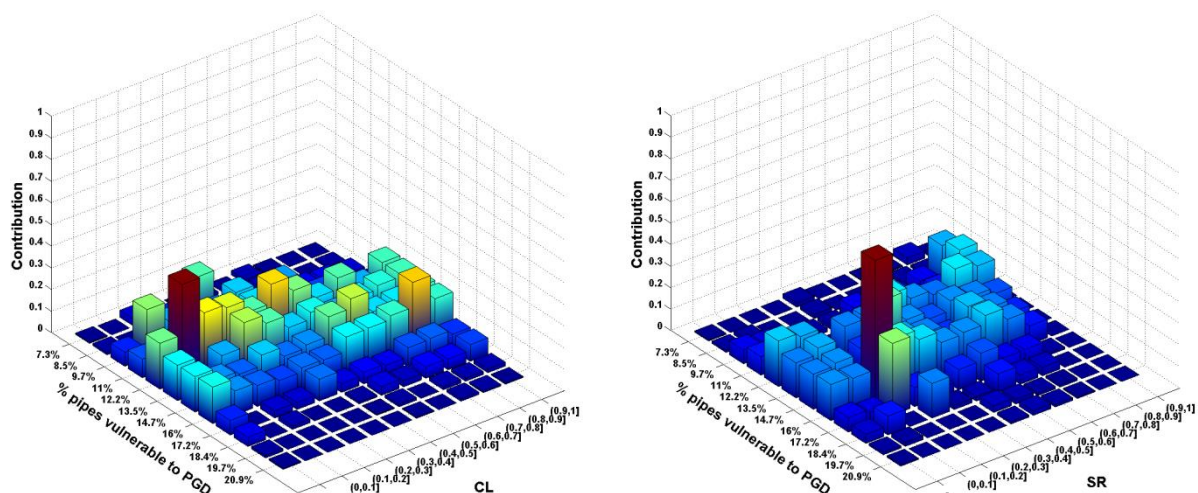


Fig. 7.39 Relative frequency of percentage of pipes vulnerable to PGD conditional to CL (left) and SR (right)

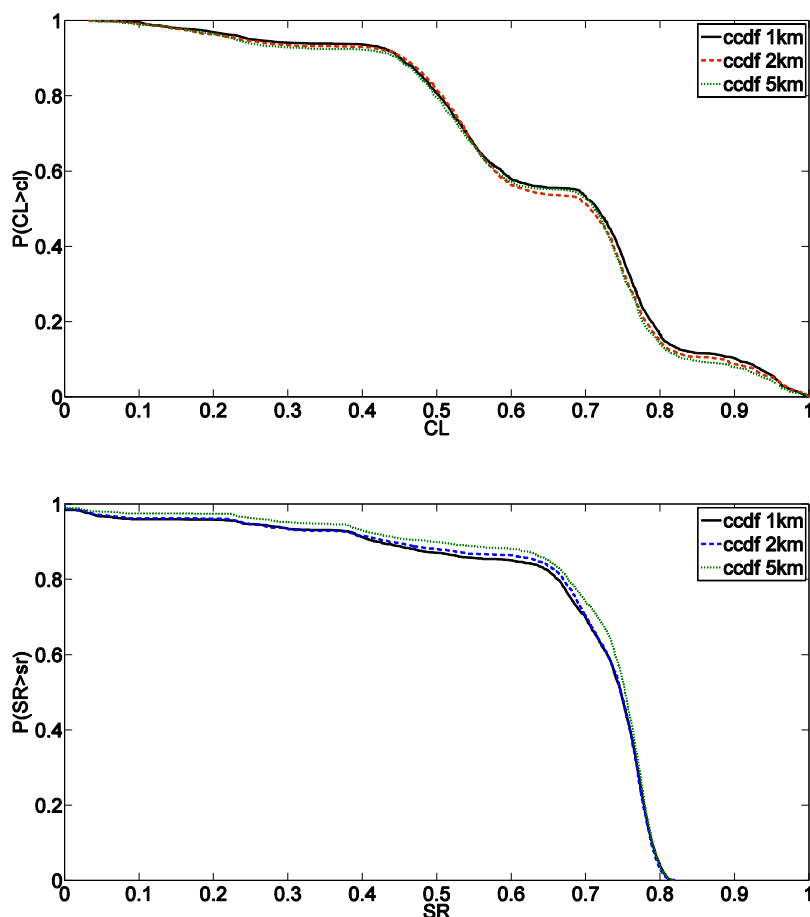


Fig. 7.40 Exceedance curve of CL (top) and SR (bottom) for the three grid sizes

Finally, in order to study the effects of regular grid size for the computation of the primary IM, three analyses were set up according to three grid sizes employed: 1 km, 2 km and 5 km. For each grid size an intra-event residual correlation value for PGA was calculated starting

from correlation models estimated by Esposito and Iervolino (2011a), i.e., 0.80, 0.64 and 0.33 respectively. These values characterize the correlation of PGA at points located at the extremity of each cell that are assumed instead perfectly correlated. Therefore, the larger is the size of the grid, the larger is the approximation.

Results for the three grid sizes are presented in the following figures. In particular, Fig. 7.40 shows the probability of exceedance for the two performance indicators. Although it seems that higher grid sizes tend to underestimate the risk, differences are not so pronounced.

7.6.4 Road network in Calabria region, Southern Italy

Three types of simulations have been carried out: a plain Monte Carlo (MCS) and two improved simulations employing variance reduction techniques, i.e., Importance Sampling (ISS) and Importance Sampling with k-means clustering (ISS-KM). The reader can refer to SYNER-G report D2.1 (Franchin et al. 2011) for an exhaustive description of such simulation schemes.

The analysis results as obtained from a plain MCS of 20,000 runs are presented in the following figures. The chosen number of runs has been shown to yield stable estimates for all considered PIs.

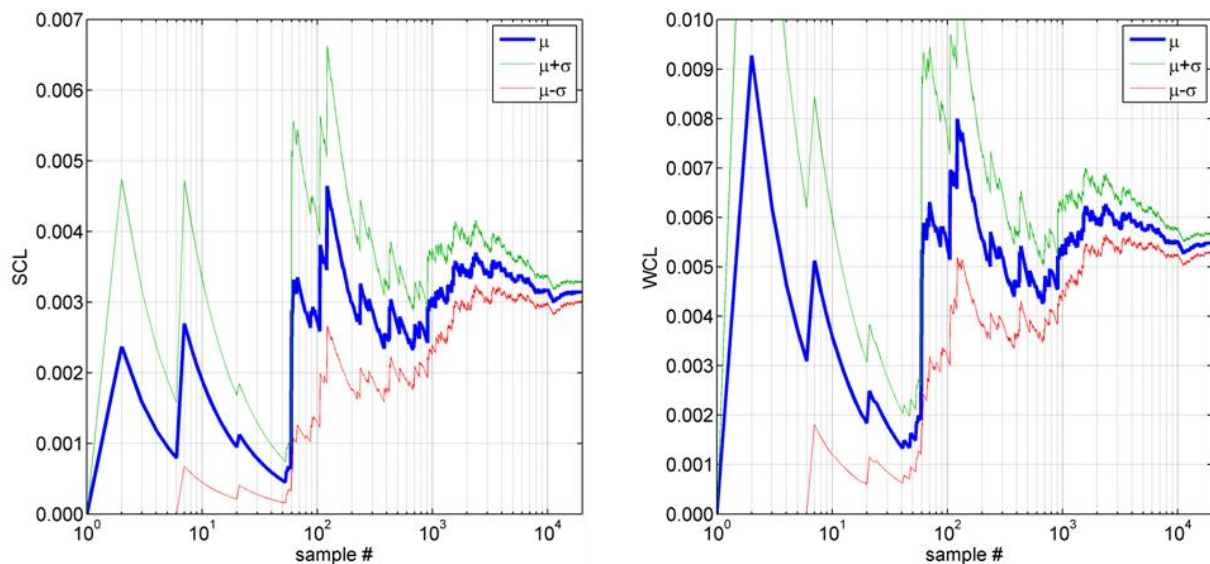


Fig. 7.41 Moving average μ , $\mu+\sigma$ and $\mu-\sigma$ curves for SCL (left) and WCL (right)

Fig. 7.41 shows the moving average μ curves for SCL (left) and WCL (right), as well as the $\mu+\sigma$ and $\mu-\sigma$ curves for the two PIs. The figure indicates that the expected value of connectivity loss given the occurrence of an earthquake is higher for WCL than for SCL, as expected. In fact, WCL takes into account not only the existence of a path between two TAZs, but also the increase in travel time due to the seismically induced damage suffered by the RDN. The jumps present in the plots are located in correspondence of simulation runs/samples in which at least one TAZ results disconnected from at least one TAZ, leading SCL and WCL to yield values greater than 0.

Fig. 7.42, left, shows the MAF of exceedance curves for SCL and WCL. As expected, weighting the computation of connectivity loss with the path travel times yields higher values of exceedance frequency.

Fig. 7.42, right, displays, in a matrix form with a grey scale, the values of TR for each pair of TAZs. The matrix, which is symmetric due to the graph being undirected (recall that even if the model is directed this particular network is in practice undirected because there is always a pair of opposite edges between connected nodes, sharing the same vulnerability), indicates that the probability of connection is very high over all the region, with lower reliability concentrated in the northern part of Calabria (approximately the first 100 TAZs).

Fig. 7.43, left, shows the contour map of travel time to the closest hospital for the entire region, in non-seismic or undamaged conditions. The blue “islands”, with zero travel time, clearly indicate the hospitals’ positions in the region.

Fig. 7.43, right, shows the contour map of expected travel time increment in damaged conditions, obtained dividing the expected value of minimum travel time in seismic conditions (averaged on the whole simulation) by the reference minimum travel time. Such increment results to be very low and concentrated in the central mountainous part of the region.

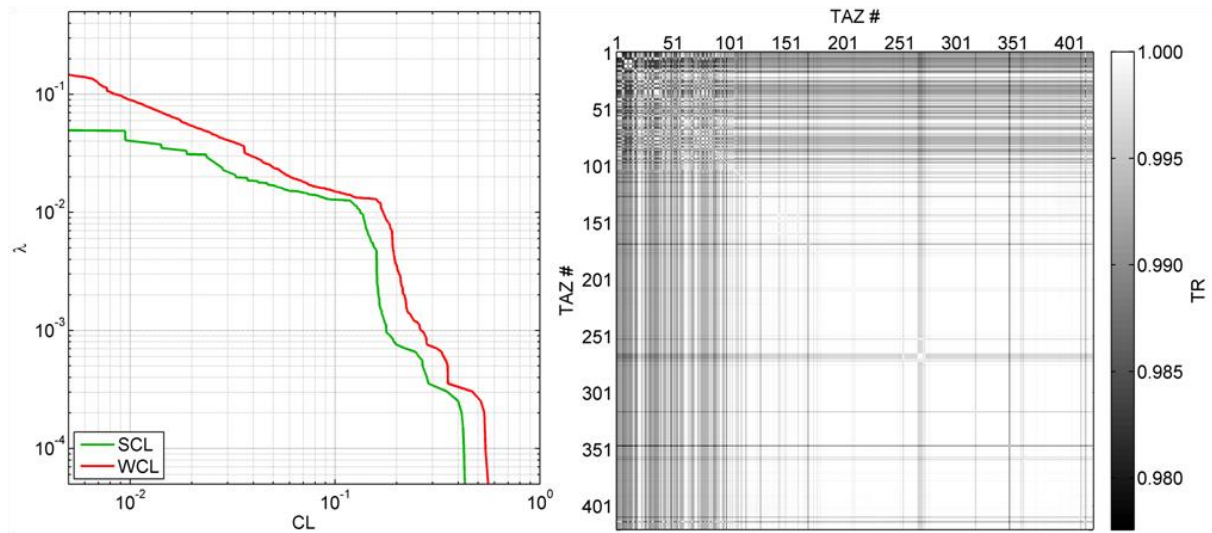


Fig. 7.42 MAF curves for SCL and WCL (left) and TR matrix (right)

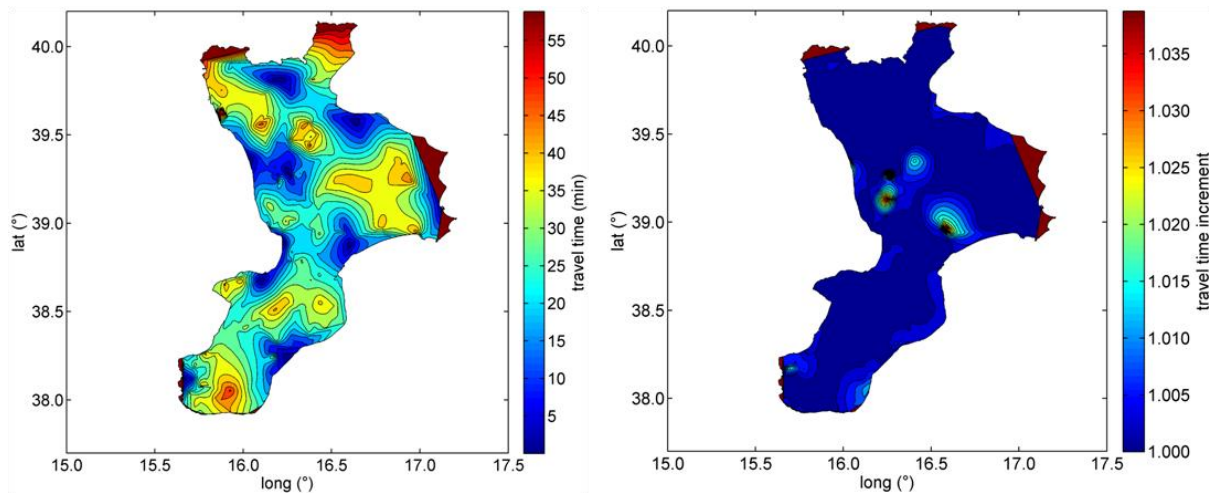


Fig. 7.43 Contour maps of minimum travel time to hospitals, in non-seismic conditions (left) and of expected increment of minimum travel time to hospitals (right)

With reference to some PIs, the results coming from MCS have been taken as the reference solution and compared with those obtained from the two variance reduction techniques, ISS (2,000 runs) and ISS-KM (200 runs). In particular, in Fig. 7.44 the comparison is relative to moving average curves of SCL (left) and WCL (right), while in Fig. 7.45 it is referred to MAF curves of the same indicators.

The match of the curves is shown to be quite good in all cases, with comparable orders of magnitude. The efficacy of ISS and ISS-KM has been tested with reference to some case studies (mostly buildings and networks) and some particular PIs, noting that the results of such tests were fully satisfactory only in some cases. The conclusion has been that the effectiveness is strongly case-dependent and PI-dependent. Further studies on different systems analyzed with different approaches (connectivity/capacitive) are needed to draw guidelines for the use of such variance reduction techniques as a practical alternative to the cumbersome and time-consuming MCS.

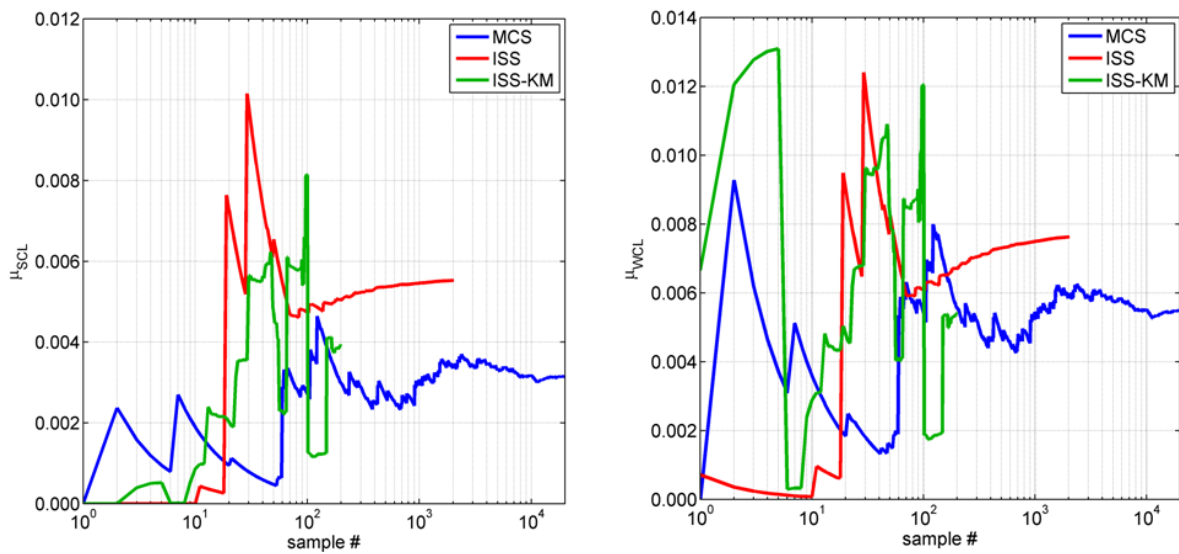


Fig. 7.44 Comparison of moving average μ obtained from MCS, ISS and ISS-KM, for SCL (left) and WCL (right)

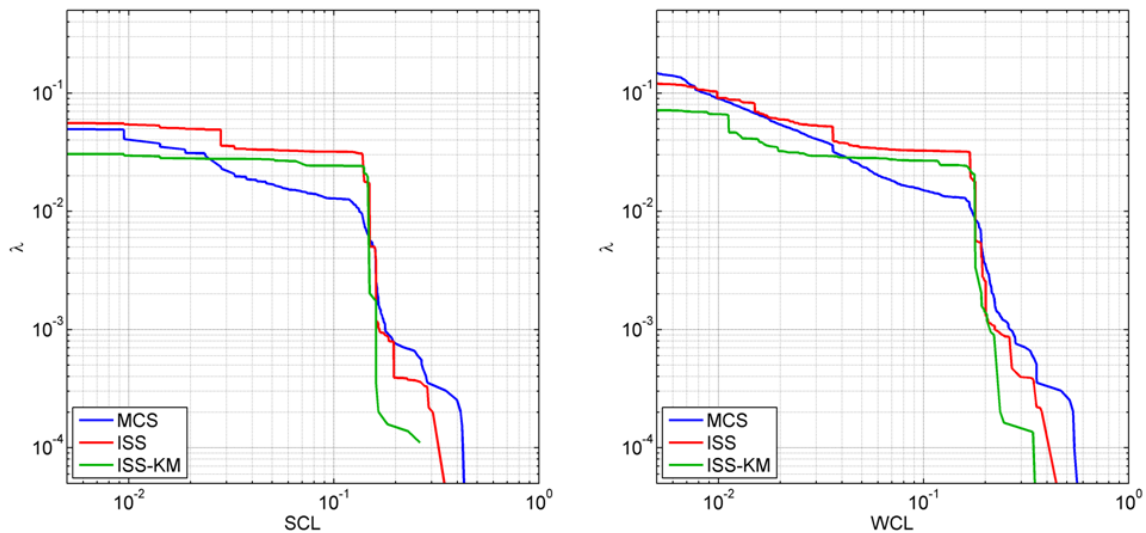


Fig. 7.45 Comparison of MAF curves obtained from MCS, ISS and ISS-KM, for SCL (left) and WCL (right)

7.6.5 Electric power network of Sicily

Three types of simulations have been carried out: a plain Monte Carlo (MCS) and two improved simulations enhanced with variance reduction techniques, i.e., Importance Sampling (ISS) and Importance Sampling with k-means clustering (ISS-KM). The reader can refer to SYNER-G report D2.1 (Franchin et al. 2011) for an exhaustive description of such simulation schemes.

The analysis results as obtained from a plain MCS of 20,000 runs are presented in the following figures. The chosen number of runs showed to yield stable estimates for all considered PIs.

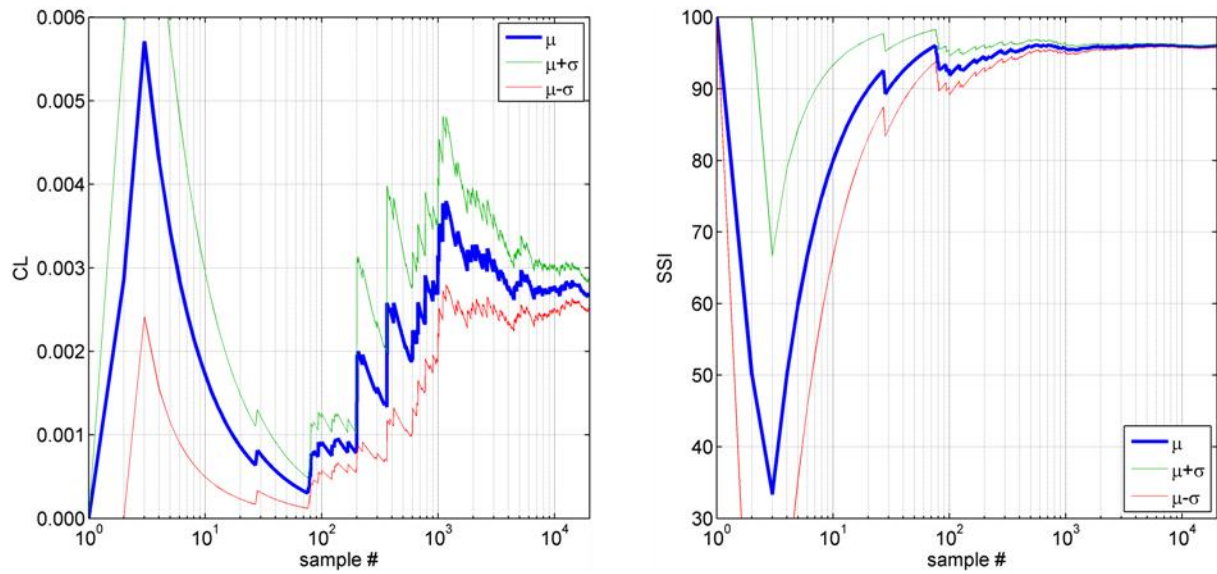


Fig. 7.46 Moving average μ , $\mu+\sigma$ and $\mu-\sigma$ curves for CL (left) and SSI (right)

Fig. 7.46 shows the moving average μ curves for CL (left) and SSI (right), as well as the $\mu+\sigma$ and $\mu-\sigma$ curves for the two PIs. The minimum sample size is strongly dependent on the chosen PI; in fact, SSI stabilises with less than 1,000 runs, whereas CL requires a much larger number of runs. The reason for this difference is that CL depends on the number of connected sources, rather than on the actual demand satisfaction at load buses. The number of connected sources is a more variable quantity, being affected by the uncertainty on short-circuit propagation, that causes a line to be turned off every time a short-circuit tries to spread outside one of the substations in the network.

Fig. 7.47 shows the MAF of exceedance curves for CL and SSI. The same feature highlighted by the moving average of the two PIs is observed by looking at the MAF curves. In fact, while the CL MAF presents a wide range of variation, SSI confirms to be a very stable indicator, with MAF values ranging in a small interval.

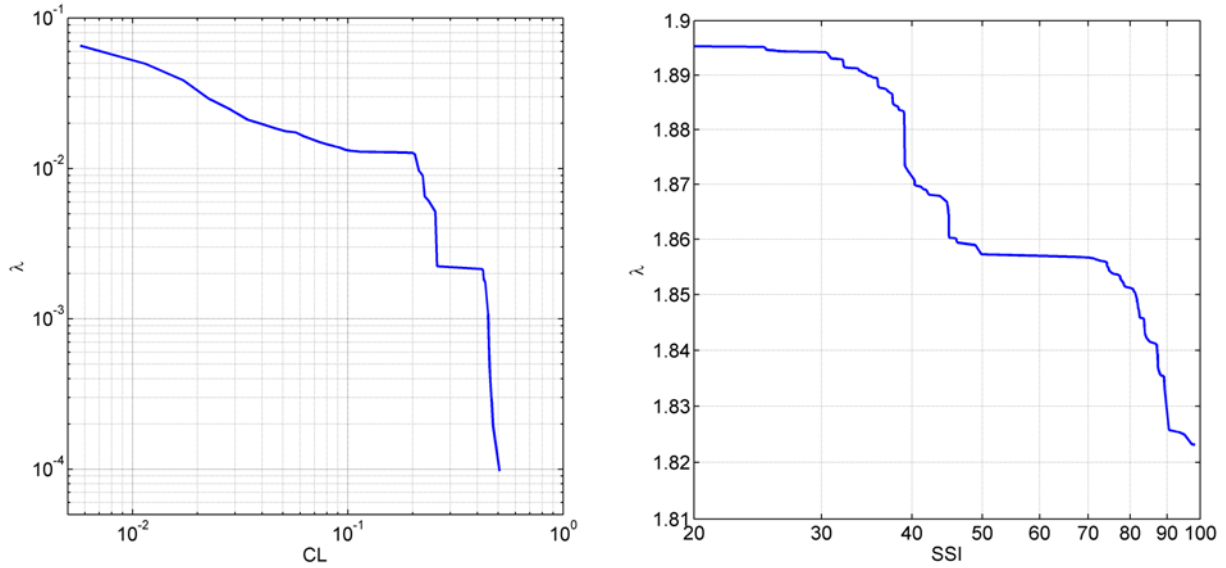


Fig. 7.47 MAF curves for CL (left) and SSI (right)

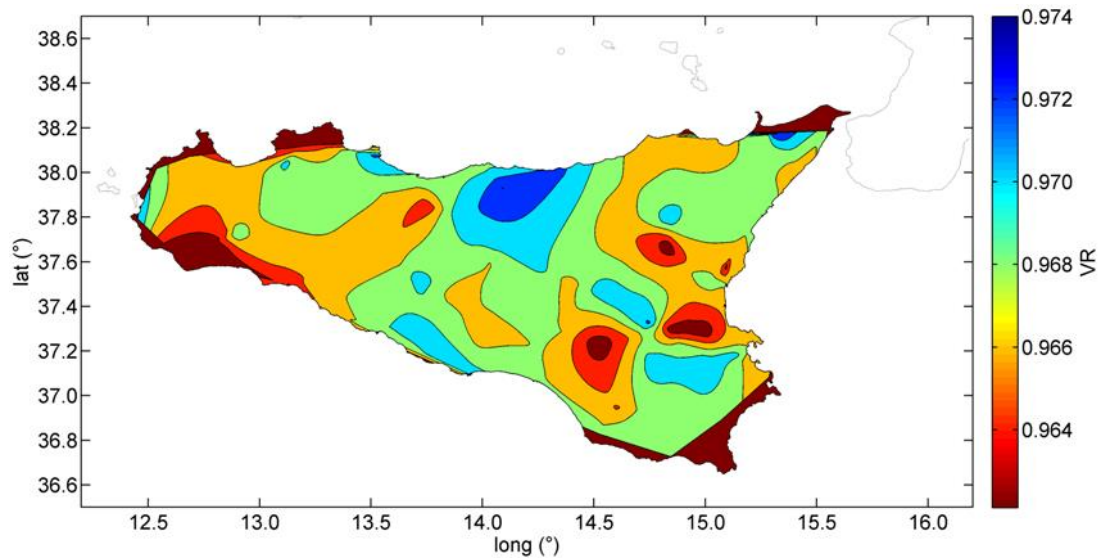


Fig. 7.48 Contour map of expected values of VR

Fig. 7.48 displays a contour map of the expected values of VR, averaged on the whole simulation for each demand node. It can be seen that the reduction in voltage due to seismically induced damage is less than the tolerated threshold of 10%, allowing the power demand delivery everywhere in the island, consistently with the very large value of SSI and very low value of CL.

With reference to some PIs, the results coming from MCS have been taken as the reference solution and compared with those obtained from the two variance reduction techniques, ISS (2,000 runs) and ISS-KM (200 runs). In particular, in Fig. 7.49 the comparison is relative to moving average curves of CL (left) and SSI (right), while in Fig. 7.50 it is referred to MAF curves of the same indicators.

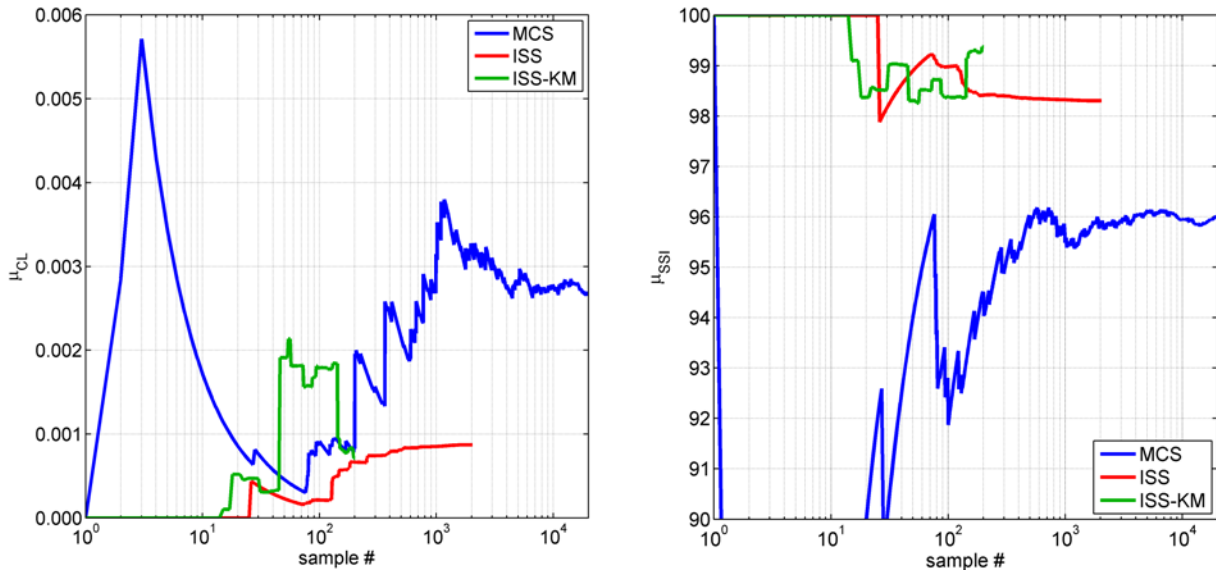


Fig. 7.49 Comparison of moving average μ obtained from MCS, ISS and ISS-KM, for CL (left) and SSI (right)

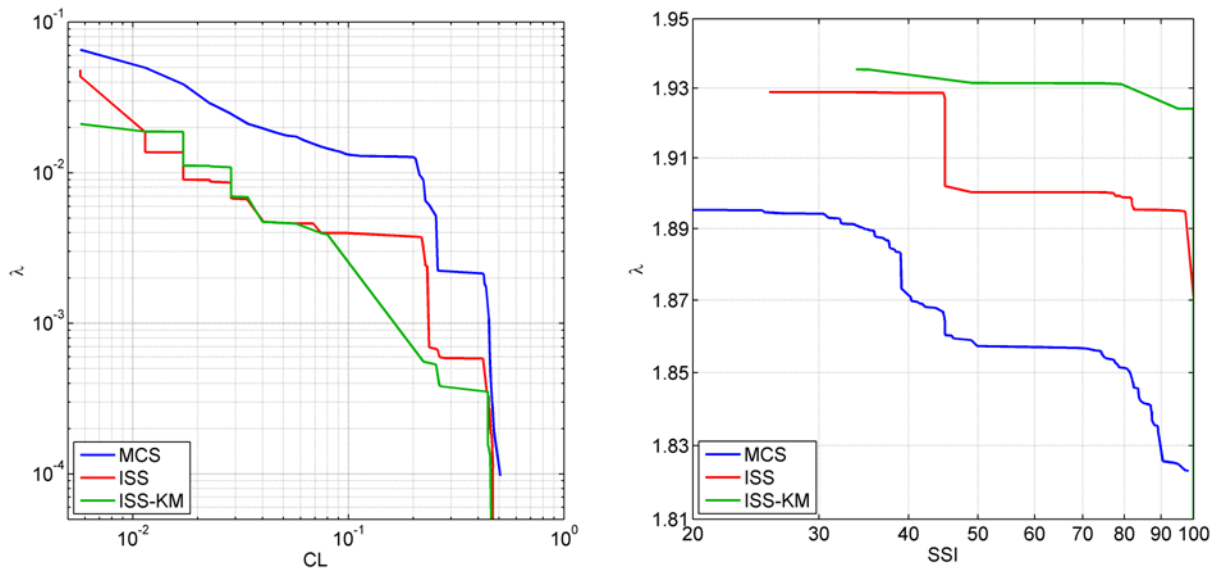


Fig. 7.50 Comparison of MAF curves obtained from MCS, ISS and ISS-KM, for CL (left) and SSI (right)

The match of the curves is shown to be not very good in all cases, although the order of magnitude of values is comparable for μ curves and MAF curve of SSI. The effectiveness of ISS and ISS-KM was tested before with reference to some case studies (mostly buildings, not networks) and some particular PIs. The results of such tests were fully satisfactory. Therefore, the unsatisfactory match in this case hints at the fact that the match quality is strongly case-dependent and PI-dependent. Further studies on different systems analyzed with different approaches (connectivity/capacitive) are needed to draw guidelines for the use of such variance reduction techniques as a practical alternative to the cumbersome and time-consuming MCS.

7.6.6 Hospital facility and regional health-care system IN Italy

A plain Monte Carlo simulation with 10,000 runs is carried out to test the proposed methodology. The expected value of the total number of casualties, N_{r+y} , over the 10,000 runs is equal to 75 (0.07% of the regional population); among those, the expected HTD are 52, while the \overline{HTD} are 23. It is noted that these figures do not include deaths (blue and black tag) and lightly injured people (green tag).

The first indicator to measure the resilience of the regional health-care system is the number of victims that cannot receive the medical care. This is expressed in terms of Mean Annual Frequency (MAF) of exceedance (or, equivalently, of return period of the event which causes the exceeding of un-hospitalised victims). The corresponding curves for the HTD and \overline{HTD} , normalised to the regional population, are shown in Fig. 7.51. For example, the return period of the event with the 0.1% of the regional population that cannot receive the (needed) surgical treatment (red curve) is 100 years.

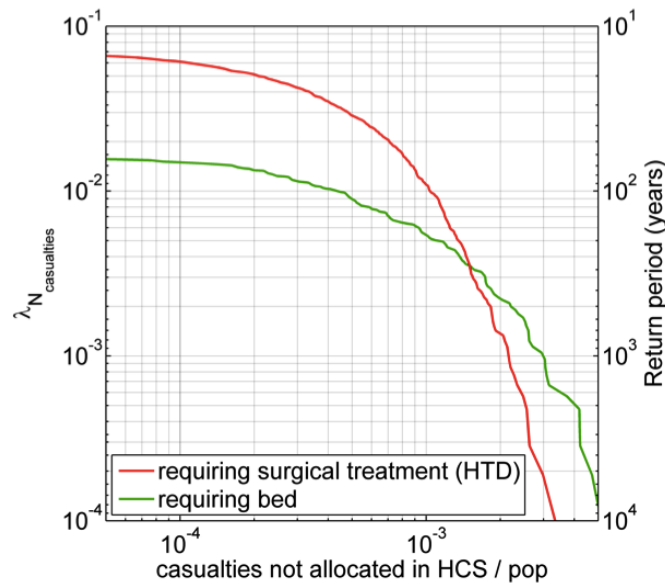


Fig. 7.51 MAF curves of normalised casualties (divided in two categories) that are not allocated in hospitals

A second indicator is the maximum hospitalisation travel time. The moving average μ and moving standard deviation σ are computed at each simulation run. Corresponding curves of μ and $\mu \pm \sigma$ are shown in Fig. 7.52. For the investigated system, the expectation of the maximum hospitalisation time is 36 min. The mean of the indicator becomes stable after about 1,000 runs, and this justifies the adopted number of runs.

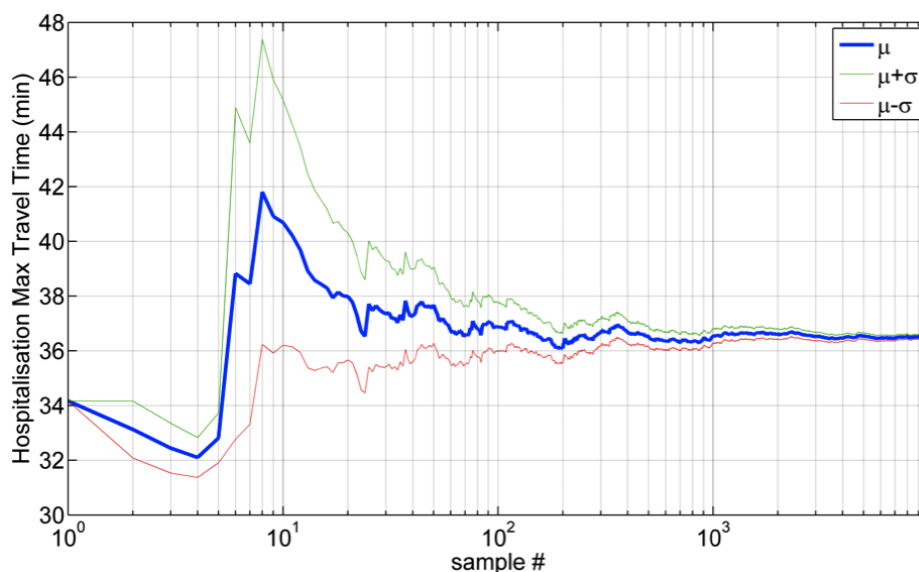


Fig. 7.52 Evolution of maximum travel time for hospitalisation

The resilience of the hospitals in the region is expressed by the probability of not being able to provide the required surgical treatments to victims if an earthquake strikes the region (i.e., the *seismic risk*), as shown by the bar plot in Fig. 7.53. The results are in agreement with the treatment capacity curves employed for hospitals and the assumed configuration of the study area, where the seismic sources are located in the western part. In fact, the distribution of the seismic risk reflects both the source to hospital-site distance (hospital in TAZ #5 is the closest) and the assumed vulnerability of the facilities in terms of *HTC* fragility curves (hospital in TAZ #5 has the lowest treatment capacity).

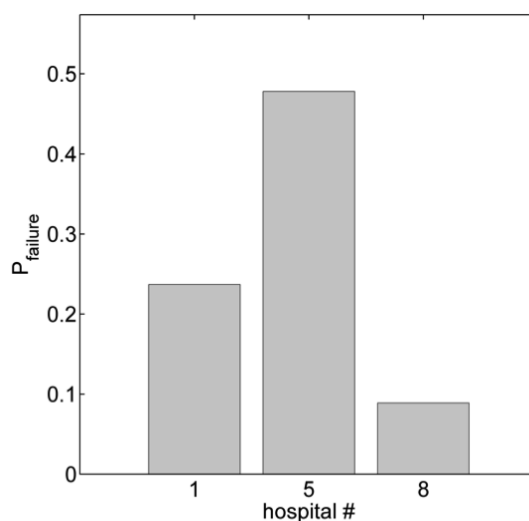


Fig. 7.53 $P(HTD \geq HTC)$, for the three region hospitals

7.6.7 Harbour of Thessaloniki

The analysis results obtained from a plain MCS of 10,000 runs is presented in the following figures. The chosen number of runs has been shown to yield stable estimates for the considered PIs.

All PIs are normalized to the respective value referring to normal (non-seismic) conditions. For the container terminal this value is equal to $PI_{a_{max}}=1,032$ TEUs per day. For the cargo terminal the max value for non-seismic conditions is equal to $PI_{o_{max}}=43,512$ tons per day. These values refer to the max capacity of the port, since they are estimated assuming that all cranes are working at their full capacity for 24 hours a day.

Fig. 7.54 shows the moving average (mean) curves for TCoH (left) and TCaH (right), as well as the mean+stdv and mean-stdv curves for the two PIs. The figures indicate that the expected value of loss given the occurrence of an earthquake is higher for TCoH than for TCaH. At the end of the analysis (10,000 runs) the moving average is stabilized. Comparison of the moving average (mean) curves for TCoM and TCaM with TCoH and TCaH respectively, shows no difference, meaning that no road closures are observed. This can be attributed to the small length of roadways considered in the analysis, as well as the limited number of low-height buildings in large building-road distances. Given the fact that no road closures are observed in the present analysis, results are presented hereinafter only for the TCoH and TCaH PIs.

Mean Annual Frequency (MAF) of exceedance values for all PIs are given in terms of normalized performance loss ($1-PI/PI_{max}$). Fig. 7.55 shows the MAF of exceedance curves for TCoH and TCaH. For performance loss values below 20% TCaH yields higher values of exceedance frequency, while for performance loss over 20% TCoH yields higher values of exceedance frequency. The estimated MAF of exceedance curves (in terms of normalized performance loss) for TCoH and TCaH with and without interaction with building collapses (road blockage due to collapsed building is not considered in the analysis) are illustrated in Fig. 7.56. As expected, in both cases, there is no difference, since no road closures are observed; this type of interactions is not important in this particular case to the port's overall performance. In other cases, for example in the Port Island in Kobe, it could be crucial. Fig. 7.57 compares the estimated MAF of exceedance curves for TCoH and TCaH when all interactions are taken into consideration (EPN and road closures) and no interactions are considered in the analysis. The effect of interaction (mainly of the EPN to cranes) can be very important for performance loss levels over 10% for TCoH and 5% for TCaH. As an example the TCoH performance loss is increased from 21% to 46% for $\lambda=0.01$ ($T_m=100$ years) when all interactions are included in the analysis. In the TCaH MAF curves, for performance loss levels of 50-60% there seems to be practically no change in the exceedance frequency values, and values with no interactions are higher than those corresponding to the all interactions case. This can be considered as the point of max performance loss for TCaH, only due to direct seismic damage occurred to cranes.

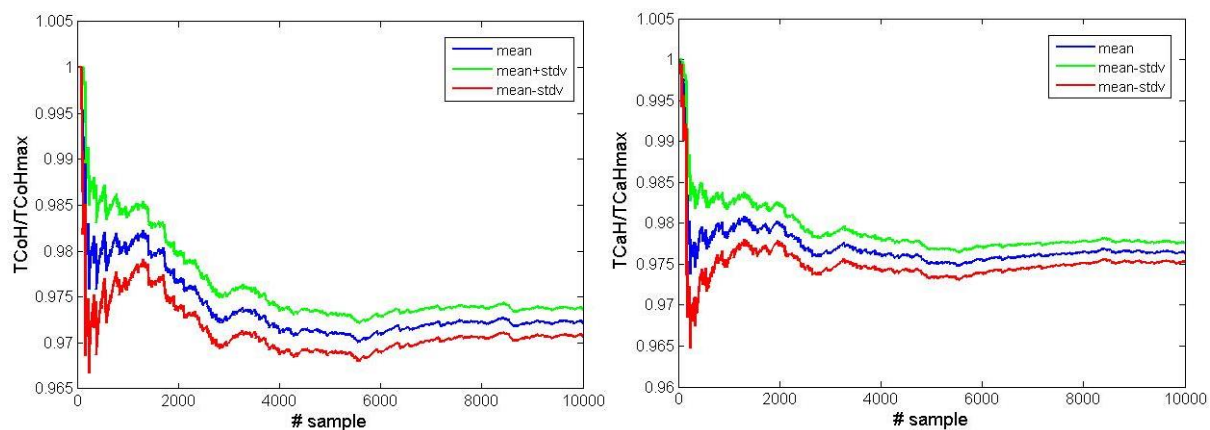


Fig. 7.54 Moving average μ , $\mu+\sigma$, $\mu-\sigma$ curves for TCoH (left) and TCaH (right)

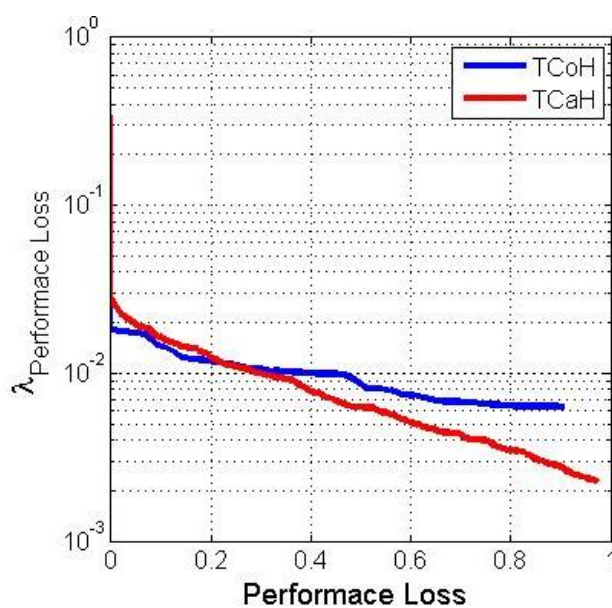


Fig. 7.55 MAF curve for TCoH and TCaH performance loss

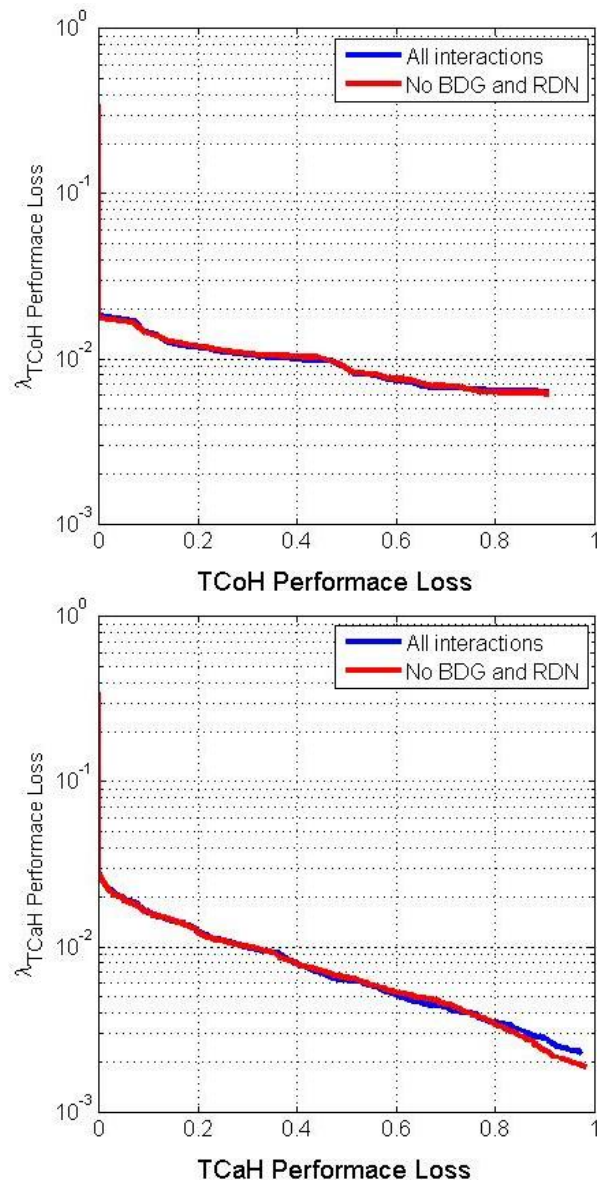


Fig. 7.56 MAF curves for TCoH (left) and TCaH (right) for Thessaloniki's port, with and without interaction with building collapses

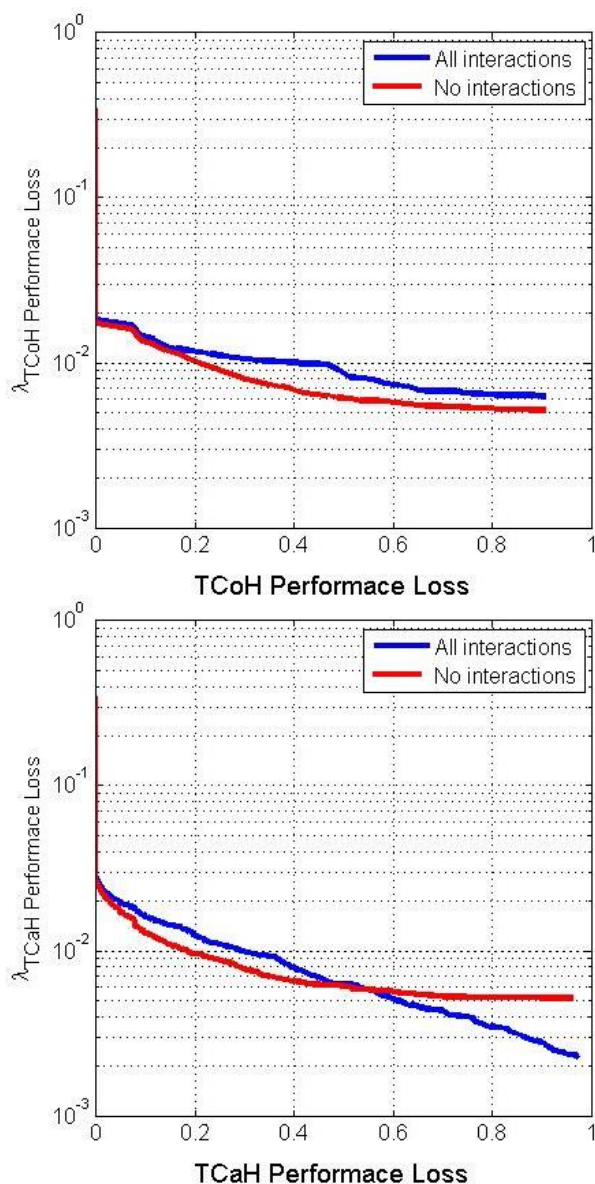


Fig. 7.57 MAF curves for TCoH (left) and TCaH (right) for Thessaloniki's port, with and without interaction with EPN and building collapses

Fig. 7.58 and Fig. 7.59 show the level of correlation between the TCaH and the distribution of damages in cranes and non-functionality of electric power distribution substations respectively. In this way the most critical components can be defined in relation with their contribution to the performance loss of the system. All cranes have medium (40-70%) to high (over 70%) levels of correlation, indicating their great importance to the functionality of the overall port system. A higher level of correlation is estimated for the EPN distribution substations, with 40% of the components having values greater than 70%.

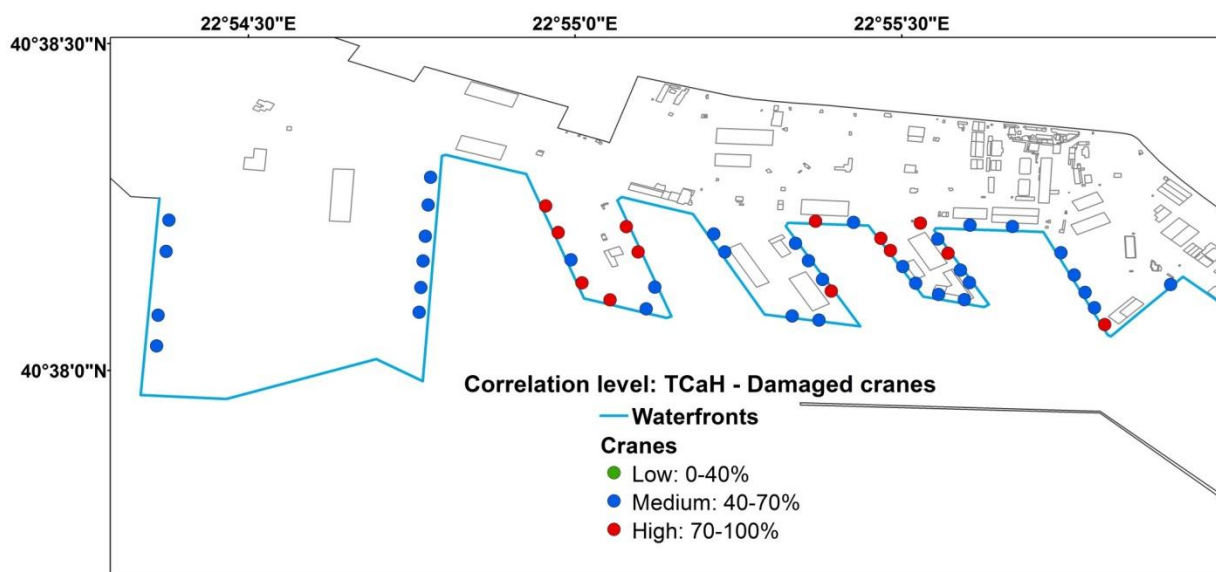


Fig. 7.58 Correlation of damaged cranes to port performance (PI=TCaH)

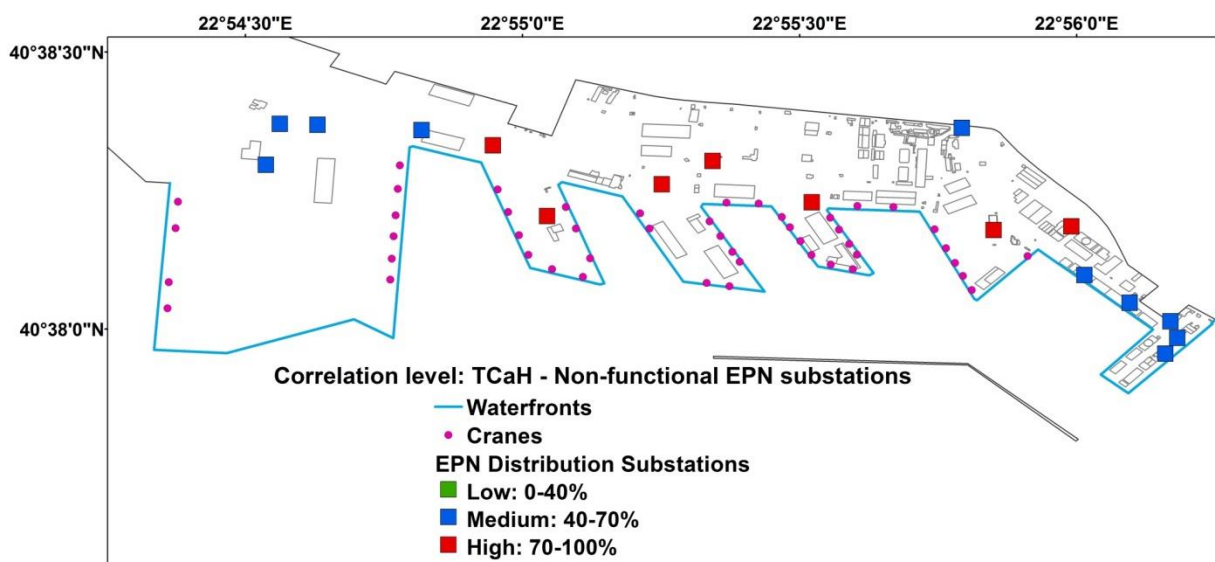


Fig. 7.59 Correlation of non-functional electric power distribution substations to port performance (PI=TCaH)

7.7 CONCLUSIONS

The SYNER-G methodology and software tools have been applied and tested in selected case studies at urban and regional level. In particular, the following case studies have been undertaken and presented in this synthetic reference report:

At city/urban level:

1) The city of Thessaloniki, a high seismicity area in North Greece. The application includes buildings, road network, water supply system and electric power network with specific interdependencies between them. New analytical fragility curves developed for buildings

(RC/masonry) and bridges based on the inventory of Thessaloniki area are also presented. An accessibility and shelter needs analysis is also performed.

2) A district of the city of Vienna in Austria, a low seismicity area. The application is performed in one district of the city. It includes buildings, road network, water supply system and electric power network with specific interdependencies between them.

At regional level:

4) The medium-pressure gas system of L'Aquila in Italy. The process makes use of probabilistic seismic hazard analysis, empirical relations to estimate pipeline response, fragility curves for the evaluation of facilities' vulnerability and connectivity performance indicators to characterize the functionality of the network.

5) The road network of Calabria region in Southern Italy. A level I analysis has been performed, focusing the attention on the network's pure connectivity, considering bridges and road pavements as vulnerable elements.

6) The electric power network of Sicily. A capacitive study has been performed, with power flow analysis that follows the analysis of short-circuit propagation, in which circuit breakers are active components playing a key role in arresting the short-circuit spreading. The substations are not modeled as vulnerable points; in fact, their full internal logic is modeled to account for partial functioning.

At complex infrastructure level:

7) A hospital system in Italy, composed of hospitals, area districts and a road network. The road network is deputed to connect districts and hospitals allowing the transportation of injured and sick people. To properly assess the response of the system, the vulnerability of the system components, i.e., hospitals and roads, as well as the interaction among them are accounted for.

8) The harbour of Thessaloniki in Greece where system performance is assessed considering specific interdependencies between the components. Port Performance Indicators (PIs) are calculated based on the estimated damages and functionality loss of the different components.

Seismic hazard

A probabilistic approach is followed which samples earthquake events based on the hazard characterization of each area. Each sampled event represents a single earthquake (shakefields method, Weatherhill et al. 2011b) and all systems are analyzed for each event. The results are then aggregated all over the sampled events. For each site of the grid the averages of primary IM from the specified GMPE were calculated, and the residual was sampled from a random field of spatially correlated Gaussian variables according to the spatial correlation model.

The source models provided in SHARE project are applied either as seismic zones (e.g. Thessaloniki case study, harbour of Thessaloniki) or as faults (e.g. transportation network in S. Italy and electric power network in Sicily). In other cases, specific faults are used as sources (e.g., Paganica fault in L'Aquila case study) or historical earthquakes are modeled (e.g., Vienna case study).

The performance of spatially distributed systems may be conditional upon the failure of many components each one being sensitive to different IMs. Therefore seismic input assessment has to take into account the possibility of the existence of a cross-correlation

between IMs. To address this issue, spatial correlation models and conditional hazard approach are considered. For each site of the grid the averages of primary IM from the specified GMPE were calculated, and the residual sampled from a random field of spatially correlated Gaussian variables according to the spatial correlation model. The value of the primary IM at each site of the network (i.e., the vulnerable elements' sites) was then obtained interpolating the grid values.

Different amplification methods are available in the SYNER-G code (i.e Eurocode 8, NEHRP, Choi&Stewart, context-specific). Such methods amplify the shaking intensity measure (IM) at vulnerable sites *a posteriori*, i.e., after the ground motion calculation stage. It can also be used the within-GMPE amplification method, using the Vs30 values for site classification. In case no soil classification data are available IM values are computed on stiff soil conditions (e.g. transportation network in S. Italy and electric power network in Sicily).

Fragility curves

Appropriate fragility curves are selected for the components of each case study considering the typology/taxonomy of the network or infrastructure (see Reference Report 4, Kaynia 2013). In case of Thessaloniki application, new analytical fragility curves have also been developed for bridges and buildings respecting the specific typologies and features of the Thessaloniki structures.

Systemic analysis and performance indicators

Connectivity analysis is performed in most case studies (e.g. networks in Thessaloniki and Vienna, road network in South Italy, gas system in L'Aquila, regional hospitals system in Italy). This is simply due to lack of all required information or due to large computational demand required for a complete flow analysis. However, in case of road network at least, this type of analysis is coherent with the time-frame of the study, that is limited to rescue operations in the aftermath of the seismic event. The interest is the identification of the portions of the network which are critical with respect to the continued connectivity of the network. In case of electric power network in Sicily, a power flow analysis is performed. For complex systems (Thessaloniki harbour, health-care facilities) their internal logic and functions are simulated.

The risk assessment is performed in terms of appropriate performance indicators for each system. In this way, performance indicators that are able to quantify the degree to which the system is able to meet established specifications and/or customer requirements following an earthquake event give the quantitative measure of the functionality of each network.

Results

The overall performance of each network and system is expressed through the moving average μ and moving standard deviation σ (averaged over simulations), as well as the Mean Annual Frequency (MAF) of exceedance of the PIs. The average loss is defined based on the moving average graph. Through the MAF graphs the annual probability of exceeding specific levels of loss can be defined and the loss for specific mean return period of the particular PI can be estimated. The earthquake event(s) that correspond to a particular return period (i.e., 500 year) are identified and maps with the distribution of damages are produced for this event(s).

Correlation of damaged components to system performance

In order to evaluate the contribution of certain components on the overall performance of the network the correlation between damaged components and system's functionality is estimated.

In the case of Thessaloniki the correlation of each component (EPN, WSS, RDN) to the system PIs is estimated. This type of analysis is based on the results of each single event, and thus it preserves the information about systems' topology and its behavior in case of spatial correlated damages (related to single earthquakes). Thus, it allows identifying the most critical elements for the functionality of each system (i.e., the damaged components that more closely control the performance of the network).

In case of L'Aquila gas system, the percentages of sites vulnerable to PGD as well as the number of broken pipes and damaged M/R stations are correlated with the performance indicators of the network in order to evaluate possible linear dependencies. The results indicate that the number of damaged M/R stations is better correlated with the considered PIs. The distributions of number of broken pipes and percentage of pipes vulnerable to PGD, conditional to the performance of the network are somewhat flat.

Uncertainties

Several sources of uncertainties are inherent in the analysis which are related among others to the seismic hazard and spatial correlation models, the fragility assessment or the functionality thresholds of each component.

In case of the Thessaloniki harbour, the epistemic uncertainty related to different fragility functions and functionality definitions is investigated through a sensitivity analysis with the use of alternative fragility curves and functionality thresholds for the waterfront structures. Similar results are obtained when different fragility curves are applied. This can be attributed to the small frequency of damage occurrence to the waterfront structures and the fact that the total port performance is mostly prescribed by the cranes functionality.

The effect of grid size for the computation of the primary IM was investigated in case of L'Aquila gas network, where different analyses were set up for three grids (i.e., 1 km, 2 km and 5 km). These were chosen via specific values of correlation of intra-event residuals for the primary IM. The results show that the larger the grid size, the larger is the approximation. As expected, coarser discretization tends to (slightly) underestimate the risk.

Socioeconomic analysis

A socio-economic analysis has been performed in the case of Thessaloniki. In particular, a GIS-based accessibility modeling has been implemented for shelter and healthcare services. It is a representative example, without considering the whole city and related networks. It is shown that the SYNER-G methodology and analysis is an important tool for seismic risk management purposes before, during and after disaster. GIS based accessibility modeling can directly provide a vital support to disaster managers in terms of accessibility, location/allocation of available resources and service/catchment related issues. A shelter needs analysis has been also applied. The shelter model simulates households' decision-making and considers physical, socio-economic, climatic, spatial and temporal factors in addition to modeled building damage states and utility loss. From the analysis, different SCDs are identified, as "Hot Spots" for shelter needs. These results can help for the planning of shelter allocation.

8 Guidelines, recommendations and dissemination

8.1 MAIN DISSEMINATION ACTIVITIES

A graphical representation of all dissemination schemes is given in Fig. 8.1. The activities for dissemination are given in the following list:

- Publication of Seven Reference Reports, documenting the methods, procedures, tools and applications developed in SYNER-G. The list of the Reference Reports, with its corresponding editors, reviewers and address audience, is given in Table 8.1.
- Development of a website platform for the project (www.syner-g.eu) set up early in the project, providing general, non-confidential information to external users, such as key publications and deliverables, newsletters and announcement of meetings and workshops. The address of the home page of the public website is www.syner-g.eu.
- Preparation of a Project Leaflet and a Project Presentation, prepared at the beginning of the project.
- Issuing of three Newsletters.
- Organization of two Technical Workshops, the first in Thessaloniki (1/3/2013) and the second on Vienna (5/3/2013), presenting the case studies for these two cities.
- Organization of the Final Workshop in Milano (21-22/3/2013), with the participation of the International Advisory Committee and invited experts.
- Preparation of a demo explaining the use of the software tool.
- Participation at key events and Conferences, in particular: i) 14th European Conference on Earthquake Engineering, held in Skopje, FYROM, from 30/8 to 3/9/2010; ii) 4th International Disaster and Risk Conference IDRC “Integrative Risk Management in a Changing World – Pathways to a resilient Society”, held on 26-30/08/2012 in Davos, and iii) 15th World Conference on Earthquake Engineering (15WCEE), held in Lisbon, Portugal, on 24-28/9/2012, with a special session organized on 24/9 describing the objectives and main outcomes of SYNER-G.
- Publication of scientific results in peer reviewed journals, conferences proceedings and magazines, including an article on “Assessing earthquake protection” in the magazine Research Media Ltd (<http://www.research-europe.com>).
- Production of a 76 page High-Quality brochure describing the main project products and the key results of the applications to the European urban, infrastructure and network sites.

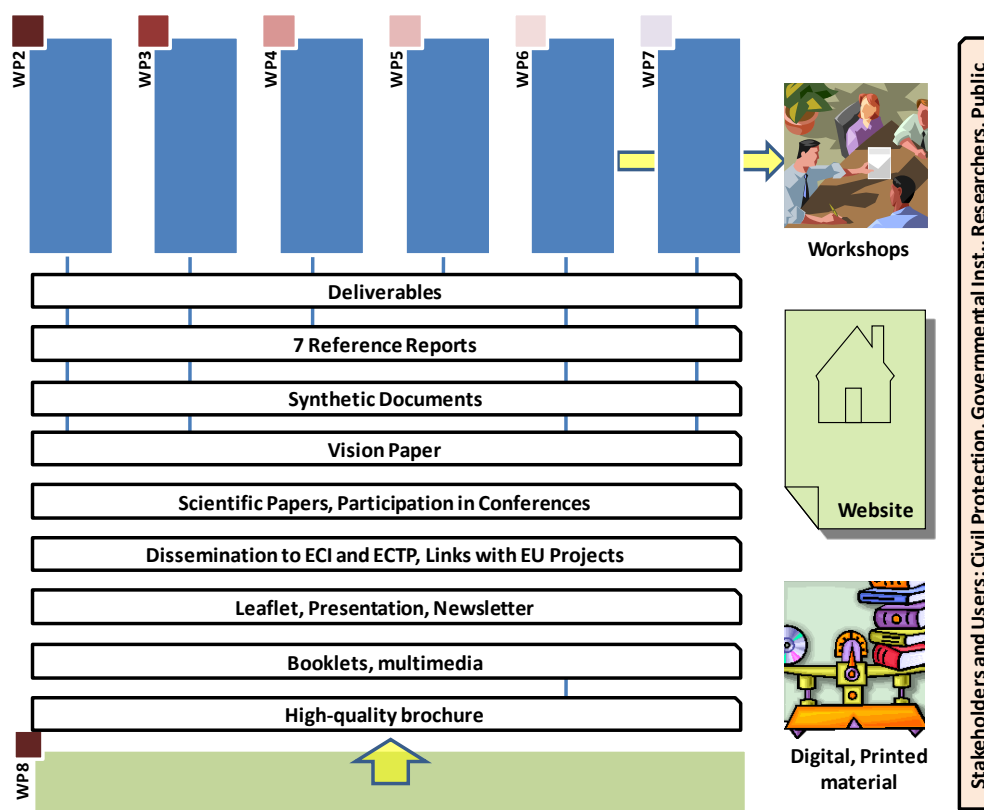


Fig. 8.1 Graphical representation of SYNER-G Dissemination scheme

Table 8.1 Consolidated List for the production of the SYNER-G Reference Reports

#	Report Title	Contributors	Lead Editor	Reviewer	Target Addressees*
1	Methodology for systemic seismic vulnerability assessment of buildings, infrastructures, networks and socio-economical impacts	AMRA, AUTH, BRGM, KIT-U, UPAV, UROMA	UROMA	UILLINOIS	SC
2	Guidelines for typology definition of European physical assets for earthquake risk assessment	AUTH, BRGM, JRC, NGI, UPAT, UPAV, UROMA	JRC	UPAT	SC, TC, PA, CP
3	Development of inventory datasets through remote sensing and direct observation data for earthquake loss estimation	AUTH, BRGM, JRC, UPAV, VCE	JRC, UPAV	NGI	SC, TC, PA, CP
4	Guidelines for deriving seismic fragility functions of elements at risk: Buildings, lifelines, transportation networks and critical facilities	AUTH, BRGM, KIT-U, METU, NGI, UPAT, UPAV, UROMA	NGI	AMRA	SC, TC, CP
5	Guidelines for the consideration of socio- economic impacts in seismic risk analysis	AMRA, KIT-U, METU, NGI	KIT-U	AUTH	SC, TC, PA, CP
6	Systemic seismic vulnerability and loss assessment: Validation studies	AMRA, AUTH, KIT-U, METU, UPAT, UROMA, VCE	AUTH	NGI, METU	SC, TC, PA, CP
7	Systemic seismic vulnerability and loss assessment: Software Users Manual	KIT-U, UROMA, VCE	VCE	METU	SC, TC, CP
*Target Addressees [Examples (non-exhaustive)]: Scientific community, Technical community, Public administration (Commission, National, Regional, Local), Civil protection Agencies					
** The final reviewer will be assigned during the meetings					

9 Conclusions and recommendations for further improvement and actions

SYNER-G has developed a highly innovative and powerful methodology and tool for modern and efficient seismic risk assessment and management. It is probably the first time that so many important components of this complex problem have been put together in a comprehensive and scientifically sound way. The whole methodology and tools have been extensively validated with different case studies of variable typology and complexity. The numerous Reference Reports that have been prepared provide a detailed description of all output. The dissemination process is in progress, besides the three general workshops that have been organized in Thessaloniki, Vienna and Milano. Numerous journal papers and the publication of two books with the main results of the project are also in progress.

In the following are summarized the main issues and recommendations gathered from the various discussions and interventions at the Final Workshop of the project:

- The definition of the taxonomy of elements at risk was one of the main outcomes of the project. However, for several elements, especially those of complex networks (e.g. industrial facilities), it will be necessary to extend the taxonomy and define appropriate fragility curves. It was also suggested to start working towards the production of European guidelines on taxonomy, with a possible view for future standardization. It was suggested to seek interaction with the INSPIRE Directive.
- In Horizon 2020 the issue of seismic and single natural risk may have a reduced importance with respect to FP7, with a shift towards multi-hazard risk and energy issues. It is important that the consortium and the scientific community as a whole explore ways on how to respond to the evolving needs of the society. The JRC proposed to combine seismic retrofit with energy upgrading, analyzing the impact of different options in economic terms.
- To this end (Horizon 2020) the Strategic Research Agenda on Earthquake Risk should be updated with contributions from SYNER-G and other on-going EU projects, as well as from the seismologists' community.
- The consortium should improve the communication of results to stakeholders, shifting from the impact of an earthquake event to the impact of mitigation measures. It is important that the scientific community does not promise zero losses, but rather a reduction of risk through constructive suggestions and recommendations.
- The active participation of stakeholders in future applications is essential for the improvement of results and for more practical use of outputs. It is also important to make the results more accessible and easily understood to the wider community of potential end users. For example the use of average values over a large number of Monte Carlo runs was questioned, as it does not provide a physical quantity that can be communicated to stakeholders. The homogeneity and clarity of the various presentations of the results of the applications is necessary to this extend.

- The SYNER-G software and tools (pre and post processing) needs to be upgraded and further improved in order to be more “friendly” to end-users as well as to improve its computation performance.
- SYNER-G presented the state-of-the-art in systemic risk. It was questioned, however, that the method, as it is proposed, is far more detailed than the level of data available (elements at risk, fragility curves). Therefore, it is necessary to invest in data mining to refine the inventories of elements at risk we have today. It is also necessary to invest more to quantify better the effects of various uncertainties, including the available data, in the accuracy of the results.
- Other issues discussed: The SYNER-G webpage will run for the next two years under the NERA platform. Then a more permanent administration mechanism should be proposed. The SYNER-G DEMO will be prepared after the final reporting under the coordination of AUTH and VCE; JRC will contribute to its dissemination.

References

- Akkar S. and Bommer J.J. 2010. Empirical equations for the prediction of PGA, PGV and spectral accelerations in Europe, the Mediterranean Region and the Middle East. *Seismological Research Letters*. 81(2): 195-206.
- American Lifelines Alliance 2001. Seismic fragility formulations for water systems. Part 1 – Guideline, ASCE-FEMA, 104 p.
- Argyroudis et al. 2011. D5.4-Systemic vulnerability and loss for water and waste-water systems, Deliverable of SYNER-G EC project.
- Argyroudis et al. 2013. D6.1-Application and validation study to the city of Thessaloniki (Greece), Deliverable of SYNER-G EC project.
- Borzi B., H. Crowley, R. Pinho. 2008. Simplified Pushover-Based Earthquake Loss Assessment (SP-BELA) Method for Masonry Buildings. *International Journal of Architectural Heritage*, 2(4): 353-376.
- Borzi B., R. Pinho and H. Crowley. 2007. SP-BELA: un metodo meccanico per la definizione della vulnerabilità basato su analisi pushover semplificate. In Twelfth Conference “L’Ingegneria Sismica in Italia”, Pisa, Italy (in Italian).
- Campbell K., Borzognia Y. 2006. Next generation attenuation (NGA) empirical ground motion models: Can they be used in Europe?. First European Conference on Earthquake Engineering and Seismology, Geneva, Paper No.: 458
- Cavalieri F., Franchin P., Gehl P., and Khazai B. 2012. Quantitative assessment of social losses based on physical damage and interaction with infrastructural systems. *Earthquake Engineering and Structural Dynamics* 41(11): 1569–1589.
- Cornell C.A., Jalayer F., Hamburger R.O., Foutch D.A. 2002. Probabilistic basis for 2000 SAC/FEMA steel moment frame guidelines. *Journal of Structural Engineering* 1284: 526-533.
- Crowley et al. 2011. D3.1 - Fragility functions for common RC building types in Europe. Deliverable of SYNER-G EC project.
- Der Kiureghian A., Ditlevsen O. 2009. Aleatory or epistemic? Does it matter? *Structural Safety* 31: 105-112.
- Erberik M.A. & A. S. Elnashai. 2004. Vulnerability analysis of flat slab structures. In Thirteenth World Conference on Earthquake Engineering, Vancouver, Canada
- Erberik M.A. 2008. Fragility-based assessment of typical mid-rise and low-rise RC buildings in Turkey. *Engineering Structures*, 30(5): 1360-1374
- Esposito S., Iervolino I. 2011a. PGA and PGV spatial correlation models based on European multievent datasets. *Bulletin of the Seismological Society of America* 101(5): 2532-2541.
- Esposito S., Iervolino I. 2012. D6.5-Application and validation study to a gas pipeline network, Deliverable of SYNER-G EC project.
- Esposito S., Iervolino I. 2011b. D5.3 - Systemic vulnerability and loss for gas and oil networks, Deliverable of SYNER-G EC project.
- Fardis M., Tsionis G. Askouni P. 2011. D3.6-Fragility functions for roadway bridges, Deliverable of SYNER-G EC project.
- Franchin et al. 2011. D2.1-General methodology for systemic vulnerability assessment, Deliverable of SYNER-G EC project.

- Franchin P. (ed.) 2013. Methodology for systemic seismic vulnerability assessment of buildings, infrastructures, networks and socio-economic impacts. SYNER-G Reference Report 1, Publications Office of the European Union, ISBN 978-92-79-28975-0.
- Franchin P. and Cavalieri F. 2012. Seismic vulnerability of a complex interconnected infrastructure. In "Seismic risk analysis and management of civil infrastructure systems", Editors: S. Tesfamariam and K. Goda. Woodhead Publishing Limited, Cambridge, UK, (in preparation).
- Gehl P., Desramaut N., Monfort-Clement D., Argyroudis S. 2011. D5.1-Systemic vulnerability and loss for building aggregates in urban scale, Deliverable of SYNER-G EC project.
- Hancilar U., Taucer F. (eds): Guidelines for typology definition of European physical assets for earthquake risk assessment. SYNER-G Reference Report 2, Publications Office of the European Union, (2013), ISBN 978-92-79-28973-6.
- Ichii K. 2003. Application of Performance-Based Seismic Design Concept for Caisson-Type Quay Walls. PhD Dissertation, Kyoto University.
- International Navigation Association (PIANC) – Chairman: Iai S. 2001. Seismic design guidelines for port structures. Bakelma, 474p.
- Kakderi K. and Pitilakis K. 2010. Seismic analysis and fragility curves of gravity waterfront structures. In Fifth International Conference on Recent Advances in Geotechnical Earthquake Engineering and Soil Dynamics and Symposium in Honour of Professor I. M. Idriss, San Diego, CA, Paper No. 6.04a.
- Kakderi K., Raptakis D., Pitilakis K. 2010. D3.9-Fragility functions for harbor elements, Deliverable of SYNER-G EC project.
- Kappos A., Panagopoulos G., Panagiotopoulos Ch. and Penelis Gr. 2006. A hybrid method for the vulnerability assessment of R/C and URM buildings, Bulletin of Earthquake Engineering, 4(4), 391-413.
- Kappos A.J., Panagiotopoulos C., Panagopoulos G., Papadopoulos E. 2003. WP4 – Reinforced Concrete buildings (Level I and II analysis), RISK-UE Report.
- Kaynia et al. 2011a. D3.7-Fragility functions for roadway system elements, Deliverable of SYNER-G EC project.
- Kaynia A.M., Johansson J., Argyroudis S., Pitilakis K. 2011b. D3.8 - Fragility functions for railway system elements, Deliverable of SYNER-G EC project.
- Kaynia A.M. (ed.) 2013. Guidelines for deriving seismic fragility functions of elements at risk: Buildings, lifelines, transportation networks and critical facilities. SYNER-G Reference Report 4, Publications Office of the European Union, ISBN 978-92-79-28966-8.
- Khazai B. (ed.) 2013. Guidelines for the consideration of socio-economic impacts in seismic risk analysis. SYNER-G Reference Report 5, Publications Office of the European Union, , ISBN 978-92-79-28968-2.
- LESSLOSS. 2005. Deliverable 84 – Report on Building Stock Data and Vulnerability Data for each Case Study.
- Mackie K., Stojadinovic B. 2003. Seismic demands for performance-based design of bridges. PEER Report 2003/16. Pacific Earthquake Engineering Research Center, University of California, Berkeley, CA.
- Mackie K., Stojadinovic B. 2005. Fragility basis for California highway overpass bridge seismic decision making. PEER Report 2005/12. Pacific Earthquake Engineering Research Center, University of California, Berkeley, CA.
- Mehanny S.S.F. 2009. A broad-range power-law form scalar-based seismic intensity measure. Engineering Structures 31(7): 1354-1368.
- National Institute of Building Sciences (NIBS) 2004. HAZUS-MH: Users's Manual and Technical Manuals. Report prepared for the Federal Emergency Management Agency,

- Washington, D.C.
- Nies S., 2008. Oil and Gas Delivery to Europe, IFRI 2008.
- Padgett J.E., Nielson B.G., DesRoches R. 2008. Selection of optimal intensity measures in probabilistic seismic demand models of highway bridge portfolios. *Earthquake Engineering & Structural Dynamics* 37(5): 711-725.
- Pinto P., Cavalieri F., Franchin P., Lupoi A. 2012a. D5.5-Systemic vulnerability and loss for transportation systems, Deliverable of SYNER-G EC project.
- Pinto P.E., Lupoi A., Cavalieri F., 2012b. D5.7- Systemic vulnerability and loss for health care facilities, Deliverable of SYNER-G EC project.
- Pinto P.E., Cavalieri F., Franchin P. and Vanzi I. 2011c. D5.2 - Systemic vulnerability and loss for electric power systems, Deliverable of SYNER-G EC project.
- Pinto P.E., Cavalieri F., Franchin P., Vanzi I. , Pitilakis K. 2010. D3.3-Fragility functions for electric power system elements, Deliverable of SYNER-G EC project.
- Pinto P.E., Lupoi A., Franchin P., 2011b. D3.10-Fragility functions for elements within health care facilities. Deliverable of SYNER-G EC project.
- Pinto P., Cavalieri F., Franchin P., Vanzi I. 2011a. D2.3-Definition of system components and the formulation of system functions to evaluate the performance of electric power systems. Deliverable of SYNER-G EC project.
- Pitilakis K., Argroudis S. (eds.) 2013. Systemic seismic vulnerability and loss assessment: Validation studies. SYNER-G Reference Report 6, Publications Office of the European Union.
- RISK-UE. 2001-2004. An advanced approach to earthquake risk scenarios with applications to different European towns. WP4: Vulnerability of current buildings
- Rossetto T., Elnashai A. 2003. Derivation of vulnerability functions for European-type RC structures based on observational data. *Engineering Structures* 25: 1241-1263.
- Saadi H. 2002. Power system analysis - second edition. McGraw-Hill Primis Custom Publishing.
- Schäfer D., Bosi A. (2013). Systemic seismic vulnerability assessment: Software users manual. SYNER-G Reference Report 7, Publications Office of the European Union, in press.
- SRMLIFE 2003-2007. Development of a global methodology for the vulnerability assessment and risk management of lifelines, infrastructures and critical facilities. Application to the metropolitan area of Thessaloniki. Research Project, General Secretariat for Research and Technology, Greece.
- Vanzi I. 1996. Seismic reliability of electric power networks: methodology and application. *Structural Safety* 18(4): 311-327.
- Vargas Y.F., L.B. Pujades and A.H. Barbat. 2010. Probabilistic assessment of the global damage in reinforced concrete structures, In Fourteenth European Conference on Earthquake Engineering, Ohrid, Macedonia
- Weatherill G., Crowley H., Pinho R. 2011a. D2.12- Efficient intensity measures for components within a number of infrastructures. Deliverable of SYNER-G EC project.
- Weatherill G., Crowley H., Pinho R., Franchin P., Cavalieri F., Iervolino I., Esposito S., 2011b. D2.13-A review and preliminary application of methodologies for the generation of earthquake scenarios for spatially distributed systems, Deliverable of SYNER-G EC project.
- Werner S. D. 1998. Seismic guidelines for ports. TCLEE Monograph No 12, ASCE, 366p.

European Commission

EUR 26157 EN – Joint Research Centre – Institute for the Protection and Security of the Citizen

Title: Systemic Seismic Vulnerability and Risk Analysis for Buildings, Lifeline Networks and Infrastructures Safety Gain

Authors: Kyriazis Pitilakis, Sotiris Argyroudis, Kalliopi Kakderi, Helen Crowley, Fabio Taucer

Luxembourg: Publications Office of the European Union

2013 – 164 pp. – 21.0 x 29.7 cm

EUR – Scientific and Technical Research series – ISSN 1831-9424

ISBN 978-92-79-33135-0

doi: 10.2788/23242

Abstract

This report summarizes the main achievements and results of the work carried out within the European collaborative research project SYNER-G. SYNER-G developed an innovative methodological framework for the systemic assessment of physical as well as socio-economic seismic vulnerability at urban and regional level. The built environment is modeled according to a detailed taxonomy into its component systems, grouped in the following categories: buildings, transportation and utility networks, and critical facilities. Each category may have several types of components. The framework encompasses in an integrated fashion all aspects in the chain, from regional hazard to fragility assessment of components to the socioeconomic impacts of an earthquake, accounting for relevant uncertainties within an efficient quantitative simulation scheme, and modeling interactions between the multiple component systems in the taxonomy. The prototype software (OOFIMS) is implemented in the SYNER-G platform, which provides several pre and post-processing tools. The methodology and software tools are applied and validated in selected sites and systems in urban and regional scale: the city of Thessaloniki (Greece), the city of Vienna (Austria), the harbour of Thessaloniki, the gas system of L'Aquila (Italy), the electric power network in Sicily, a roadway network in South Italy and a hospital facility again in Italy. Adequate guidelines and appropriate dissemination schemes for all products of the project at European and international level have been proposed, including among others seven comprehensive Reference Reports, synthetic documents and deliverables, high quality brochure and leaflet, three technical workshops, a special session in the 15WCEE, peer review publications in journal and conferences, and preparation of two books in Springer Editions.

As the Commission's in-house science service, the Joint Research Centre's mission is to provide EU policies with independent, evidence-based scientific and technical support throughout the whole policy cycle.

Working in close cooperation with policy Directorates-General, the JRC addresses key societal challenges while stimulating innovation through developing new standards, methods and tools, and sharing and transferring its know-how to the Member States and international community.

Key policy areas include: environment and climate change; energy and transport; agriculture and food security; health and consumer protection; information society and digital agenda; safety and security including nuclear; all supported through a cross-cutting and multi-disciplinary approach.



ISBN 978-92-79-33135-0

